

---

---

## Fire chemistry — Generation and measurement of aerosols

*Chimie de la combustion — Production et mesurage des aérosols*





**COPYRIGHT PROTECTED DOCUMENT**

© ISO 2013

All rights reserved. Unless otherwise specified, no part of this publication may be reproduced or utilized otherwise in any form or by any means, electronic or mechanical, including photocopying, or posting on the internet or an intranet, without prior written permission. Permission can be requested from either ISO at the address below or ISO's member body in the country of the requester.

ISO copyright office  
Case postale 56 • CH-1211 Geneva 20  
Tel. + 41 22 749 01 11  
Fax + 41 22 749 09 47  
E-mail [copyright@iso.org](mailto:copyright@iso.org)  
Web [www.iso.org](http://www.iso.org)

Published in Switzerland

# Contents

Page

<b>Foreword</b>	<b>iv</b>
<b>Introduction</b>	<b>v</b>
<b>1 Scope</b>	<b>1</b>
<b>2 Normative references</b>	<b>1</b>
<b>3 Terms, definitions, symbols and abbreviated terms</b>	<b>2</b>
3.1 Terms and definitions	2
3.2 Symbols and abbreviated terms	2
<b>4 Aerosol properties</b>	<b>3</b>
4.1 General	3
4.2 Movement and evolution of fire aerosol	4
4.3 Measurable properties of aerosols	5
<b>5 Methods of measurement</b>	<b>11</b>
5.1 Applications	11
5.2 Categories of aerosol measurement	12
5.3 Initial considerations for sampling and analysis of aerosols	19
5.4 Selection of methods	20
5.5 <i>In situ</i> measurement methods	21
5.6 Extractive measurement methods	27
<b>6 Aerosol measurement metrology</b>	<b>43</b>
6.1 Standard aerosol generators for calibration of instrumentation	43
6.2 Qualification (Verification) of generators	45
6.3 Calibration methods exigencies	46
6.4 Validation	47
<b>7 Presentation of results</b>	<b>51</b>
7.1 Calculations	51
7.2 Measurement report	53
7.3 Uncertainties	53
<b>Annex A (informative) Experimental measurements of <math>D_{pp}</math>, <math>N_{pp}</math>, <math>R_g</math>, <math>D_f</math> and <math>k_f</math></b>	<b>55</b>
<b>Annex B (informative) Adsorption of combustion gases on particles</b>	<b>57</b>
<b>Annex C (informative) Inhalation dynamics and toxicity of particles</b>	<b>60</b>
<b>Annex D (informative) Non-toxicological effects of particles</b>	<b>64</b>
<b>Annex E (informative) Example of report</b>	<b>65</b>
<b>Bibliography</b>	<b>68</b>

## Foreword

ISO (the International Organization for Standardization) is a worldwide federation of national standards bodies (ISO member bodies). The work of preparing International Standards is normally carried out through ISO technical committees. Each member body interested in a subject for which a technical committee has been established has the right to be represented on that committee. International organizations, governmental and non-governmental, in liaison with ISO, also take part in the work. ISO collaborates closely with the International Electrotechnical Commission (IEC) on all matters of electrotechnical standardization.

The procedures used to develop this document and those intended for its further maintenance are described in the ISO/IEC Directives, Part 1. In particular the different approval criteria needed for the different types of ISO documents should be noted. This document was drafted in accordance with the editorial rules of the ISO/IEC Directives, Part 2. [www.iso.org/directives](http://www.iso.org/directives)

Attention is drawn to the possibility that some of the elements of this document may be the subject of patent rights. ISO shall not be held responsible for identifying any or all such patent rights. Details of any patent rights identified during the development of the document will be in the Introduction and/or on the ISO list of patent declarations received. [www.iso.org/patents](http://www.iso.org/patents)

Any trade name used in this document is information given for the convenience of users and does not constitute an endorsement.

The committee responsible for this document is ISO/TC 92, *Fire safety*, Subcommittee SC 3, *Fire threat to people and environment*.

## Introduction

Aerosols generated in fires are complex, non-homogeneous mixtures of liquid droplets of tar or water, solid-phase carbonaceous agglomerated soot with adsorbed organic compounds, or mineral particles. After formation through complex chemical and physical processes, fire aerosols continuously undergo changes in physical size, structure, and chemical composition as the particles may coalesce, agglomerate, absorb gases, evaporate or deposit on surfaces. The aerosol concentration, particle size, temperature, and gas-phase composition also play a role in the rate of change.<sup>[1][2][3]</sup>

There are multiple mechanisms by which fire-generated aerosols affect the fire threat to people and the environment. First, small particles are respirable and can penetrate deep into the lung structure. Inhaled particles themselves can be irritating, reducing the ability of people to escape from a fire.<sup>[4][5]</sup> Next, these particles can adsorb and/or absorb toxic and irritant gases and vapours, providing a means for transport past the respiratory tract natural defences and deep into the lungs.<sup>[5][6]</sup> Third, even less or non-respirable particles may effectively reduce the concentration of toxic gases and vapours in the fire effluent and can deposit them on surfaces. Fourth, aerosols may obscure vision, potentially reducing the ability of people to move effectively toward safety (see ISO 13571). Finally, the aerosol fraction in fire effluents also has significant potential to adversely affect the environment, particularly where the fires are large and of long duration.<sup>[2][4]</sup>

Therefore, it is important, within the context of the mechanisms of generation and evolution of aerosols, to be able to measure aerosol concentrations and size distributions accurately; to appreciate the scope and limitations of the apparatus and methodologies available for these measurements; and to interpret such measurements effectively, consistent with the hazards and risks being evaluated. This International Standard provides details of a range of sampling and measurement methods and guidance on which ones to use for particular applications, together with an interpretation scheme based on current knowledge. This document also includes informative annexes that summarize the physical aspects of fire aerosol generation, aerosol movement and modification with and away from the fire plume, the aerosol contribution to fire growth through flame radiation, and the roles of particulates in threat to life and the environment.



# Fire chemistry — Generation and measurement of aerosols

## 1 Scope

This International Standard provides a guide to the generation of aerosol particles in fires, defines apparatus and procedures for the sampling and measurement of aerosols, and provides procedures for the interpretation and reporting of the data. It is intended to assist fire test designers and those making measurements at unwanted fires to choose and use appropriate methods for aerosol measurement for differing hazards to people and the environment.

This International Standard identifies the scope, applicability, and limitations of each method. The interpretation of the data from these measurements is strongly dependent on the end use of the data.

Fire-generated aerosols may present a direct risk of restricting escape from fire by obscuring an exit route, or they may produce chronic health and environmental hazards from chemical compounds contained in the aerosol (for example, toxic chemicals like polycyclic aromatic hydrocarbons in soot or radionuclides from nuclear plant fires.) Aerosol particles may be inhaled to various depths in the lungs, depending on their size and density, or may be released into the environment and deposited on land and in watercourses.

In particular, this International Standard addresses the following aspects of aerosol generation and measurement in fires:

- Adsorbed/dissolved gas or vapour phase species;
- Physical mechanisms involved in the transport of aerosols, dispersal in the fire plume, coagulation/agglomeration leading to variation in particle sizes and fractions, “thermophoresis” (main cause of soot deposition), “diffusiophoresis” and, sedimentation.
- The interactions between gases and vapours and aerosol: adsorption and removal of species from gas phase, transportation of adsorbed gases into the lungs;
- Sampling and measurement methods, including their principles of operation, method description, the data provided, and in each case their scope, field of application, advantages and disadvantages;
- Metrology of the measurement methods, and in the generation of “standard aerosols”, and the related uncertainties;
- Physiological and environmental effects of aerosols insofar as these effects can be used to define the measurement method for specific applications; and
- Hazards of carbon particles present in the fire effluent as visible “smoke” through their size, morphology, chemical nature, and the nature of the effluent in which they are (or were) suspended.

This International Standard is not oriented toward the aerosols generated from controlled combustion. (e.g. incineration). However, much of the material in this document is common to such aerosols.

## 2 Normative references

The following documents, in whole or in part, are normatively referenced in this document and are indispensable for its application. For dated references, only the edition cited applies. For undated references, the latest edition of the referenced document (including any amendments) applies.

ISO 13943, *Fire safety — Vocabulary*

### 3 Terms, definitions, symbols and abbreviated terms

#### 3.1 Terms and definitions

For the purposes of this document, the terms and definitions given in ISO 13943 and the following apply.

##### 3.1.1

##### **aerosol**

suspension of liquid droplets, or solid particles in a gas phase matrix which are generated by fires and range in particle size from under 10 nm to over 10 µm

##### 3.1.2

##### **particles**

solid-phase products present in aerosols

Note 1 to entry: There are two categories of fire aerosol particles: unburned or partially burned particles containing a high proportion of carbon (i.e. "soot"), and relatively completely combusted, small particle sized "ashes". Soot particles of small diameter, (i.e. about 1 µm), typically consist of small elementary spheres of between 10 nm and 50 nm in diameter. Formation of soot particles is dependent on many parameters including nucleation, agglomeration and surface growth. Oxidation of soot particles (i.e. further combustion) is also possible.

##### 3.1.3

##### **droplets**

liquid-phase products present in aerosols, typically generated through pyrolysis (reduced oxygen combustion conditions) from both flaming and smouldering fires and which may condense into tarry-like, spherically-shaped droplets

Note 1 to entry: Water produced from combustion may also condense around particles forming aerosol droplets.

##### 3.1.4

##### **inhalable fraction**

mass fraction of the total particles suspended in air, which can be inhaled into the nose and the mouth and depends on particle diameters, the velocity and direction of gas containing the particles, and on the respiratory frequency

##### 3.1.5

##### **extrathoracic fraction**

mass fraction of the inhaled particles which cannot penetrate beyond the larynx

##### 3.1.6

##### **thoracic fraction**

mass fraction of the inhaled particles penetrating beyond the larynx

##### 3.1.7

##### **tracheobronchic fraction**

mass fraction of the inhaled particles penetrating beyond the larynx but not penetrating into the non-ciliated respiratory system

##### 3.1.8

##### **alveolar fraction**

mass fraction of the inhaled particles which penetrates into the non-ciliated respiratory system

#### 3.2 Symbols and abbreviated terms

$D_p$	Physical diameter of a particle
$D_a$	Aerodynamic diameter of a particle
$D_m$	Electrical mobility equivalent diameter of a particle



$D_{ev}$	Volume equivalent diameter of a particle
$D_g$	Diameter of a spherical shell with the same mass and inertial component as the considered combustion particle
$D_{50}$	Mass median diameter of a set of particles
$D_{pp}$	Diameter of primary particles of an agglomerate
$N_{pp}$	Number of primary particles constituting an agglomerate
$R_g$	Gyration Radius of a particle
$D_f$	Fractal Dimension of a particle
$k_f$	Logarithm of the prefactor for fractal dimension of a particle
$\chi$	Dynamic shape factor
$\rho$ :	Mass density of the particle
$\mu$	Viscosity of the surrounding gas
$L$	Optical path followed by light through the aerosol (m)
$K_{ext}$	Extinction coefficient of light by the aerosol ( $m^{-1}$ )

## 4 Aerosol properties

### 4.1 General

Fire effluents consist of combustion gases and vapours, water droplets and aerosols (solids and liquids formed during and after combustion) combustion. The aerosol component of fire effluents forms the visible portion of smoke and is made up of particles and droplets of small size. Aerosols are organic and inorganic particles and droplets produced during the incomplete combustion of fuels.

The liquid droplets present in aerosols are mainly spherical. Solid carbon particles have quasi-fractal morphology, and can be present over a relatively large range of sizes. Inorganic mineral particles can have various forms, depending on their initial form in the fuel and on the fire “history”.

The nature of fire products are less dependent on the fuel type at high fire temperatures (i.e. around 1000 °C) than at lower temperatures and at high temperatures appear to depend on the local conditions during formation. It has been demonstrated that combustion of cellulose, tobacco, various polymers can generate approximately the same yield<sup>[8]</sup> of soot at an imposed high temperature of 1000 °C.

With open, well-ventilated fires, production of soot is therefore highly dependent on the temperatures in the flame (or smouldering) zone, the oxidation conditions (e.g. degree of air access to the fire), and the extent of aerosol agglomeration or re-oxidation.

The similarity of aerosol types during the combustion of different fuels can be partly explained by the fact that many fuels are based on hydrocarbons or hydrocarbon polymers which have relatively similar “cracking” patterns during thermal decomposition, generating common products such as methane, ethane and ethylene, propane.

Depending on the end use of data from the measurement of the various properties of the aerosol portion of fire effluents, these properties will have a varying prominence. For example:

- a) For studying escape from fire, the aerosol opacity will affect human visibility (see ISO 13571). In many fire scenarios, the impact of aerosols on visibility is one of the most important parameters in determining the ability to escape. Pre-movement actions and movement speed are strongly dependent

on the visibility in smoke-filled spaces. It has been suggested that above a certain opacity of smoke, many would consider that escape would be seriously impeded. See [Annex D](#) for further details.

- b) In fire modelling, soot yield is an important input parameter. It has a very significant effect on the heat radiation properties of flames (often a sub-model of the main model), and therefore on the general heat transfer by radiation, which can affect escape from a fire (see ISO 13571) and can significantly influence fire growth and the occurrence of “flashover”. See [Annex D](#) for further details.
- c) The direct physiological effect of aerosols on people is related to the size fractions within the aerosol and the morphology of the particles and droplets. It is therefore often more important to know the particle and aerosol distribution by size rather than the total aerosol mass for the determination of physiological effects. Unfortunately, size distribution is a parameter, which is often difficult to measure, principally due to the processes of agglomeration over short time intervals. Agglomeration can greatly affect the structure of the particles and droplets, as well as their density and optical (i.e. obscuration) properties. In addition, volatile species that may evaporate to a varying degree while being sampled and measured will influence the data recorded. Furthermore, measuring instruments operating on different principles will give different effective size fractions, and the methods cannot be assumed to be equivalent. The main parameter to consider for physiological effect of aerosols is their deposition in the respiratory tract. Different classes of particle size, based on their relation to physiological effects, have been defined: “PM10”, “PM2.5”, “inhalable” ( $D_p < 100\ \mu\text{m}$ ), “thoracic” ( $D_p < 10\ \mu\text{m}$ ), “respirable” ( $D_p < 4\ \mu\text{m}$ ), “ultrafine” ( $D_p < 0,1\ \mu\text{m}$ ), and “nanoparticulates” ( $D_p < 0,050\ \mu\text{m}$ ). See [Annex C](#) for further details.

Mass concentration and particle and droplet size fraction can also be valuable parameters for computational fluid dynamics (CFD) computer modelling of fire processes. This is especially true as models become capable of simulating the evolution of the aerosols and the effects of the evolution on flame radiation.

## 4.2 Movement and evolution of fire aerosol

Knowing how and where to sample the fire effluent is critical to obtaining an accurate and useful aerosol distribution. Thus, it is important to take into account the local transport processes that can result in non-uniform particle distributions.

The generation of particles begins within the flame or combustion zone in smouldering. Upon release into the fire atmosphere, agglomeration can occur to varying degrees. In the fire plume, because of thermophoresis (movement of particles due to a temperature gradient) and due to the upward, buoyancy-driven movement of the fire plume, particles will be entrained and carried initially upwards above the fire. Glowing carbon particles are the most important contributor to heat radiation from the fire plume, especially because these particles are typically present in a relatively high concentration, have an emissivity close to blackbody (i.e. radiate over a very large spectral range), and are present at high temperature.

Thermophoresis is a very important parameter governing the movement of aerosols in a hot fire and their deposition on any relatively cool surfaces. Thermophoretic movement may be considered as the mechanism by which the aerosols are repelled by a hot body and attracted to a cooler body resulting in a movement of particles and droplets from hot to cold areas. This results in the observed deposition of particles and droplets onto cool surfaces such as windows and walls in the structure containing the fire. Hot zones can be relatively free of particles, but are potentially capable of generating them if temperature conditions change. This is because, as the temperature drops, gaseous organic molecules can condense to form aerosols. In fact, the very act of sampling from these areas of apparently low or zero particles can give rise to measured particles through the intrusive (particularly cooling) effect of the measuring apparatus.

The phenomenon of particle deposition can, for example, damage property at considerable distances from the fire. The pattern of smoke deposits after a fire, typically as an inverted “V” from the source can provide valuable evidence on the origin of the fire when arson is suspected. The same pattern can also be used to determine areas of the fire scenario which are likely to be free from contamination by

smoke – an important economic consideration for example with respect to restoration requirements following a fire.

There are three other transport processes that can affect the distribution of aerosols within the airflow away from a fire:

- Diffusiophoresis is the process by which suspended particles in a hot medium with a concentration gradient move from areas of high concentration to areas of low concentration.
- Photophoresis characterizes reaction of the particle with light. In photophoresis, a particle absorbs light and is heated by this absorbed energy in the highlighted direction. In reaction, the particle then moves away from the light (toward a cooler region).
- Sedimentation is the downward movement of the particles due to gravity and to the properties of the surrounding matrix (especially viscosity). The rate of sedimentation is dependent on the viscous properties of the overall flow, the temperature, and the aerosol size and mass. Large, heavy particles settle quickly, whereas fine, low mass particles can remain suspended indefinitely.

In the presence of an electrical field, movement of the particles (especially carbon particles) will be modified. The effects of this phenomenon are largely influenced by gravity and thermophoresis. This phenomenon is the principle of measurement of some instruments described in this Standard.

The agglomeration and coagulation processes, present during the formation of the aerosol may continue at considerable distances from the fire source, although the effects decrease as the aerosols become diluted in increasing volumes of air. Thus, at relatively great distances from the fire, large-mass clusters of particles may be formed and may sediment rapidly. As an illustration of the importance of time in decreasing the concentration of particles through coagulation effects, [Table 1](#), [see Reference (2)], shows the relationship between an initially monodispersed aerosol over a range of initial concentrations and the corresponding times needed to double the diameter and halve the concentration of the particles. This shows that if such particles are to be sampled for meaningful measurement, rapid dilution is necessary to preserve as much as possible the original particle size distribution and total aerosol mass.

**Table 1 — Measured change of the size and mass concentration of an initially monodispersed aerosol due to coagulation, according to Reference [2]**

Initial concentration (particles/mL)	Time to double the mean diameter of aerosol	Time to halve the mass concentration
$10^{14}$	140 $\mu$ s	20 $\mu$ s
$10^{12}$	0,014 s	0,002 s
$10^{10}$	1,4 s	0,2 s
$10^8$	140 s	20 s
$10^6$	4 h	33 min
$10^4$	16 days	55 h
$10^2$	4 years	231 days

Under conditions of fixed temperature, the aerosol size distribution tends towards a state known as “self preserving”, i.e. equilibrium tends to exist between the rate of agglomeration and the rate of separation.<sup>[2]</sup>

### 4.3 Measurable properties of aerosols

#### 4.3.1 Size and shape

Aerosol droplets are spherical at the time of their formation and typically remain spherical as they grow by aggregation or condensation. The droplet diameters range from under 1 nm to more than 100  $\mu$ m.

Carbaceous particles formed initially are spherical, with diameters  $D_p$ , are homogenous, and have a size range varying between 10 nm and 50 nm. The frequency distribution of such particles is normally

Gaussian.[2][3] However, as these small particles stick together to form larger particles, aged and agglomerated carbon particles in fire effluents are rarely spherical, their fractal structure being a result of the growth process. Therefore, they need to be characterized using parameters other than those used to describe a sphere. The main parameters used are the aerodynamic diameter and the electric mobility diameter. These and some additional parameters are defined below.

#### 4.3.1.1 Aerodynamic diameter

This diameter  $D_a$  represents the diameter of a sphere of density  $1 \text{ g/cm}^3$  having the same settling velocity in calm air as the aerosol particle being considered. For an unspecified particle, the following relation links this diameter to the mass median diameter of the distribution:

$$D_a = \sqrt{\frac{\rho}{\chi}} \cdot d_{50}$$

#### 4.3.1.2 Electrical mobility equivalent diameter

This diameter represents the diameter of a sphere, having the same electric mobility  $Z_p$  as the considered particle, following the relation:

$$D_m = \frac{Cc}{3\pi\mu B}$$

where

$Cc$  is the Cunningham correction factor

$B$  is the dynamic mobility, which characterizes forces produced by surrounding gas on the particle.

#### 4.3.1.3 Volume equivalent diameter

This diameter represents the diameter of a sphere with the same mass as the considered particle and the same density.

$$D_{ev} = \left[ \frac{m}{(\pi/6)\rho} \right]^{1/3}$$

#### 4.3.1.4 Gyration diameter

This diameter,  $D_g$ , represents the diameter of a spherical shell with the same mass and inertial moment as the considered combustion particle. This diameter is particularly useful in order to describe the fractal morphology of combustion aerosol and will be described in [5.2.3](#).

#### 4.3.1.5 Additional diameters

Other diameters can be used to define particles, see References [2] and [3] They include diameter of primary particles  $D_{pp}$ , aggregate diameter  $D_{agr}$  (diameter of a sphere, which includes totally the particle), Martin diameter, Feret diameter or Stokes diameter. [Figure 1](#) presents these different diameters for a carbon particle.

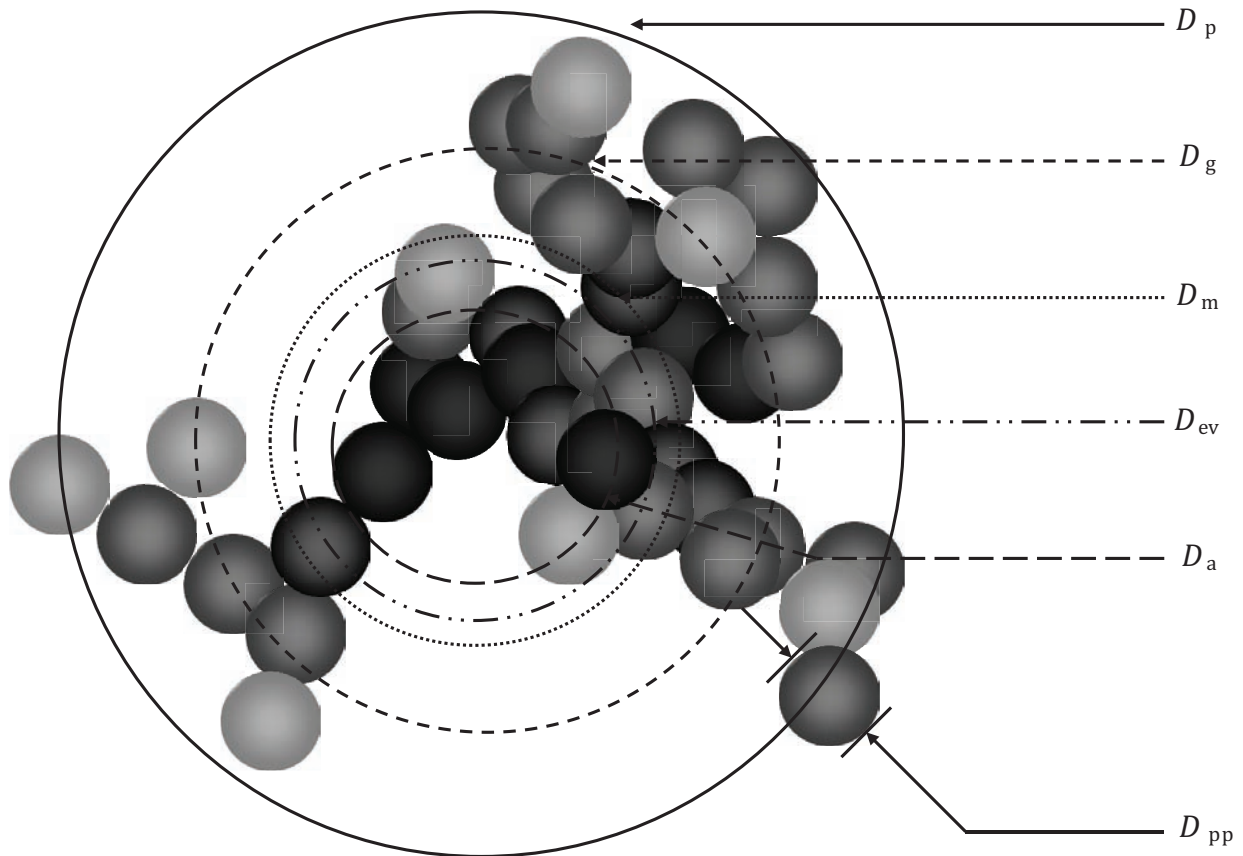


Figure 1 — Different characteristic diameters of a carbon particle

#### 4.3.1.6 Aerosol morphology

The shape of combustion aerosol particles and droplets has been intensively investigated since the pioneering work of Witten and Sander[9] and Julien and Botet.[10] Due to their mode of formation, particles produced by flames have a shape mainly governed by the “diffusion limited aggregation” phenomenon (DLA). A quasi-fractal relationship has been introduced in order to fully describe the morphology of a combustion aerosol through the aggregation process from a small number of primary particles  $N_p$  to a large number in the mature aggregate:

$$N_{pp} = k_f \cdot \left( \frac{D_g}{D_{pp}} \right)^{D_f}$$

This relationship is regarded as a *quasi-fractal* as it is only possible to define the morphology of the smallest primary particles and the highest limit for the agglomerated particles. Some measurements of  $D_{pp}$ ,  $N_{pp}$ ,  $R_g$ ,  $D_f$  and  $k_f$  are presented in [Annex A](#).

#### 4.3.1.7 Aerosol size distribution

The parameters typically used to characterize the granulometric distribution of the aerosol are the mass median aerodynamic diameter (MMAD), the standard deviation of the diameters, and the distribution function. This distribution is generally assumed to fit a log/normal distribution.

### 4.3.2 Aerosol global parameters

#### 4.3.2.1 Optical extinction coefficient

The Bouguer-Beer-Lambert relation describes the attenuation of light through a suspension of particles, usually normalized for fire studies for a unit path length. The law is dependent upon the wavelength of the light, although an approximation is normally used and ignores this spectral dependence. The extinction coefficient of light depends on soot concentration and the particles' propensity to absorb light, characterized by their specific extinction surface. The average attenuation of the light beam is stated through the expression:

$$\frac{I}{I_0} = e^{-K_{\text{ext}} \cdot L}$$

where

$L$  is the optical path (path followed by the light through smoke) (m)

$K_{\text{ext}}$  is the extinction coefficient of the light ( $\text{m}^{-1}$ )

The extinction coefficient of an aerosol depends on the extinction cross section of aggregates stated through the expression:

$$K_{\text{ext}}(N, m) = N \int f(d) C^{\text{ext}}(d, m) dd$$

where

$N$  is the particle concentration ( $\text{m}^{-3}$ )

$m$  is the soot refractive index (/)

$f(d)$  is the particle diameter distribution function (/)

$d$  is the particle diameter (m)

$C^{\text{ext}}(d, m)$  is the extinction cross section for the particle diameter  $d$  ( $\text{m}^2 \text{sr}^{-1}$ )

When the size parameter  $x_p = \pi d_p / \lambda$  is small enough,  $C^{\text{ext}}$  is given by the Rayleigh approximation:

$$C^{\text{ext}} = \frac{-\pi^2}{\lambda} E(m) d^3$$

$$\text{With } E(m) = \text{Im} \left( \frac{m^2 - 1}{m^2 + 2} \right)$$

The extinction coefficient is the main value used to represent smoke opacity. It provides information on the ability of people to find egress paths, see exit signs, etc, in a smoke-filled building.

#### 4.3.2.2 Mass concentration of soot

An extinction coefficient value can be used to estimate the mass concentration of soot, as follows:

$$C_s = \frac{\sigma_s}{k}$$

where

$C_s$  is the mass concentration of soot particles ( $\text{kg}\cdot\text{m}^{-3}$ )

$\sigma_s$  is the specific extinction surface per mass unit of soot ( $\text{m}^2\cdot\text{kg}^{-1}$ ). In the related literature,  $\sigma_s = 10 \text{ m}^2/\text{g}$  and more exactly,  $(9,6 \pm 3) \text{ m}^2/\text{g}$ <sup>[1]</sup> for hydrocarbon gas. This value depends on numerous parameters and can be precisely known only for the simple combustibles under ideal combustion conditions

#### 4.3.2.3 Soot volume fraction

From the extinction coefficient, the soot volume fraction may be deduced from:

$$F_v = \frac{\lambda}{6 \pi \operatorname{Im} \left( \frac{m^2 - 1}{m^2 + 2} \right)} K_{\text{ext}}$$

where

$\lambda$  is the wavelength of the source

#### 4.3.2.4 Soot yield

Soot yield is the ratio between the mass of soot and the mass loss of the fuel. This parameter is in general expressed for the fuel either in global way independently of conditions, or for given conditions (fuel oxygen ratio, temperature, pressure). The soot yield generally varies over the phases of burning, from ignition to extinction of the fuel. It is normally expressed in kg of soot per kg of fuel. The value can be determined experimentally, from integration of the extinction coefficient, or from direct measurement. The soot yield parameter is commonly used as input data to the flame models that are used to calculate fire spread.



#### 4.3.2.5 Scattering coefficient

The scattering coefficient of aerosols depends on the scattering cross section of aggregates through the expression:

$$K^{\text{sca}}(N, m) = N \int f(d) C^{\text{sca}}(d, m) dd$$

where

$N$  is the particle concentration ( $\text{m}^{-3}$ )

$m$  is the soot refractive index (/)

$f(d)$  is the particle diameter distribution function (/)

$d$  is the particle diameter (m)

$C^{\text{sca}}(d, m)$  is the scattering cross section for the particle diameter  $d$  ( $\text{m}^{-2}\text{sr}^{-1}$ )

$K^{\text{sca}}(d, m)$  is the scattering coefficient ( $\text{m}^{-1}$ )

When the size parameter  $x_p = \pi d_p / \lambda$  is small enough,  $C^{\text{sca}}$  is given by the Rayleigh approximation:

$$C^{\text{sca}} = \frac{\pi^4}{4\lambda^4} F(m) d^6$$

where

$$F(m) = \left| \frac{m^2 - 1}{m^2 + 2} \right|^2$$

and

$$K^{\text{sca}} = N C^{\text{sca}}$$

With the Rayleigh approximation, the particular concentration is defined as:

$$N = \frac{1}{4\lambda^2} \frac{F(m)}{E^2(m)} \frac{(K^{\text{ext}})^2}{K^{\text{sca}}}$$

and primary particles are defined as:

$$d_p = \left( \frac{-4\lambda^3}{\pi^2} \frac{F(m)}{E(m)} \frac{K^{\text{sca}}}{K^{\text{ext}}} \right)^{1/3}$$

Different approaches are in use to provide a formula for the relationship between the scattering coefficient of the aerosol and scattering cross section of primary particles, (i.e. the primary components of fractal aggregates of the aerosol). These approaches can be separated on two families:

- The first uses many approximations and hypotheses and has the advantage of providing an analytical formulae linking the properties of a primary particle to that of an aggregate and the aerosol itself.
- The second uses powerful mathematical techniques in order to compute the scattering of aggregates aerosols by solving Maxwell equations in an analytical or in a numerical way. In order of decreasing



approximation the main techniques are the Rayleigh theory, the Rayleigh-Debye-Gans theory, and the Rayleigh-Debye-Gans theory for fractal or polydispersed aggregates.<sup>[1]</sup>

The degree of approximation depends on the size parameter  $x_p = \pi d_p / \lambda$ .

Integral methods (Volume Integral Equation Method, Method of Moment, Discret Dipole SCATtering...) or differentials methods (T-Matrix Method, Generalized Lorenz-Mie Theory for fractal aggregates, etc) are also used for the resolution of Maxwell equations.<sup>[1][12][13]</sup>

#### 4.3.2.6 Refractive index

The refractive index is a mathematical function of real and imaginary parts and is defined as:

$$m = n - i * k$$

where

$n$  is the real part of the refractive index

$k$  is the imaginary part of the refractive index

The refractive index is necessary to determine properties such as the volume fraction when using experimental measurements. Inversion methods have been developed to determine the refractive index of aerosols using extinction and scattering coefficients from experimental studies and coupling these results with extinction and scattering coefficients estimated with calculations that can take into account the fractal aggregate shape.

#### 4.3.3 Warnings considering aerosols characteristic parameters

The majority of particles in fire effluent are rich in carbon. Nevertheless, it is important to consider aerosols other than carbon-based solid particles which can be present in significant quantities. For example, these include solid mineral particles derived from the burning item when the item contains mineral fillers. In these cases, care has to be taken with the expression of descriptive parameters of the aerosol. Some of the relations presented previously are subject to caution when extended to non-carbon-based aerosols.

## 5 Methods of measurement

### 5.1 Applications

The nature of aerosol measurements in this International Standard is driven by fire safety objectives. These objectives include assessment of personal injury, reduction in escape possibilities, and impact on the environment. All areas normally have direct and indirect effects, and a key parameter in most is the transportation of adsorbed species. Some species like sulfur compounds or radioactive metals have a high affinity for carbon aerosols. They can be transported in lungs (see above) or far from fire source

The main adverse physiological factors affecting people exposed to fire aerosols are the granulometric distribution, the chemical nature and the morphology of the aerosols. Granulometric distribution affects the penetration of the aerosol into the respiratory tract where its chemical nature and morphology are the main adverse factors. The effect of larger particles is mainly due to their ability to act as a mechanical blockage within the bronchioalveolar tree. These larger particles may also produce acute effects due to tissue damage where they lodge, through the presence of adsorbed chemical species. Micronic particles are difficult to expurgate and can accumulate in alveoli, where they can be ingested by phagocytosis making them difficult to remove. This accumulation can cause loss of breathing capacity and possibly promote cancers. There are both acute and sub-acute effects. The smallest nanometric particles have a

toxic effect due more to their chemical nature rather than their morphology. Such effects are linked to molecular biological processes, which are currently being studied.

The indirect effect of aerosols on health and the environment can be linked to their environmental impact generally. Two aspects are frequently taken into consideration here: the effect of aerosols themselves and the effect of adsorbed species. Aerosols from large fires, especially of long duration may be transported far from the fire source. Many industrial or wildland fires have been reported as depositing aerosols some hundreds of kilometres from the source, but generally the most significant area of deposition is within a few kilometres around the source. Deposition of aerosols on vegetables can decrease photosynthesis depending on the optical properties of the aerosol, and adsorbed chemical species can have a lasting and detrimental effect on plants and surface water. These aspects are currently being studied and guidance on these processes and the mitigation of their effects are being developed within ISO TC92/SC3/WG6.

The impact of aerosols on filtration systems is very important in controlled atmosphere environments where ventilation and pressure effects must be carefully controlled to ensure minimal escape of hazardous material. As examples, if fire occurs in biohazard laboratories or nuclear facilities, efficient filtration of fire effluent is clearly vital to ensure that external areas do not become contaminated. In such situations fire dampers may be installed in extract ducts to prevent fire and fire products from migrating to unwanted areas. To limit the release of fire aerosols, such installations may be equipped with gas absorbers and high efficiency filters. Because of the sealed nature of such installations and the over-pressure effects of fire, these filters must be designed so that they are not rapidly plugged during fire. Design of these filtration stages requires a knowledge of the nature of effluents, particularly aerosols likely to be released in the fire.

Impact on electrical systems is also an important hazard from aerosols in fire effluents, having both immediate and delayed effects. Because of the electrical conductivity of aerosols, if they contaminate electronic circuits, this conductivity can cause severe functional impairment. This is especially serious if the circuits are in safety devices. Delayed effects can occur when such circuitry is re-commissioned after restoration following a fire when residual corrosivity (e.g. from adsorbed species such as hydrogen chloride) can continue to adversely affect the function of the circuitry. Such aspects are hazards and risks which need to be considered in any fire safety engineering study.

## 5.2 Categories of aerosol measurement

### 5.2.1 Measurement of concentration

The concentration of an aerosol is defined as some integrated measure per unit volume. For example, the aerosol number concentration is the total number of particles (regardless of size) per unit volume and the mass concentration is the total aerosol mass per unit volume. Other concentration measures include: aerosol diameter, surface area, light scattering, and electrical charge per unit volume. Typically, a measurement device will be constrained to provide a single measure of concentration over a wide range or to provide a concentration measurement over a number of limited size ranges. Optical particle counters are effective in giving the number concentration and even the particle size distribution for particles greater than about 300 nm. Condensation particle counters are effective in providing the number concentration for particles greater than about 10 nm. Gravimetric sampling of aerosols can be tailored to provide mass concentration measurements of particles below a certain size through inertial impaction of large particles.

A limited number of large particles can dominate mass concentration, surface area concentration, or light scattering concentration. Conversely, under-counting, or not sampling a small number of large particles may not affect the number distribution appreciably. Likewise, not weighing a large quantity of very small particles may not affect the mass concentration appreciably.

Typically, direct concentration measurements are performed on extracted fire aerosol samples drawn into an instrument, or onto a filter. *In situ* measurements tend to be indirect measurements, such as by light extinction. The benefit of an *in situ* measurement like light extinction is its simplicity and the fact that it does not disturb the aerosol or flow. However, light extinction is spatially averaged over a path length. Extractive sampling may disturb flows, and is subject to biases due to non-isokinetic

sampling, diffusive losses in sampling lines, sedimentation and impaction losses, and electrostatic losses depending on sampling line materials and aerosol electrical charge. In general, particle losses in sampling tubes must be considered for any aerosol measurements. The design of the experimental setup, and the sampling system should be tailored to minimize the losses of particles in the size range of interest. For instance, beyond the shortest possible sampling lines, metallic or conductive plastic tubing will minimize electrostatic losses, large radius bends and short horizontal lines will reduce impaction and sedimentation losses, and large volumetric flow rates will reduce diffusion losses. The temperature and humidity of the aerosol as it flows to instrumentation and gets mixed with any dilution air may affect its particle size distribution. Heated lines will reduce condensation when extracting fire aerosols at temperatures above the ambient. Dilution air at the same temperature and relative humidity will reduce evaporation and condensation of volatiles and water.

The aerosol concentration measured may be an average value over a time interval, or may be time-resolved, depending on the instrumentation used. Time averaging over a test is usually called for when a limiting quantity is prescribed such as the total smoke production from a burning sample, or when a yield is computed from the total sample mass loss. Gravimetric filter sampling may require time averaging in order to accumulate sufficient mass to weigh the deposit accurately. Likewise, gravimetric cascade impactor sampling must be over a time interval long enough to accumulate sufficient mass on the separate stages, related to the size range of interest.

### 5.2.2 Measurement of size distribution

The aerosol size distribution is a statistical representation of the quantity of all the particle sizes contained in a sampled aerosol. A monodisperse aerosol is represented by a single parameter since all particles are identical. Polydispersed aerosols have individual particles within a range of sizes. Fire aerosols are polydispersed and may range in diameter over two to three decades. The size distribution can represent any concentration measurement contained in discrete size ranges, or as a continuous function of the particle size.

Frequently the size distribution is represented graphically as a histogram with the discrete concentration contained in a size bar or “bin”. Many instruments produce binned data, for example cascade impactors, scanning mobility particle sizers, optical particle sizers, etc. [Figure 24](#) (see [7.1](#)) is an example of a histogram plot. A frequency distribution or cumulative distribution curve are convenient representations of size distributions because the mathematical properties allow for computation of size related information of interest. From a cumulative distribution one can readily ascertain the fraction above or below a fixed size. The shape of the frequency distribution is asymmetrical for most aerosols with long tails at larger sizes and in some cases they are multimodal. Unlike a normal distribution, the mode, median and mean sizes are different and the particle diameter distributions are typically ranked from smaller to larger values of the mode, median and mean. The mode is the most frequent size, the median is the size that splits the distribution into two equal areas, and the mean is the average value.

Because of the skewed distribution consisting of a long tail at larger sizes, aerosol size distributions are frequently represented by a log-normal distribution. It is equivalent to a normal distribution of the logarithm of the particle size.

### 5.2.3 Measurement of morphological characteristics

The morphology of the particles is an important characteristic of combustion aerosols, especially in order to describe their potential toxicity. Since the 1980s, soot particles have been described as quasi-fractal objects. Several experimental procedures of determination of fractal parameters of combustion aerosols are presented hereafter. The presented list is not exhaustive, and additional approaches can be found in the literature.<sup>[14]</sup> However, these are not always adaptable to fire measurements. For example, Angular Light Scattering,<sup>[15]</sup> which is widely used to measure soot morphology in combustion, needs to be adapted to fire effluents.

### 5.2.3.1 Micrograph analysis of combustion particles

The first approach is simple and the most cited in the literature. This procedure is based on *in situ* sampling and image analysis of a combustion particles micrograph. The first point of this procedure is most utilized one and several works described sampling procedure, one may cited three commonly used procedures.

#### 5.2.3.1.1 *In situ* sampling

##### 5.2.3.1.1.1 Thermophoretic precipitator (TP)

This procedure, largely used in aerosol studies since the works of Green and Watson<sup>[16]</sup> who developed a thermal precipitator for measuring dust concentrations in mines. It is based on the motion of particles from a cold to hot surface inside a temperature gradient. This physical phenomenon has been recently used in the combustion community<sup>[17][18]</sup> for soot characterization inside flames or in plume of various laminar and turbulent flames. In this case, the TEM grid, mounted on thermophoretic probe is inserted briefly into the flame zone using a pneumatic piston. Use of this device has been widely used in the literature but it is currently still at a prototype stage. Also of note is the recent commercial device of the Fraunhofer Institute of Toxicology and Experimental Medicine (ITEM). This unit is composed of a sampling tube, which heats the aerosol to 180 °C and a thermophoretic precipitation zone composed of a TEM grid fixed on a “Peltier-effect” cooler. This device has been used to study nanoparticles generated by an aluminium smelter.<sup>[19]</sup> The main advantage of thermophoretic sampling is the low-influence of particle diameter on thermophoretic collection efficiency for sub-micron particles. Moreover, direct deposition of particles on TEM grids allows direct observation, without any post-treatment of particles.

##### 5.2.3.1.1.2 Electrostatic precipitator (EP)

The second procedure is based on the motion of a charged particle inside an electrical field. In this situation, charged particles experienced electrostatic forces directly linked to the flow conditions of the particle and intensity of the electric field. This physical behaviour of charged particles is used in the Differential Mobility Analyser (DMA) for production of size-selected aerosol or for size distribution measurement of submicron particles. A commercial device, called the Nanometer Aerosol Sampler (NAS 3089),<sup>[20]</sup> has been recently developed by TSI, in order to sample submicron aerosols directly on Transmission Electron Microscope (TEM) grids. Due to its design, this device is especially suited to particles with a diameter lower than 100 nm but modification is possible to extend this size range.

##### 5.2.3.1.1.3 Filtration sampling (FS)

The last approach for aerosol sampling, in order to analyse particle morphology, is based on filtration. This method is similar to the gravimetric method presented in 5.6.2. The major difference is the sampling medium, which is, in this case, a “nucleopore” membrane composed of polycarbonate. In use, the nucleopore membrane is placed inside a filter housing and a sampling period is chosen such that the number concentration of particles can be measured before aggregation of particles occurs at the surface of the membrane. After sampling a carbon film is applied to the surface of the membrane then the “nucleopore” filter is dissolved by a flow of chloroform in order to transfer the particles on a TEM grid. Spurny<sup>[21]</sup> describes this method.

The main advantage of this method is its capability of measuring a wide range of particle sizes. With different pore-sized filters, nanoparticles (<0,1 µm) or large particles (>10 µm) can be sampled using the same method. The main disadvantage of this procedure is the post-treatment of the “nucleopore” filter. In contrast with thermophoretic or electrostatic precipitators, the method is based on carbon film deposition/chloroform dissolution, which may in certain cases modify the morphology of the studied particles.

#### 5.2.3.1.2 Transmission Electron Microscopy (TEM) Image analysis procedure

After sampling a combustion aerosol, a large number of TEM micrographs must be retrieved in order to be representative of the global population of combustion aerosol. Primary particle diameter  $D_{pp}$  is determined directly on TEM micrographs and calibrated polystyrene sphere latex (PSL) is used in order

to calibrate the micrograph pixels to a nanometer scale Then grey-levels micrographs are converted to binary format for image analysis:

- a) The primary particle surface  $S_{pp}$  is determined using its diameter,
- b) The number of pixels composing the particles is determined and brings the 2D-projected pixel surface of the aggregate  $S_{ag\ 2D}$ ,
- c) The 2D-projected number of primary particles which compose the particles is then computed using the previously determined surfaces of the primary particle and of the aggregate;

$$N_{pp\ 2D} = \frac{S_{ag\ 2D}}{S_{pp}}$$

- d) The 3D number of primary particles is then computed using an empirical relation:[22][23][24]

$$N_{pp3D} = k_a \cdot N_{pp2D}^\alpha$$

where  $k_a$  and  $\alpha$  are empirical, non-dimensional constants, respectively ranging from 1,15 to 1,16 for  $k_a$  and from 1,09 to 1,10 for  $\alpha$ .

- e) The 2D-projected gyration radius  $R_{g\ 2D}$  is computed on the TEM micrograph by meaning the square distance  $r_i$  between the centre of mass of the aggregate and the different primary particle:

$$R_{g\ 2D}^2 = \frac{1}{N_{pp2D}} \cdot \sum_i r_i^2$$

- f) The 3D gyration radius  $R_{g\ 3D}$  is also computed from empirical relationship and using iteration method on  $D_f$ :

$$R_{g\ 3D} = \left( \frac{D_f + 2 \cdot \alpha}{D_f + 2} \right)^{1/2} \cdot R_{g\ 2D}$$

The final results are several experimental sets of  $(N_{pp\ 3D}, R_{g\ 3D})$ , which allow the fractal relation between these two parameters to be established. General representation is on a log-log scale between  $N_{pp}$  and the ratio  $D_g/D_{pp}$ . In this case the slope of the linear regression applied to experimental results is the fractal dimension  $D_f$  and the intercept is the logarithm of the prefactor  $k_f$ . An example of experimental result is presented on [Figure 2](#), where the fractal dimension is 1,85, and the fractal prefactor is 2,32.

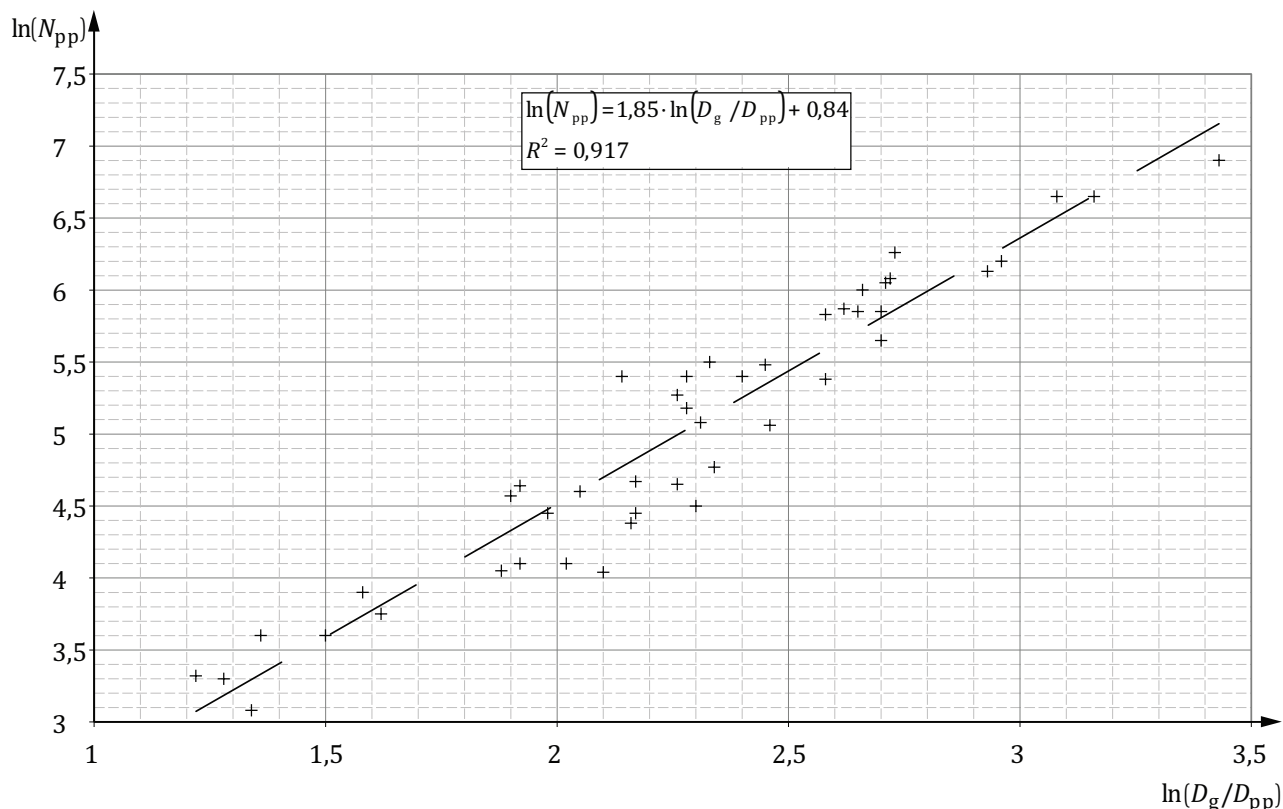


Figure 2 — General representation between  $N_{pp}$  and the ratio  $D_g/D_{pp}$

Similar analysis can be performed by other microscopy techniques. One can cite Atomic Force Microscopy (AFM) as suitable for nanometric particles. This technique allows knowledge of 3D parameters, where TEM allows only enables determination of 2-D projections. The third dimension allows direct determination of the 3D gyration radius,  $R_{g\ 3D}$ , and the 3D number of primary particles.

### 5.2.3.2 DMA-ELPI serial analysis

TEM analysis of combustion aerosols is a powerful but time consuming method of determination of morphology. One way is a comparison of the response of an Electrical Low Pressure Impactor to a monodispersed mobility diameter soot particle classified using a Differential Mobility Analyser.<sup>[25]</sup> The first technique, the ELPI, provides a measure of number distribution in terms of aerodynamical diameter, while the DMA describes a monodispersed aerosol in terms of electrical mobility diameter. A sketch of the experimental device is detailed on [Figure 3](#).<sup>[25]</sup>

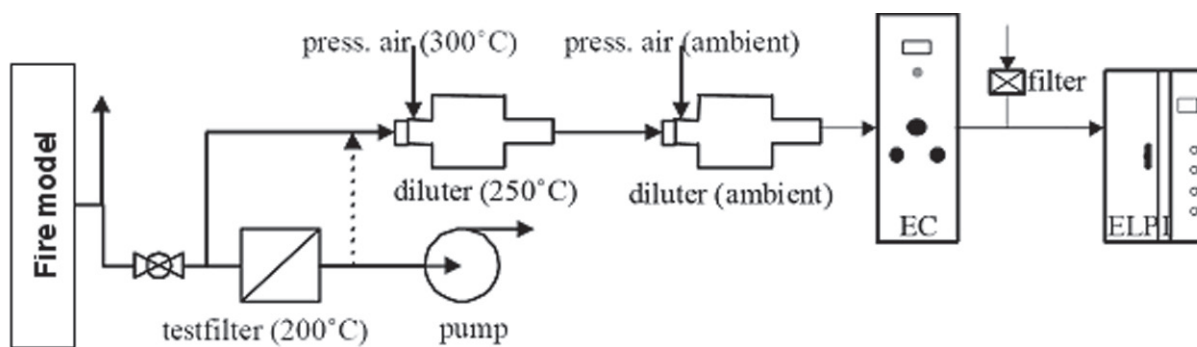


Figure 3 — Experimental device for DMA-ELPI morphology analysis



In the transition regime (particle diameter similar to the mean free path of the molecule of the gas), the aerodynamic and electrical mobility diameters of fractal aggregates are defined as follow:

$$\frac{D_a}{D_{pp}} \propto \left( \frac{D_{m,trans}}{D_{pp}} \right)^{\frac{D_f - \alpha'}{3 - \alpha'}}$$

where

$$\alpha' \text{ is defined as } C_c \propto \left( \frac{2\lambda}{D_p} \right)^{\alpha' - 1}$$

Then the fractal dimension can be retrieved by several ELPI measurements of DMA classified combustion particles. An example of  $\log(D_a) = f(\log(D_m))$  function is presented in [Figure 4](#). The slope of this relationship is proportional to the fractal dimension and the  $\alpha'$  constant. In this case  $\alpha' = 1,83$  yields a fractal dimension of 2,4, in good agreement with previous measurements.

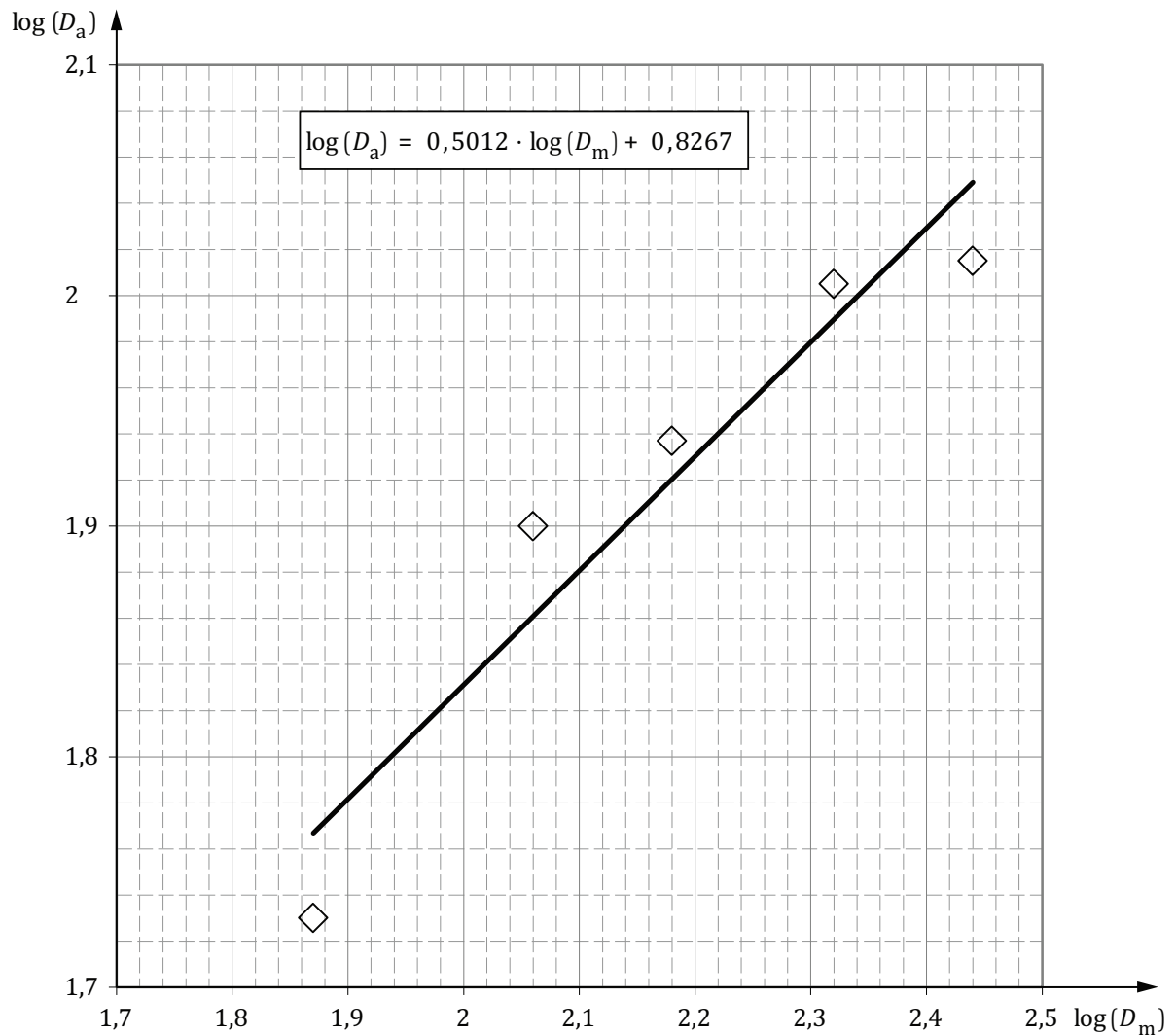


**Figure 4 — Calculation of fractal dimension by DMA-ELPI serial analysis**

This second approach of measurement of the fractal dimension has an advantage, in that it allows measurement in quasi real-time. This direct method allows determination of fractal dimension at various times during a fire. It must be noted, however, that this procedure is based on a set of theoretical hypotheses, which is currently the subject of debate.<sup>[1]</sup>

## 5.2.4 Chemical measurements

### 5.2.4.1 Chemical nature of aerosols

Following an appropriate sampling procedure (see above for sampling techniques), aerosols can be characterized chemically. An important factor in chemical analysis of aerosol particles or droplets is the nature of the surface on which the aerosols have been collected (e.g. a filter). When granulometric analysis indicates the presence of a polydispersed aerosol, it is important to appreciate that the various granulometric size ranges may each have a different chemical nature. It is therefore necessary in these cases to carry out a particle or droplet size range determination.

Some combustible materials or products can contain mineral-based fillers or other additives that can be present in the aerosols generated in a fire. Examples are titanium oxides, aluminium trioxides and clays. Characterization by X-Ray fluorescence and X-Ray scattering of collection filters allow a qualitative and semiquantitative analysis respectively of elements and crystal structures present at the surface of the collection. Analysis of metals in aerosols can be carried out by the use of selective solvents on the trapping filter followed by treatment with acid, for example, Regal solution or sulphuric acid. The resulting solution can be analysed by ion liquid chromatography, inductively coupled plasma (ICP), or atomic absorption. In all these cases, quantitative analysis is possible. It is important to note that metals can be reduced or oxidized in a flame, resulting in compounds that cannot be measured by this technique.

For all these techniques, when a filter is used for sampling, a “blank” analysis of the filter is essential. Other compounds can be analysed on the basis of a knowledge of the likely combustion products from a fire. However, this can be difficult, as these products may be different from those expected from the nature of the fuels, due to the combustion conditions and other interactions.

### 5.2.4.2 Analysis of adsorbed gas products

Many gaseous products can be adsorbed onto soot aerosols. In particular, carbon aerosols can have a structure and surface properties close to those of activated charcoal, which is a commercial gas adsorbing product. Adsorbed species on aerosols can be transported, for example, into the lung thereby increasing their physiological effects. Many adsorbed species can be desorbed and analysed individually, using either the liquid phase or gas phase methods.

[Table 2](#) summarizes a range of typical desorption and subsequent analysis techniques. It is also important to note that the methods are used for adsorbed gases which have a strong ionic or electrostatic bonds at a molecular level. Those species with covalent chemical bonds cannot be desorbed with these techniques. Following sampling, the host materials (e.g. filter pads) can be washed with a solvent, and the adsorbed gas species can thus be extracted in the liquid phase (solid-liquid extraction). The analysis of products trapped in liquid solvents can provide information on many adsorbed species originally trapped on the aerosol. Appropriate selections of the extraction solvent and choice of analytical technique are vital. Liquid-phase techniques are, in general, suitable for such purposes and also presented in [Table 2](#). References [\[26\]](#) and [\[90\]](#) give full details on some of these analytical techniques.



**Table 2 — Analysis of some gases trapped in carbon aerosols**

Trapped species	Desorption liquid	Analyzed species	Analytical technique
SO <sub>2</sub>	H <sub>2</sub> O + 3 % H <sub>2</sub> O <sub>2</sub>	SO <sub>4</sub> <sup>2-</sup>	HPIC
HCl, HBr	H <sub>2</sub> O	Cl <sup>-</sup> , Br <sup>-</sup>	HPIC, Titrimetry
HF	NaOH 1 M	F <sup>-</sup>	HPIC, ISE
HCN	NaOH 0,1 M	CN <sup>-</sup>	HPIC, Spectrocolorimetry
Organic compounds	CS <sub>2</sub>	Same in liquid phase	GC-MS, GC-FID

Some compounds can also be extracted by thermal desorption (TSA) or pressure desorption (PSA) and analysed in the gas phase. This technique is appropriate for organic compounds such as aliphatic and aromatic hydrocarbons, aldehydes and ketones, with carbon numbers up to 20. Common techniques used for the analysis are gas chromatography coupled with flame-ionization detector (GC-FID) or coupled with mass-spectrometry (GC-MS). [Annex B](#) presents information on the quantity of adsorbed gases that can be transported by an aerosol.

### 5.3 Initial considerations for sampling and analysis of aerosols

#### 5.3.1 Considerations for selecting a measurement device

The first consideration is whether the measurement will be “in-situ” or from samples extracted from the flame or fire effluent. In making this choice, it is critical to ensure that the method will be sufficiently non-intrusive to enable representative data to be obtained. The choice then dictates the type of measurement device or devices which can be used. *In situ* measurements are often based on optical principles and in are, in general, non-intrusive. They give time-dependent information integrated over a fixed light path. Extractive methods are intrusive and are more likely to affect the retention of the nature of the sampled aerosol.

The second consideration is whether the desired data are in the form of a concentration determination and/or size distribution.

The third consideration is the expected range of interest of the granulometric distribution of the aerosol. For example, devices designed to trap nanoaerosols are completely different and inappropriate for trapping more conventional aerosols.

The fourth consideration is the desired degree of time resolution, i.e. the time interval over which each measurement is to be made. A single optical measurement can be made in a fraction of a second. Thus, many measurements are needed to characterize the effluent over the duration of a fire. For extractive methods, such factors as the sampling volume, aerosol dilution, and the maximum aerosol mass capable of being trapped are factors that will affect the time resolution.

#### 5.3.2 Considerations for interpreting the measurements

There are additional measurements that must be measured close to the aerosol measurement point location(s). These include the fire effluent temperature, relative humidity, velocity and dynamic pressure, flow of smoke at the measurement point, and possibly the gas composition of the effluent. With such data, it is possible to establish oxygen and carbon balances for the fuels if the elemental composition of the fuel is known.

Careful and appropriate selection of materials used for sampling lines and the chemical properties of trapping substrates (including filters) is essential. These may differ from the materials used in other areas of aerosol measurement. For example, the materials used in fire effluent sampling must be resistant to “aggressive” acidic compounds. Another consideration in the selection of materials is the possible heating of the entire sampling train to avoid condensation of effluent vapours. Any cool point

could further agglomerate aerosols. Care must also be taken to ensure such sampling systems are leak-free and where losses are inevitable these should be quantified where possible. The concepts of limits of quantification and limits of detection are equally applicable to aerosols as they are for gases.

## 5.4 Selection of methods

The particle or droplet size range applicable to commonly used measurement techniques is given below in [Figure 5](#). [Table 3](#), following [Figure 5](#), summarizes the main measurement techniques used to measure aerosols in fire, with some of their important characteristics.

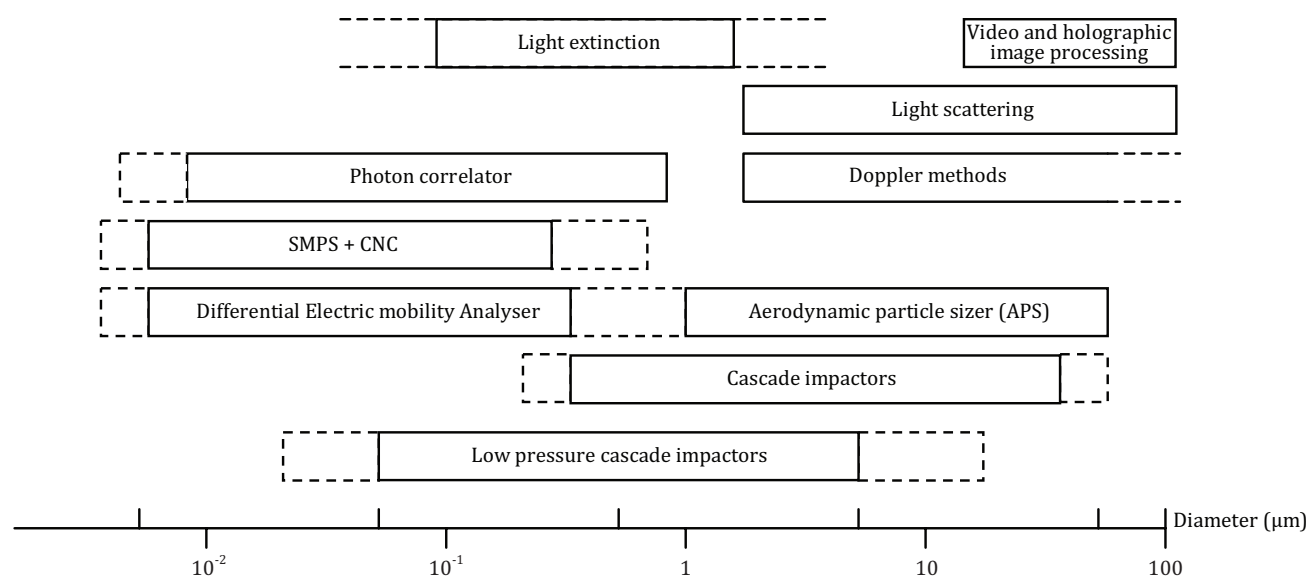


**Figure 5 — Size range of the most common aerosol measurement techniques**

**Table 3 — Summary of techniques for measurement of fire aerosols**

Principle	Kind of method	Information provided	Usage	Diameter range (μm)	Resolution	Max conc.	Ease of usage <sup>a</sup>	Ease of interpretation
Light extinction	In situ, Non intrusive Time-dependent	Extinction coefficient, Soot concentration and soot yield	Modelling, Regulation	0,1 – 1	NA	Not limited	+++	+++
Light scattering	In situ, Non intrusive Time-dependent	Extinction coefficient, particles size distribution	Modelling	> 1	NA	Limited by signal	++	++
Microphotography / ombroscopy	In situ, Non intrusive Time-dependent	Soot concentration and size distribution	-	>5	-	Low concentrations	++	+
Holography	In situ, Non intrusive Time-dependent	Soot concentration and size distribution	-	>10	-	Low concentrations	++	+
Photon correlation spectrometry	In situ, Non intrusive Time-dependent	Soot concentration and size distribution	Research	0,01-1	-	Low concentrations	+	+
Doppler method	In situ, Non intrusive Time-dependent	Soot concentration and size distribution	Research	>1	-	Low concentrations	+	+
<sup>a</sup> Flexibility, to use on different fire models. <sup>b</sup> Standard cascade impactors. <sup>c</sup> Low-pressure impactors (DLPI).								

Table 3 (continued)

Principle	Kind of method	Information provided	Usage	Diameter range (µm)	Resolution	Max conc.	Ease of usage <sup>a</sup>	Ease of interpretation
Direct gravimetric method	Extractive, integrated	Soot main concentration and soot yield	Comparisons, Modelling	Total	NA	Limited by device	+++	+++
Cascade impactor	Extractive, integrated	Granulometric distribution (aerodynamic diameter)	Toxicity	0,3 – 30 <sup>b</sup> 0,02 – 30 <sup>c</sup>	+	0,1 – 1g	++	++
Electrical low pressure cascade impactor (ELPI)	Extractive, time-dependent	Granulometric distribution (aerodynamic diameter)	Toxicity	0,02 – 30	+	0,1 – 1g	+	++
Tapered Element Oscillating Microbalance (TEOM)	Extractive, time-dependent	Soot yield at a given cut-off size	Regulation	0,5 - 100	NA	-	+++	+
Crystal vibration frequency	Extractive, time-dependent	Soot yield at a given cut-off size	Regulation	0,5 - 100	NA	-	+++	+
Scanning mobility Particle Sizer (SMPS)	Extractive, time-dependent	Granulometric distribution (electric diameter)	Research, Nanoaerosols	0,01 - 1	+++	-	+++	++
Engine Exhaust Particle Sizer (EEPS-FMPS)	Extractive, time-dependent	Granulometric distribution (electric diameter)	Research, Nanoaerosols	0,005-0,56	++	-	++	+
Aerodynamic Particles Sizer (APS)	Extractive method, time-dependent	Granulometric distribution (aerodynamic diameter)	Research	0,5 - 20	++	< 1000 part/cm <sup>3</sup>	+++	++
<sup>a</sup> Flexibility, to use on different fire models. <sup>b</sup> Standard cascade impactors. <sup>c</sup> Low-pressure impactors (DLPI).								

## 5.5 In situ measurement methods

### 5.5.1 General

*In situ* measurement methods are based on optical techniques such as light extinction (photometry), laser scattering, or image processing. Traditionally, these measurements are made through windows in the apparatus in order to separate smoke from the delicate optics. However, during a test, soot can be deposited on the windows, resulting in baseline drift. This requires post-test corrections to the optical data. More recently, windowless design has become possible due to the availability of very small diameter laser light sources. To avoid particle deposition on the optics, a very small hole is drilled in the apparatus wall; and long, narrow lightbeam tubes are affixed to the exterior. Especially if the inside of the apparatus is at negative pressure with respect to the room outside, there is minimal leakage of the effluent. Any particles will deposit on the tube walls instead of on the optics further out from the duct.

### 5.5.2 Light extinction (photometry)

#### 5.5.2.1 Principle

Measurement of both light extinction and light scattering allows the determination of some geometrical parameters of aerosols such as the number of primary particles, *N*, the component particles in aggregates as defined in [Figure 1](#), and the diameter of primary particles.

As with light transmission measurements, light scattering in the beam is compared with the light scattering in the absence of smoke by using a reference gas (often helium) with a low scattering cross

section. If smoke enters the optical path between the light source and the detector, part of the luminous flux is lost under the influence of several phenomena:

- The direct absorption of the light beam through the soot particles simply physically blocking the light path. This occurs with particles of a size between a few micrometers to a few millimetres.
- The diffraction or scattering of the light beam on the small particles and soot that have a size comparable to the wavelength of the diffracted beam.
- The spectral absorption by coloured gases which have absorption bands in the spectrum of the light beam.

The value measured depends on the mass concentration of smoke and on the intrinsic characteristics of smoke, mainly its extinction coefficient, but also its geometrical characteristics. The wavelength of the light beam is important and will influence the measurements. There are two types of light sources for the “opacimeters” available on the market:

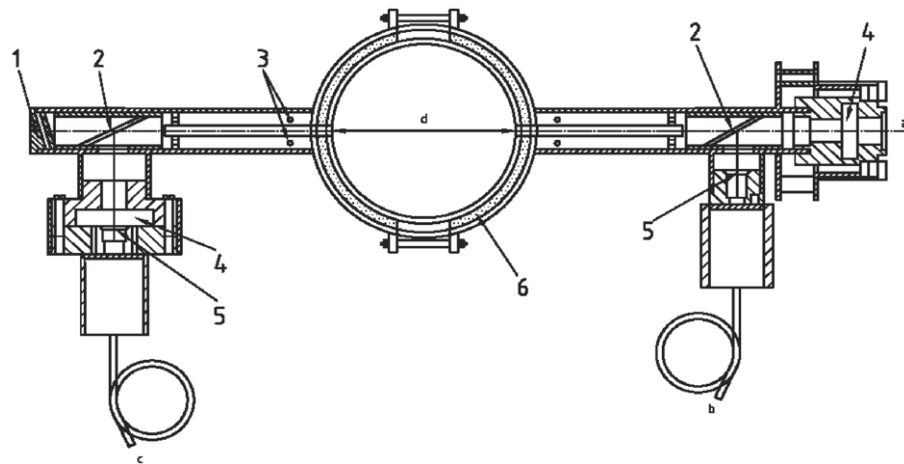
- Monochromatic lasers, which illuminate with one single wavelength (e.g. 350 nm or 632 nm, for He-Ne lasers).
- Polychromatic sources, typically white light, which are closer in spectral content to normal ambient light, but do not allow an exact use of the Beer-Lambert law. Rasbash and Phillips<sup>[27]</sup> indicated that one stable source of white light working at a colour temperature of  $(2900 \pm 100)$  K can be provided by a stabilized voltage supply.

When using a polychromatic light source, the choice of detector is also important. Different detectors will be sensitive to different wavelengths of light. In addition, the detectors vary in their response time. Those based on a selenium oxide photocell tend to have a relatively slow response time and are suitable for slowly changing events. Those based on a silicon photodiode has a preferential sensitivity to red and near infrared radiation up to 1100 nm wavelength and have fast response time, particularly suitable for detecting fast moving or changing transients in a more dynamic situation such as chimney stacks. Note that the scattering properties of light are wavelength dependent, so measurements with He-Ne lasers need to be corrected for direct comparison to scattering measured with a white light source.

### 5.5.2.2 Method description

#### 5.5.2.2.1 Experimental aspects

[Figure 6](#) shows an example of a stack-mounted light extinction system. The system is that used in ISO 5660-2. It consists of a He-Ne laser beam as light source and two detectors, one for measurement of attenuation and one for compensation. This kind of system is frequently used in fire laboratories.



#### Key

- 1 Cap
- 2 Beam splitter
- 3 Purge air orifices
- 4 Filter slot
- 5 Opal glass
- 6 Ceramic fibre packing

**Figure 6 — Example of stack-mounted light extinction system (ISO 5660-2)**

Before use, the system can be calibrated using filters of known light attenuation at the wavelength of the source. The parameters measured are described below.

#### 5.5.2.3 Parameters measured

**5.5.2.3.1** Extinction coefficient ( $k$ ). This parameter is obtained continuously during a test. The integration of this parameter represents the total opacity produced during the fire test.

**5.5.2.3.2** Mass of soot particles per gaseous volume. This parameter is obtained by post-processing after the test. It provides the opportunity to determine the soot yield as a function of time.

**5.5.2.3.3** Specific Extinction Area (SEA). This parameter is defined as the ratio of the extinction area of smoke to the mass loss of the specimen that is associated with the production of that smoke (ISO 5660-2).

#### 5.5.2.4 Advantages and disadvantages

The advantages of the technique are principally that it provides a dynamic measurement with low response time and that it is non-intrusive. The technique is easy to use, and is often present in general fire test laboratories and for many fire test standards the results are sometimes used directly in regulations (transportation especially). The apparatus is relatively inexpensive, simple to maintain and calibrate, and does not require a high level of skill to operate.

The principal disadvantage is that only total aerosol data are obtained, without information on any granulometric aspects. The technique is subject to some interference when used for particles, especially those listed below:

- Light emission from the fire, if it is too close to the experimental device, can distort the measurement made by the detector by overvaluing the luminous transmission reaching the detector.

- Gases, especially NO<sub>2</sub>, can absorb light. White light used as described does not give accurate measurement when the data are interpreted using the Beer/Lambert law equation.
- Scattering or diffraction methods using monochromatic illumination have the potential for large errors when the wavelength of the light source is comparable to the particle sizes.
- If the optical system contains windows, measurements can be affected by soot deposit during measurement.

Data available on the accuracy of these methods indicate a repeatability of SEA over 20 % ( $r = 28,83 \pm 0,14 \times \text{SEA}$ ) and a reproducibility on SEA over 90 % ( $R = 15,03 \pm 0,56 \times \text{SEA}$ ), as stated in ISO 5660-2. SEA is proportional to the total mass concentration of the aerosol. There are no data available on bias of the measurement technique.

### 5.5.2.5 Applications

A monochromatic source is prescribed in the tests carried out to conform with ISO 5660-2. A polychromatic source is prescribed in the tests carried out to conform with ISO 21367 or ISO 5659-2.

## 5.5.3 Laser scattering

### 5.5.3.1 Principle

When a laser beam is passed through an aerosol the beam will be scattered. A scattering coefficient is measured in a fixed direction and the following relationship applies:

$$I^{\text{sca}}(\theta) = I_0 K^{\text{sca}}(\theta) V_C \Delta\Omega$$

where

$I^{\text{sca}}(\theta)$  is the flux of the scattered beam

$V_C$  is the volume of the cell

$\Delta\Omega$  is the solid angle between the beam and the detector.

$V_C$  and  $\Delta\Omega$  are difficult to obtain and in practice they are determined by using a reference gas of known scattering characteristics:

$$I_{\text{RG}}^{\text{sca}}(\theta) = I_0 K_{\text{RG}}^{\text{sca}}(\theta) V_C \Delta\Omega$$

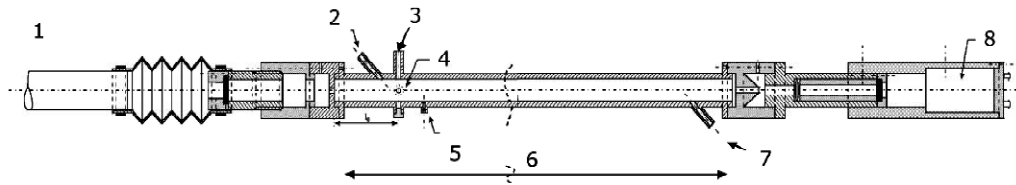
Moreover, aerosol scattering laser beam measurements are frequently obtained by using a polarized beam. The formula is then:

$$\frac{I_{\text{vv}}(\theta)}{I_{\text{vv}}^G(\theta)} = \frac{K_{\text{vv}}(\theta)}{K_{\text{vv}}^G(\theta)}$$

The subscript vv denotes the polarization state vv, where the polarization is orthogonal to the scattering plane. Note that the scattering angle  $\theta = 90^\circ$  is a value often chosen experimentally for practical reasons, although some apparatus allow these scattering measurements over a range of angles using a rotating detector.

### 5.5.3.2 Method description

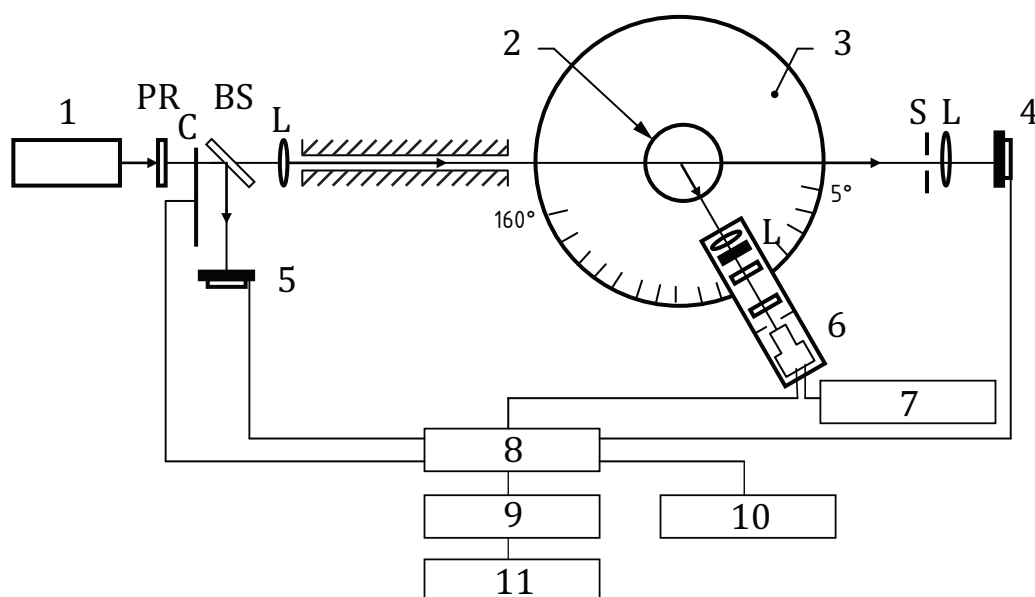
Figures 7 a) and 7 b) show a typical example of a stack-mounted light extinction and scattering system. It uses a He-Ne laser beam as a light source and two detectors for measurement of attenuation and for compensation. This kind of system is frequently used in fire research laboratories.



a) Example of extinction scattering (at 90°) measurement system bench<sup>[12]</sup>

#### Key

- 1 Laser beam (He-Ne)
- 2 Aerosol outlet
- 3 Photodetector for scattering measurement in the parallel scattering plane
- 4 Photodetector for scattering measurement in the perpendicular scattering plane
- 5 Pressure drop
- 6 Optical path
- 7 Aerosol inlet
- 8 Photodetector for extinction measurement



**b) Example of scattering measurement system bench with a rotating detector platform<sup>[13]</sup>**

**Key**

1	Ar* laser	PR	Polarizer
2	Hood exit	C	Comparator
3	Rotating platform	BS	Beam splitter
4	Detector	L	Lense
5	Detector	S	Diaphragm
6	Photomultiplier tube		
7	High-voltage supply		
8	Lock-in amplifier		
9	A-D converter		
10	Oscilloscope		
11	Computer		

**Figure 7**

### 5.5.3.3 Parameters obtained

**5.5.3.3.1** Particle concentration and particle or aerosol diameter. These parameters are determined with both extinction and scattering coefficients measurements for a given refractive index value.

**5.5.3.3.2** Refractive index. This parameter can be determined using inversion methods from both extinction and scattering coefficients measurements.

### 5.5.3.4 Advantages and disadvantages

Coupling these measurements with granulometric measurements allows the use of an inversion technique to determine refractive index of aerosols by taking into account the fractal shape of the aerosol.

Light scattering measurements are more difficult than extinction measurements because of the small values against a relatively high “noise” signal and because the scattering angles must be fixed.



### 5.5.3.5 Applications

Few applications are found in industry.

### 5.5.4 Other *in situ* measurement methods

Other *in situ* methods are all based on optical principles. The main techniques cited in the published literature are:

- Microphotography and ombroscopy (a light reflecting technique which can scan the particles thereby allowing a better visualization of their shape). These techniques rely on the light sensitivity characteristics of video recorders and the resolution of their CCD sensors. They are commonly limited to aerosols bigger than 5 µm.

Holography. This technique allows measurements with a high depth of field – i.e. a three dimensional visualization. It is carried out in two steps: The first step is the generation of a hologram using established techniques which illuminate the particles with pulsed laser light and record many facets of the particle on a single photographic plate. The second step is the restitution of the particle image in three dimensions and analysis of the image. The technique is time-consuming, complex, and limited by the granulometric minimum size of particles and difficulty in adapting to low concentrations of aerosols. There is a size limitation related to the optical path length by the relation  $D_p^2 > \lambda_0 l$ , where  $\lambda_0$  is the wavelength of the laser and  $l$  is the length between the sensitive plate and the particle during the image-saving step. In common installations, it is limited to particles larger than 10 µm.

- Doppler velocimetry. Light diffused by a moving particle is analysed by a detector, which records the frequency shift due to the particle's velocity and direction of travel with respect of the detector. The main Doppler technique used is the Phase Doppler Anemometry (PDA) technique. Interpretation of such a technique is complex. Details are available in the literature.[\[28\]](#)[\[29\]](#)
- Photon correlation spectroscopy.[\[30\]](#) For submicron aerosols, the intensity fluctuations of diffused light is related to the Brownian motion (i.e. the motion caused by collision with molecules) of the aerosol particles. This technique can work in extreme conditions of temperature or pressure. Nevertheless, it has only been adapted for use with monodispersed aerosols. Research is currently in progress to extend its use to polydispersed aerosols.
- Laser induced incandescence (LII). LII is an optical method which allows getting an image of the soot volume fraction in one or two dimensions by measuring the increased Planck radiation due to incandescence, when the soot is heated by laser radiation. The LII signal is approximately proportional to the soot volume fraction. LII can additionally be used for measuring the soot particle size by determining the decay of the LII signal. Smaller particles cool faster and thus have a shorter LII decay time. Practical applications have been demonstrated. There are disadvantages in that LII is a line-of-sight technique and that there is a need to suppress the luminosity of the background.

## 5.6 Extractive measurement methods

### 5.6.1 Sampling methods

The principal challenge with aerosol sampling is to maintain a faithful representation of the particles throughout the sampling process before detection. In particular, the aerosols in fire effluents are typically present in conditions of high temperature, moisture and pressure, which are very different from the working conditions of the detector systems.

An important constraint comes from the requirements for sampling rate. This constraint is characterized using  $R$ , the ratio of the sampling velocity to the velocity of the particles. For greatest accuracy, the sampling velocity should be identical to the velocity of the particles being sampled. This is known as "isokinetic" sampling. If  $R$  is greater than unity (i.e. the sampling velocity is greater than the original velocity of the particles being sampled), the results will be distorted by the inclusion of heavier particles in the sample. If  $R$  is less than unity, the reverse will apply (i.e. heavier particles could be missed from

the sample). Sampling velocities lower or higher than the velocities of the particles in the sampled atmosphere are termed "subkinetic" or "superisokinetic" sampling, respectively. For small particles, the effect is negligible. Effects of subkineticism and superisokineticism are shown in [Figure 8](#).

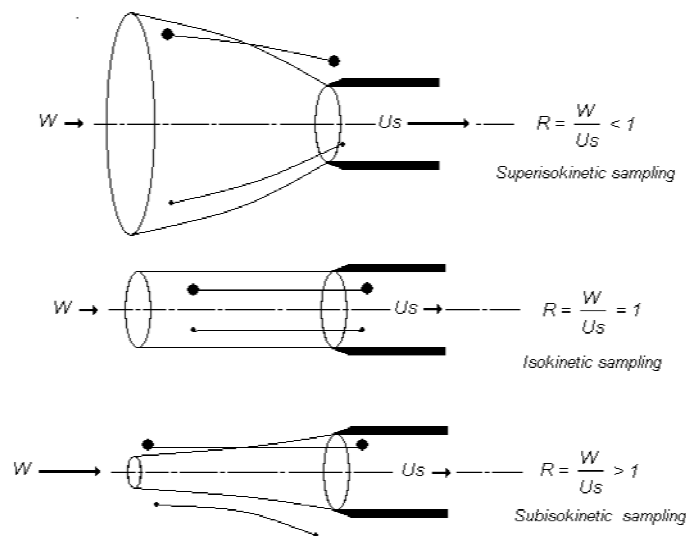


**Figure 8 — Effect of sampling: isokinetic, superisokinetic and subisokinetic [2]**

The problem is therefore to determine the extent to which the extracted sample is representative of the flow or volume from which it is being sampled. This includes how well the aerosol is mixed in the volume being sampled, as well as the character of the sample extraction flow. On the other hand, the particles can undergo coagulation or agglomeration processes within the sampling system that will largely modify their characteristics. Crane and Evans[31] and Pui, Romy-Novas and Liu[32] have studied aerosol transportation efficiency as a function of the geometry of pipes. It has been proved that this efficiency is optimized when bent pipes with a radius curve greater than 4 are used. Transportation efficiency is also function of the Stokes number of the particle, and decreases for high Stokes numbers. The Stokes number is a dimensionless number corresponding to the behaviour of particles suspended in a fluid flow. The Stokes number is defined as the ratio of the stopping distance of a particle to a characteristic dimension of the obstacle.

#### 5.6.1.1 Nozzle and probe

For extractive methods, the characteristics of the sampling nozzle are vital to ensure correct isokinetic sampling. Diameter, geometry, and positioning of the nozzle have to be defined to limit the effect of the nozzle on the movement of particles in the sampled flow. Depending on the fire effluents being studied, it is also essential to ensure that isokineticism is preserved through the duration of the fire. For all these parameters, it must be assumed that the flow is laminar flow, as characterized in terms of the Reynolds Number, a measure of the degree of laminar flow or turbulent flow. If the aerosol measurement probe is inserted into an exhaust duct (for example in ISO 5660-1 or ISO 9705 tests), conservation of a laminar flow has to be ensured during the entire test. Under normal operating velocities in a fire test with a straight exhaust duct, well-mixed flow can be ensured if the nozzle is placed at a distance of at least 10 times the diameter of the duct downstream of any obstructions and five times upstream of any obstructions. If possible, a laminar flow is better than a well-mixed turbulent flow for this purpose.

In fire effluents, knowledge of the temperature and pressure at the sampling point is also an essential parameter for interpretation of results. This requires additional sensors (e.g. thermocouples) to be placed close to the extracting point, but their positioning must be designed to limit perturbations to the effluent flow. In addition, the materials of which the nozzle and probe are constructed must be compatible with the fire effluents, e.g. resistant to corrosion, removable, and washable. Metallic parts must also be electrically grounded to limit electrostatic attraction effects and unwanted depositions. Common materials used for nozzles are stainless steel, borosilicate glass, and quartz.

The nozzle must also ideally be thin and sharp in order to limit perturbations in the main effluent stream. However, there may be mechanical reasons which will limit the thinness of the probe due to the need to have a nozzle “chamfer” which is of sufficient size to remain robust under the fire conditions. It is also necessary to ensure that the uncertainty about the actual sampling area is less than 10 % in order to meet the criteria for isokinetic sampling. To achieve this, it is recommended that a nozzle of inner diameter greater than 6 mm is used. For gas velocities greater than 20 m/s, it is possible to use 4 mm diameter nozzles. To minimize disruptions caused by the hole in the nozzle, the following requirements shall be observed:

- The internal diameter of the nozzle must be consistent over a length of at least one inner diameter and at least 10 mm from the end of the nozzle.
- Any change in the internal diameter must be tapered and have an angle less than 30°.
- Bends are allowed only when they are placed after at least 30 mm of straight section. Their radius of curvature must be at least one and a half times the internal diameter.
- Any changes in the external diameter of the probe and located less than 50 mm to the orifice of the nozzle must be tapered and have an angle of less than 30°.
- No obstructions associated with sampling equipment are to be present upstream of the orifice of the nozzle. Obstructions can be present downstream if they are well over 50 mm from the hole and if the maximum size of the obstacle is one and a half times the probe size.

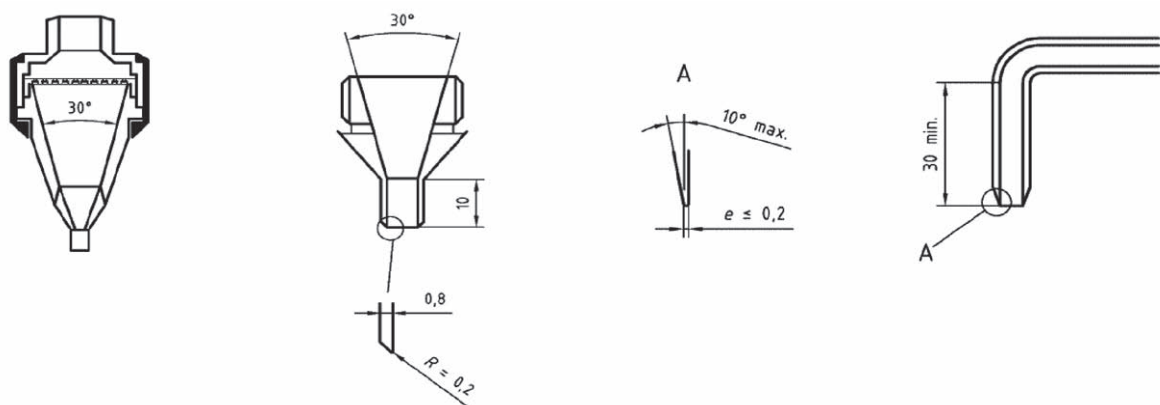


**Figure 9 — Examples of nozzles geometries**

Some probes can be designed to catch the total aerosol, whereas others are adapted to select only the smallest aerosol particles. To limit the size range of aerosols particles sampled, techniques such as “mini-cyclones” or “inertial impactors” can be used.

#### 5.6.1.2 Sampling train and sampling line

The sample path from the nozzle to the measurement device, must be designed to limit variations of the main characteristics of the aerosol particles (e.g. concentration, distribution size and morphology). With this objective, and due to the high humidity of fire effluents, it is essential to use heated devices and sample tubes or pipes. In addition, an important consideration is that aerosols are sensitive to temperature and thermophoresis phenomena. The temperature of the sampling train therefore has to be high enough to limit condensation but low enough to limit its effects on aerosols characteristics. Temperatures between 50 °C and 100 °C are generally used. The pipes must have a smooth polished internal surface, and must be so designed to enable them to be inspected and cleaned regularly. Their compatibility with corrosive effluents from fire must also be considered. Metallic parts have to be linked to an electric ground to limit electrostatic depositions.

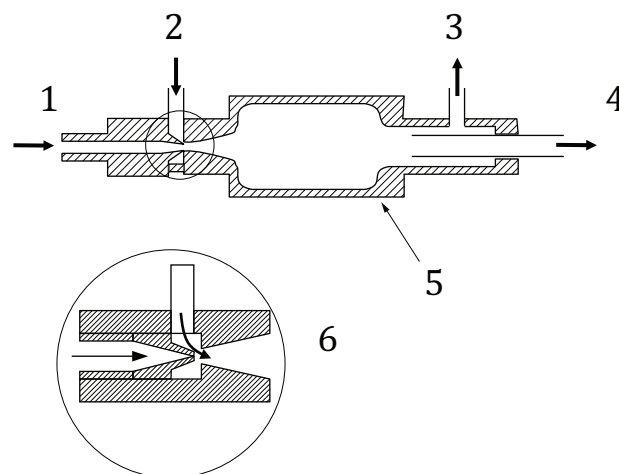
### 5.6.1.3 Dilution

Aerosols produced in combustion generally have a very wide range of characteristics. Furthermore, particle concentration and the temperature and relative humidity of the flow can change radically with time and with position. Depending on the aerosol characteristics, particle distributions may change through coagulation, condensation, and nucleation during sampling. Often, it is advisable to sample as fast as possible to reduce any changes in the morphological properties of the particles and modifications by agglomeration. These latter may require rapid dilution of the sample. The main difficulties occur when sampling a concentrated aerosol which has to be diluted to prevent the above effects occurring and where the aerosols are present in a high temperature environment that is saturated with moisture and condensable vapours. When diluting a sample, therefore, three fundamental parameters have to be considered: the residence time in the sample train, the degree of dilution, and the temperature of the diluted sample.

The influence of residence time is often the most significant and depends on the extraction conditions. During travel through the sampling train, condensation of water and other vapours can occur, depending on the composition of the aerosol and effluent stream. Another phenomenon to consider is coagulation in the sampling lines during extraction. This phenomenon can quickly become important for concentrations of particles higher than  $10^{10}$  particles/cm<sup>3</sup>. This concentration is quickly reached in fire tests, necessitating dilution of the sample.

Specialised instrumentation is available to carry out required dilutions, which is achieved in either one or two stages. A one-stage dilutor consists of an “ejector” which injects aerosol into a coaxial heated mixing chamber [Figure 10 a)]. For a two-stage dilutor [Figure 10 b)], the first dilution stage is achieved using perforated tube technology, which has been proven to be an effective tool in aerosol studies. The dilution ratio and dilution temperature of the first dilution stage are adjustable and controlled. Dilution at the initial sample temperature eliminates the effect of volatile and semi-volatile vapours, while cooled dilution maximizes the effect of nucleation and condensation. The second dilution stage is an ejector diluter as used in a single stage dilutor, but which also acts as the sample pump and returns the sample to ambient temperature. The dilution ratio of the ejector diluter is also controlled and adjustable. Many studies have been carried out to quantify the impact of such dilutions on nucleation, aggregation, or aerosol deposit in these devices.

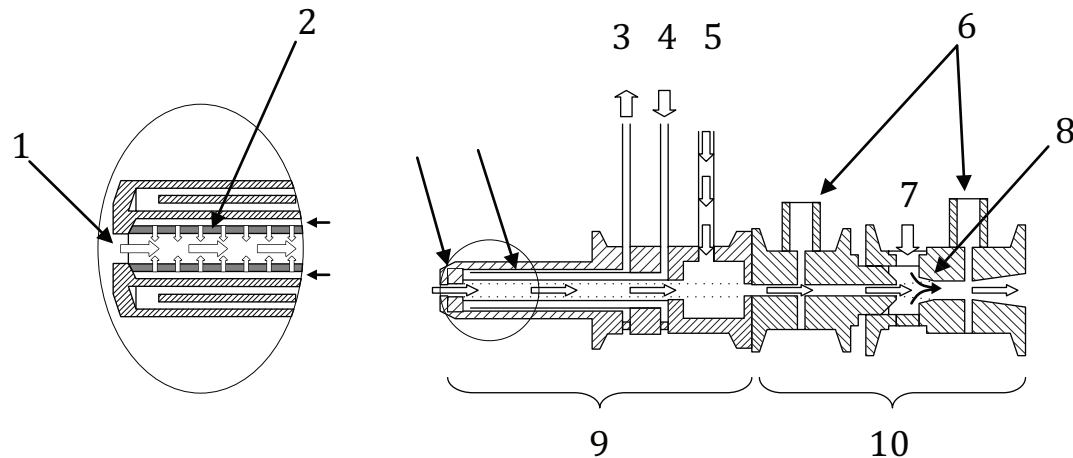
Other dilution devices are available. One can cite the fine particles sampler,[33] heated simple injectors,[34] or rotating disk diluters.[35]



a) One-stage aerosol dilution system

#### Key

1	Sample in	4	Sample out
2	Dilution air	5	Mixing chamber
3	Exhaust air	6	Ejector



b) Two-stage aerosol dilution system

**Key**

1	Aerosol in	6	Pressure sensors
2	Porous tube	7	Dilution air (hot air)
3	Cooling air out	8	Pressure drop
4	Cooling air in (cold air)	9	Primary dilution stage – Porous tube
5	Primary dilution air (hot air)	10	Secondary dilution stage

**Figure 10****5.6.1.4 Sampling quality**

Losses in the sampling and analysis/detection stages should be estimated, although in many cases this will be difficult. It is therefore important to limit as far as possible any changes to the aerosol characteristics. In fire testing, it is therefore important to consider the effect of the design of the test apparatus on the nature of the aerosols produced by the physical fire model used, prior to sampling. For example baffles, plates, and other intrusions used to produce a uniform flow in devices like the ISO 5660-1 or ISO 9705 calorimeters will affect the characteristics of the aerosol fraction generated, particularly the particle size distribution. Orifice plates used to measure flow will also modify aerosol characteristics. Variations in temperature, pressure, and relative humidity and in the dilution of the effluent will all affect the characteristics of the aerosol; and such effects must be taken into account. For other fire models, parameters like coagulation time can become important and the time history of the aerosols may be needed to assist in interpreting the results.

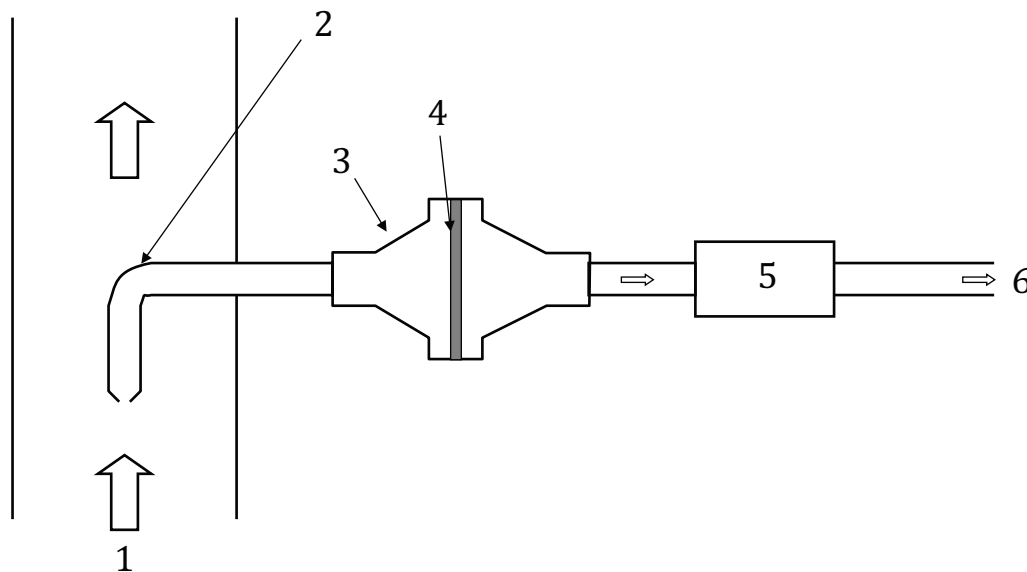
**5.6.2 Direct gravimetric method****5.6.2.1 Principle**

The gravimetric method is relatively simple. The smoke to be analysed is sampled, diluted if necessary, (see [5.6.1](#)), and filtered with a high efficiency filter. The filter is weighed before and after sampling. The mass difference and the ratio between total flow and sampled flow are used to calculate the total soot/aerosol yield.

**5.6.2.2 Method description**

The device consists of a sampling line, a filter holder containing a high-efficiency filter, a mass flowmeter, and a pump. The filter is stored in dry conditions and weighed before a test. After the sample

has been collected, it is removed from the device and dried in a desiccator before being weighed. The mass difference gives the mass quantity of aerosol trapped. For a reliable measurement, the entire sampling line and filter have to be heated at a constant temperature over 80 °C, to prevent water vapour condensation. A mass-flow controller and meter are used to provide a constant flow through the filter. It is very important in this technique to have a sampling flow velocity that is similar to that in the sampled effluent stream. The filter holder must be conically shaped, with angles not exceeding 30°. The filter holder can be placed either directly in the flow of the effluent stream or outside the stream. In the former case, temperature effects on the filter can be important and may limit the choice of filter material. In the latter case, a sampling probe transfers the sample from the duct flow to the filter ([Figure 11](#)), and the recommendations in [5.6.1](#) have to be considered.



#### Key

- 1 Exhaust flow
- 2 Sampling probe
- 3 Filter housing
- 4 High efficiency filter
- 5 Mass flowmeter
- 6 To pump

**Figure 11 — Direct gravimetric method**

#### 5.6.2.3 Parameters produced

The method is a mass concentration method. It provides the “total soot” production. The results can be expressed relative to the flow of effluent (i.e. average mass concentration in  $\text{kg}\cdot\text{m}^{-3}$ ) or relative to the mass of the tested material as a fuel mass loss (i.e. mass of “soot” per mass of fuel in  $\text{kg}/\text{kg}$ ). An additional option is to use the trapped aerosol for further chemical analysis of adsorbed species. See [5.2.4](#) for details on chemical measurements.

#### 5.6.2.4 Advantages and disadvantages

The method is relatively accurate and very easy to use. The main disadvantages are the lack of data on particle distribution size or on kinetics of the deposit.

### 5.6.2.5 Applications

The method is often used in bench-scale tests, especially the cone calorimeter ISO 5660-2 to determine soot yield.

### 5.6.3 Cascade impactors

#### 5.6.3.1 Principle

The equipment most commonly used to study aerosol size distribution is the multistage cascade impactor.<sup>[2][3]</sup> Operation of these devices is based on the inertial properties of particles. The aerosol enters an inlet cone and cascades through succeeding orifice stages with successively higher orifice velocities from the first to the last stage. From each stage, a high velocity is produced which is deviated at 90°. This has the effect of depositing or “impacting” particles that cannot remain in the stream at each stage. The diameters of the orifices decrease from the first stage to the last stage of the impactor, so that particles “unimpacted” at stage N, are accelerated slightly more at stage N+1 toward a new collecting surface, see [Figure 12](#).

The inertia of a particle is a function of three parameters: shape, density and velocity. The shape and the density of a particle are unknown in most cases for a given aerosol. The particle size associated with each stage of the impactor is therefore expressed across an “aerodynamic diameter,” which encompasses these two latter parameters. The density of the particle is therefore considered to be equal to unity, and the information that characterizes particles is linked to the Mass-Median Aerodynamical Model (MMAD), as defined in [4.3.1](#).

Each stage of the impactor is characterized by a cut-off size, denoted as  $D_{50\%}$ . The cut-off size corresponds to the aerodynamic diameter of particles trapped with an efficiency of 50 % within a given stage. Another way to characterize a stage is through the geometric mean diameter, the square root of the product of the cut-off size of the given stage and the previous stage.



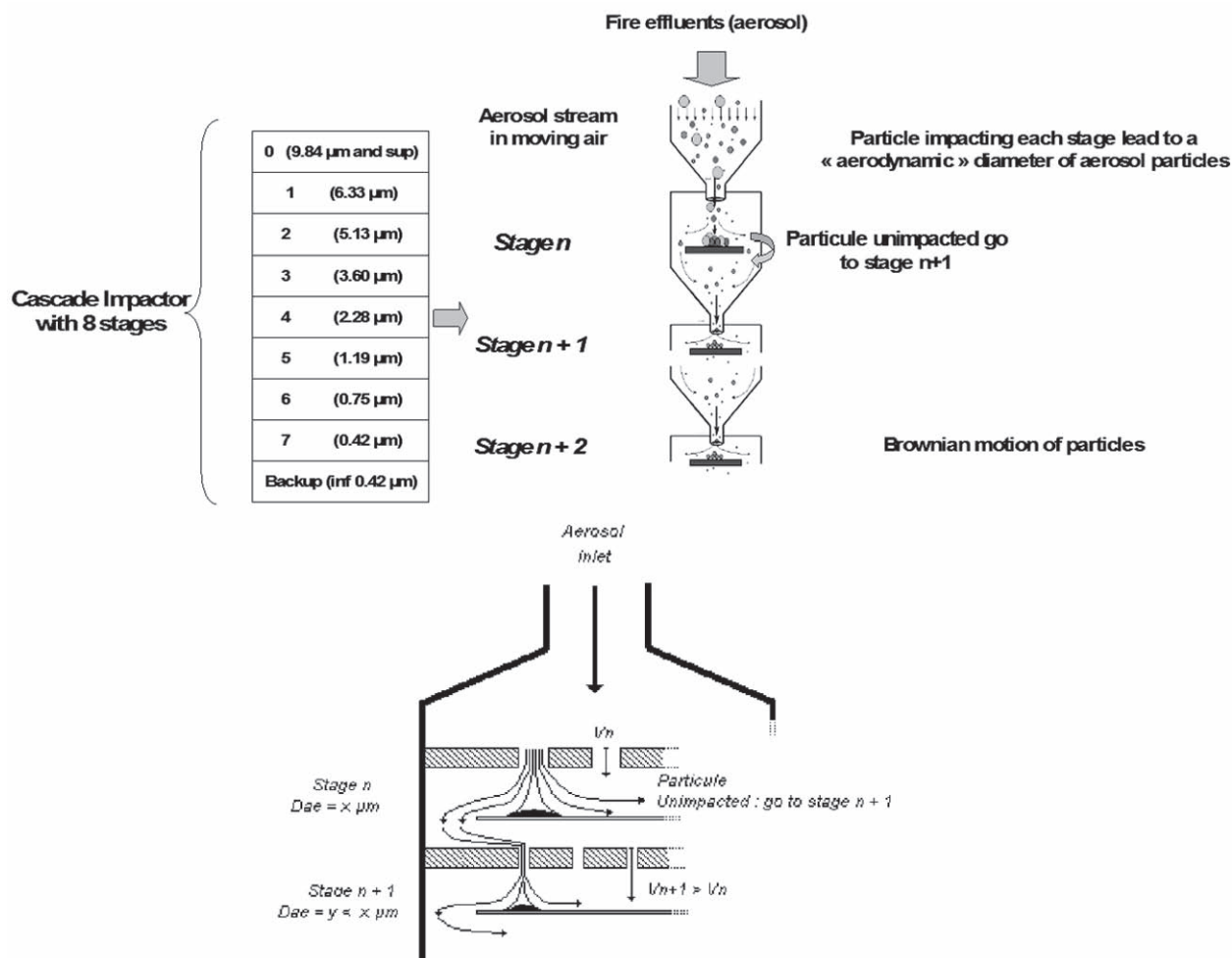


Figure 12 — Cascade impactor and impactor stages

### 5.6.3.2 Method description

In order to obtain the best possible accuracy, the sampling and analysis apparatus must be set up to reduce as nearly as possible the effect of the apparatus on the particle characteristics. Each part of the apparatus can be considered as a potential trap, having its own transmission efficiency. The analytical device itself can be considered to some extent as being potentially capable of modifying the composition of the aerosol.

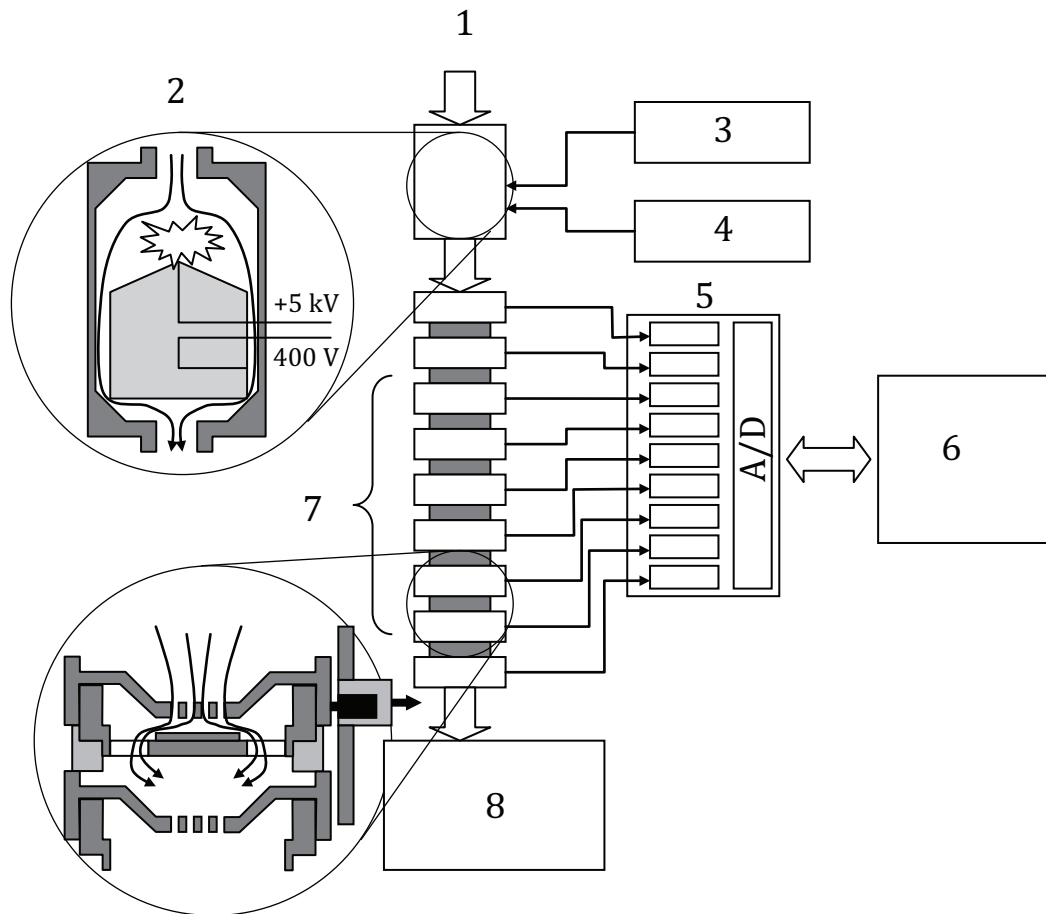
The measurements are normally achieved by collecting the impacting filters after sampling and measuring the weight difference between the start and finish of the collection period. The filters are dried and weighed before a test. After a test, they are removed from the impactor and dried in a dessicator before being weighed a second time. The mass difference gives the mass quantity of aerosol trapped between the stage and the previous stage. As shown above, this interval is characterized using the cut-off diameters of both stages. The final stage is a high-efficiency filter, which collects all particles remaining from the previous stage.

Normal cascade impactors are limited to a range of particle sizes between about 300 nm and 30  $\mu\text{m}$ . To measure smaller sizes, the impactor can be designed so that the pressure in the device is lower than atmospheric. In this case, devices are able to reach sizes from about 20 nm to 30  $\mu\text{m}$ , with typically 12 stages.

For some devices, the particles' number concentration with time can be determined by electrical measurement. Such a device is the Electrical Low Pressure Impactor (ELPI), see [Figure 13](#). Before entering the modified cascade impactor, particles are charged by a high voltage corona discharge. Each



impaction stage is effectively an electrometer, which counts the charges associated with the particles. There is a link between the charge on a particle and its aerodynamical diameter.



#### Key

- 1 Aerosol in
- 2 Coronacharger
- 3 High voltage source
- 4 Ion trap voltage source
- 5 Electrometers
- 6 Computer and control electronics
- 7 Impactors with insulators and contact needles
- 8 Vacuum pump

**Figure 13 — Electrical Low Pressure Impactor (ELPI) principle**

#### 5.6.3.3 Parameters produced

The cascade impactor provides information on total granulometric mass distribution per stage. This allows building a size distribution (7.1). ELPI devices also provide the number size distribution through kinetic measurements. Particles are quantified as a mass / diameter ratio, but the relationships can vary depending on the nature of the aerosol considered.

It is also possible to analyse the individual impactor surfaces after a test. In addition to being characterized by the cut-off diameter of the stage, these particles can be characterized by their morphology and by their chemistry. See 5.2.3 for details on morphological characteristics measurements and 5.2.4 for details on chemical measurements. Valuable information can be obtained from a morphological analysis

or a chemical analysis of the trapped particles to check if the nature of an aerosol is similar for each size range. This information is particularly important for polydispersed aerosols and has significant implications for the toxicity of the aerosol.

#### 5.6.3.4 Advantages and disadvantages

The method allows a relatively simple analysis of granulometric distribution or to enable the separation of the aerosol into its particle fractions. It has been used for many years for measurements in controlled combustion.

The link between impaction characteristics and a particle's diameter must consider the particle's shape model. This is especially important for ELPI devices. This must be considered when interpreting the results.

In a fire test apparatus, such as a calorimeter with effluent collecting hood and duct, the temperature of the effluent will vary at different locations. The variation in temperature has an influence on the isokineticism and modifies the cut-off diameter associated with each stage of the impactor. To limit the impact of temperature variations on the impactor, it is generally heated to a temperature above 80 °C. This heating also limits the condensation of water vapour on the impaction filters. However, use of the impactor under these higher temperature conditions requires a determination of the new cut-off size for each stage. See 6.3 for details.

#### 5.6.3.5 Applications

The method can be used in devices where the effluent is continuously extracted, such as calorimeters at bench-scale (ISO 5660-1, ISO 21367, etc) or large-scale tests (ISO 9705, etc) to determine the aerosol size distribution. In such devices, care has to be taken if baffles or flow stabilizers are present in the exhaust duct because these can modify distribution size by impacting a proportion of the aerosols. Reference [36] presents the design of a modified cone calorimeter exhaust duct to ensure non-impaction before the sampling point.

#### 5.6.4 Tapered Element Oscillating Microbalance (TEOM) and Crystal vibration frequency

The Tapered Element Oscillating Microbalance (TEOM) is mainly used for airborne measurements.[3] It is often equipped with a cyclone sampling system. The TEOM produces a total gravimetric measurement. All of the particles in the aerosol are collected on a vibrating substrate which produces a modification of the vibration frequency (Figure 14). The relation describing TEOM behaviour is thus derived from the equation of the movement of a harmonic oscillator. The oscillation frequency,  $f$ , of the oscillating element can be defined as the resistance,  $K$ , and the mass,  $M$ , of this element:

$$f = \sqrt{\frac{K}{M}}$$

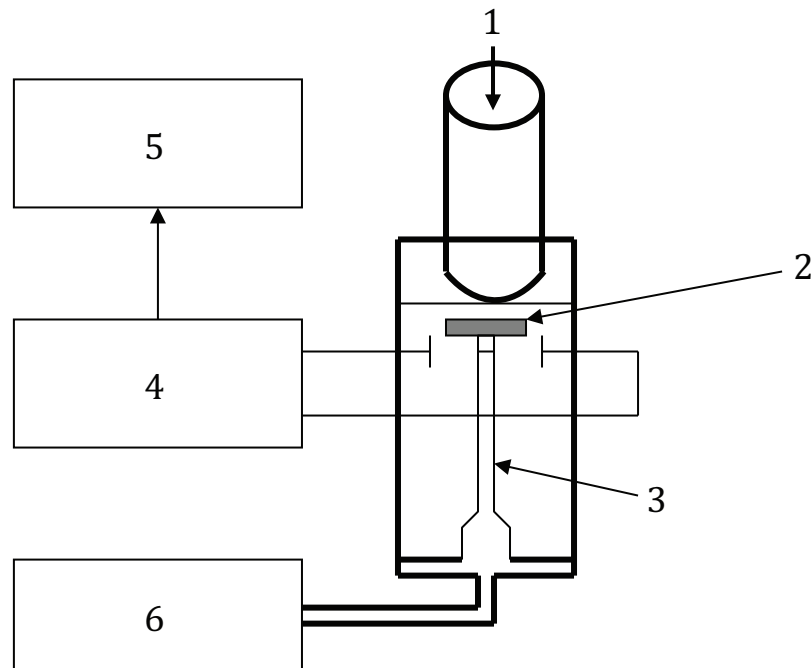
Then, the variation of the mass of the element,  $\Delta m$ , can be described as:

$$\Delta m = K_0 \cdot \left( \frac{1}{f_1^2 - f_0^2} \right)$$

where

$K_0$  is the specific conversion constant of the oscillating element.

$f_0$  and  $f_1$  are the initial and actual oscillating frequency of the element (Hz).

**Key**

- 1 Aerosol in
- 2 Removable collection filter
- 3 Oscillating element
- 4 Oscillation amplifier
- 5 Frequency measurement
- 6 Flow regulator

**Figure 14 — Tapered Element Oscillating Microbalance (TEOM)**

The device provides the total mass of aerosol collected in real time, from the smallest up to about 100  $\mu\text{m}$ . A selection cyclone is commonly used at the input of the device to select the maximum size of particles to be measured.

The Crystal Vibration Frequency device is based on very similar principles. In this case, the oscillating element is replaced by a piezo-electric crystal, which produces oscillations when electrically connected. The presence of particles on the crystal produces a variation of frequency that is linked with the particle's size

## 5.6.5 Scanning Mobility Particle Sizer (SMPS)

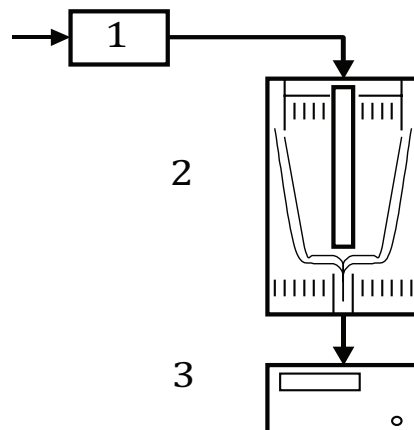
### 5.6.5.1 Principle

This method is mostly applied to measure the particle size distribution of nanoparticles in aerosols. [1][2][3] The SMPS consists of a neutralizer, a diffusion mobility analyser (DMA), and a condensation particle counter (CPC) at continuous flux. The neutralizer ensures entering a neutral aerosol before its ionization. The DMA set up suspended particles in the gas stream following their electric mobility and the CPC downstream detects these pre-selected particles, as seen on [Figure 15](#).

The size distribution of the aerosol is calculated from the number of particles detected by the CPC and the transfer function of the DMA, using an inversion data technique. However, although the SMPS is often considered to be an established technique, there remain a number of uncertainties in its use associated with the measurement of a size distribution, which have not currently been assessed.

### 5.6.5.2 Method description

The neutralized sampled effluent is ionized by a radioactive source, commonly containing  $^{210}\text{Po}$  or  $^{85}\text{Kr}$ . The largest particles are then removed by impaction. This prevents these large particles, which can accumulate more than one charge, from interfering with the measurements. The effluent then enters the DMA, where the aerosols are separated by their electrical mobility in a continuous electrostatic field. The diameter profile of the particles at the outlet is a function of the electrostatic field. Particles selected in this way then enter a condensation particle counter, where they nucleate condensation of a saturated vapour, commonly obtained by heating a liquid pool of butanol across the flow. The butanol vapour condenses to produce droplets of about  $10\text{ }\mu\text{m}$  and these droplets are counted by an optical system. This count is independent of the initial size of particles.



#### Key

- 1 Ionization –  $^{210}\text{Po}$
- 2 DMA classification
- 3 CPC counting

**Figure 15 — Scanning mobility particle sizer (SMPS)**

### 5.6.5.3 Parameters produced

The instrument is designed to measure particle number, size, surface area, and mass of particles and the main result is concentration in particles/ $\text{m}^3$ . One of the important characteristics of these devices is that separation is made on DMA on the basis of electrical diameter of the particles. The method is able to measure in real time particles from  $10\text{ nm}$  to  $1\text{ }\mu\text{m}$ .

For fractal objects like carbon soot, SMPS devices over-estimate the mass and surface area of non-spherical particles. Recent studies<sup>[37]</sup> now allow the inclusion of the fractal nature of soot particles when using a SMPS device.

### 5.6.5.4 Advantages and disadvantages

The main advantage of the SMPS is its resolution and range of measurement, especially for fine particles. The finer the particle, the more important its electric mobility will be.

A major disadvantage of this method is the multiple charge effect. During ionization in the DMA, and depending on its diameter, a particle has a significant probability of acquiring multiple charges (2, 3, or 4). Due to the principle of the SMPS method, the size distribution in terms of mobility diameter is based on the assumption of all particles being singly charged. Any multiple charged particles (especially for particles higher in size than  $150\text{ nm}$  to  $200\text{ nm}$ ) will be erroneously detected with smaller particles having a single charge. A further disadvantage of the SMPS method is the integration time of the system. A SMPS is a scanning device which progressively integrates the particle sizes. A valid size distribution

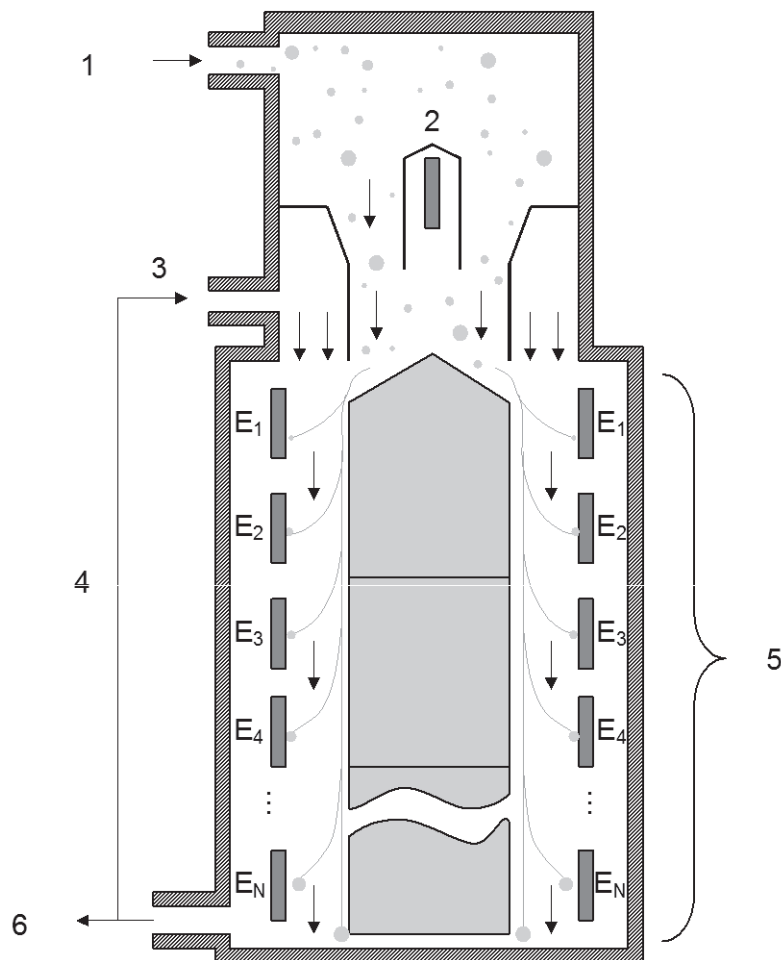
measurement takes at least 30 s. Thus, short-term, transient phenomena (occurring over a second or so) are not integrated using this device. The presence of a radioactive source for ionization results in problems with transportation of the device between organizations.

#### 5.6.6 Engine Exhaust Particle Sizer (EEPS) and Fast Mobility Particle Sizer (FMPS)

The SMPS device described above is particularly suitable for studying the size distribution of particles with a diameter of less than 1  $\mu\text{m}$ . This “granulometer” has been widely used, and the theoretical considerations linking electrical mobility diameter and morphological parameters are available in the literature.<sup>[37]</sup> On the other hand, the major disadvantage of the SMPS is that it does not do real time scanning. Recently, a device has been developed in order to use the physical principle of the DMA, but which allows the real-time measurement of size distribution. This device, named Engine Exhaust Particle Sizer (EEPS), is based on electrostatic precipitation of particles in a similar way to the DMA method.<sup>[1]</sup> The device is also called DMS by some manufacturers.

##### 5.6.6.1 Principle

At the inlet of the EEPS, the aerosol passes through a cyclone impactor with a 0.8  $\mu\text{m}$  cut-off diameter (50 %). Particles are then positively charged to a prescribed level using a unipolar diffusion charger. The charged particles are introduced into the measurement region near a centre column electrode to which a high positive voltage is applied. Positively charged particles are then repelled from the centre column to several electrometers placed on the outer surface of the measurement region. A particle with high electrical mobility (i.e. low electrical mobility diameter) will strike the electrometer at the top of the outer electrometers column while a particle with low electrical mobility (i.e. high electrical mobility diameter) flows through the column and will strike a lower electrometer. The arrangement of multiple electrometers (22 channels) allows real-time measurement of the size distribution using built-in digital signal processing hardware and software. Two designs of this device are available, the EEPS and the FMPS. The EEPS is the faster device, with a data rate of 10 Hz while the FMPS (Fast Mobility Particle Sizer) produces a data rate of 1 Hz. Due to their different response times, the FMPS sensitivity range is higher than the EEPS range, but the measurable size range is similar for the two devices. [Figure 16](#) presents the principle of EEPS device.



#### Key

- 1 Sample in
- 2 Charger
- 3 Sheath air in
- 4 Excess flow
- 5 Electrometers
- 6 Exhaust

**Figure 16 — Engine Exhaust Particle Sizer (EEPS)**

#### 5.6.6.2 Parameters produced

This instrument is designed to measure number size distribution in terms of electrical mobility diameter from 5,6 nm to 560 nm in real-time. The concentration range of the FMPS ranges from  $1 \cdot 10^2$ - $1 \cdot 10^7$  particles/cm<sup>3</sup> at 5,6 nm to  $1 \cdot 10^1$ - $1 \cdot 10^5$  particles/cm<sup>3</sup> at 560 nm.

#### 5.6.6.3 Advantages and disadvantages

The main advantage of these devices is their real-time response and their ease of operation. These devices represent an “all-in-one granulometer.” In contrast to the SMPS, no radioactive source is needed, and the measuring device is ready to use in few minutes.

A disadvantage of these devices is the high frequency of maintenance. An additional problem is that EEPS and FMPS are sensitive to large particles or fibrous particles, which may produce a bridge between electrometers.

## 5.6.7 Aerodynamic Particle Sizer (APS)

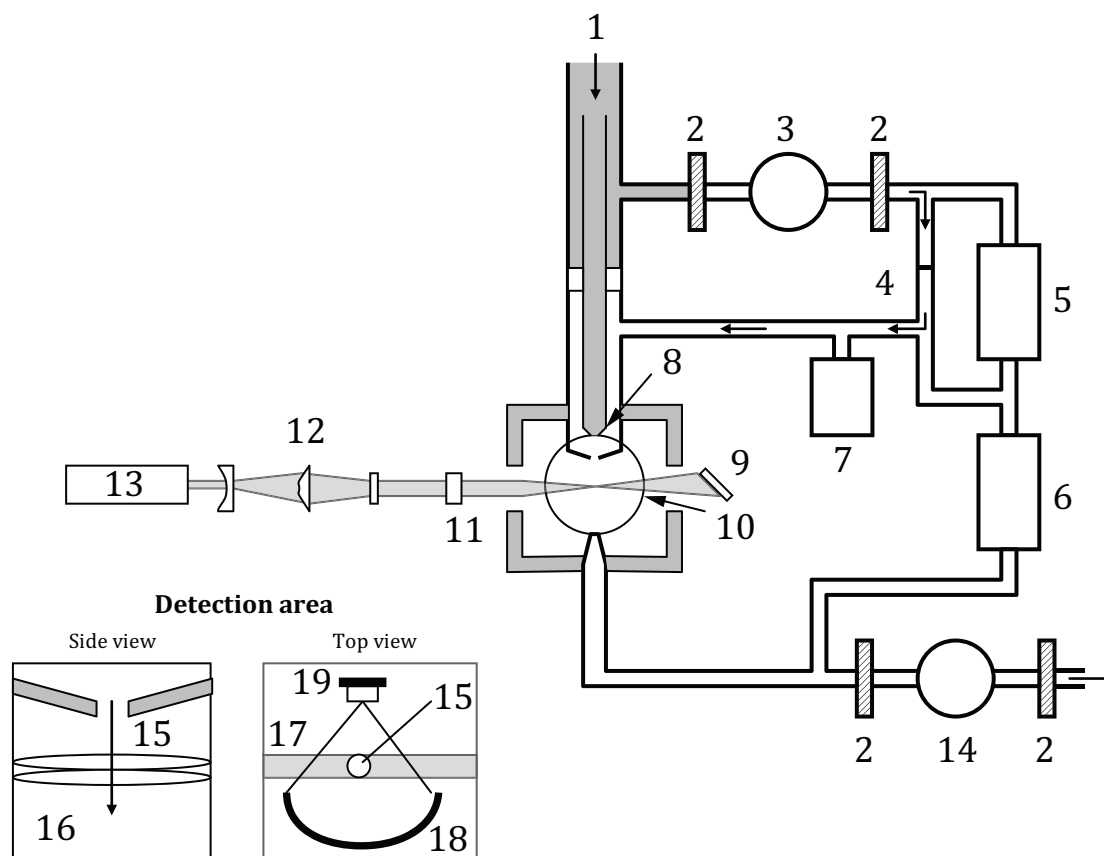
### 5.6.7.1 Principle

The Aerodynamic Particle Sizer (APS)<sup>[38]</sup> performs a granulometric classification of particles in the range from 0.5 µm to 20 µm using a time-of-flight technique that measures aerodynamic diameter in real time ([Figure 17](#)). Because time-of-flight aerodynamic sizing is dependent on the particle shape and is unaffected by an index of refraction or Mie scattering, it is superior to sizing by light scattering methods. In addition, the monotonic response curve of the time-of-flight measurement ensures high-resolution sizing over the entire particle size range.

### 5.6.7.2 Method description

In the APS method, the aerosol sample stream is initially passed through an accelerating orifice. The aerodynamic size of a particle determines its rate of acceleration, with larger particles accelerating more slowly due to their higher inertia. As particles exit the nozzle, they cross through two partially overlapping laser beams in the detection area.

Light is scattered as each particle passes through the overlapping beams. An elliptical mirror, placed at 90° to the laser beam axis, collects the light and focuses it onto a photodetector. The configuration of the detection area improves particle detection and minimizes Mie scattering oscillations in the light-scattering-intensity measurements.



#### Key

- |                                   |                        |
|-----------------------------------|------------------------|
| 1 Sample in                       | 11 Detection area      |
| 2 Filters                         | 12 Beam shaping system |
| 3 Sheath-flow pump                | 13 Laser               |
| 4 Orifice                         | 14 Total flow pump     |
| 5 Sheath-flow pressure transducer | 15 Nozzle              |
| 6 Total flow pressure transducer  | 16 Split laser beam    |
| 7 Absolute pressure transducer    | 17 Laser beam          |
| 8 Accelerating orifice            | 18 Elliptical mirror   |
| 9 Beam dump                       | 19 Photodetector       |
| 10 Elliptical mirror              |                        |

**Figure 17 — Aerodynamic Particle Sizer (APS[38])**

The use of two partially overlapping laser beams results in each particle generating a single, two-crested signal. Peak-to-peak time-of-flight between the two beams is measured with a resolution of a few nanoseconds. The amplitude of the signal is logged for light-scattering intensity. The smallest particles may have only one detectable crest and are stored separately. Particles with more than two crests, indicative of coincidence, are also stored separately, but are not used to build aerodynamic-size or light-scattering distributions.

#### 5.6.7.3 Parameters produced

This instrument is designed to measure a particle aerodynamic diameter distribution from 0,5 µm to 20 µm, and provides qualitative information on particles under 0,5 µm. One of the important



characteristics of such devices is that separation is made on the basis of the aerodynamic diameter of the particles.

#### 5.6.7.4 Advantages and disadvantages

The method is very easy to use and allows wide range of sizes to be measured in real time. Nevertheless, it is not adapted to nanoparticles, and information for particles under  $0,5\ \mu\text{m}$  has to be used with caution. Moreover, due to its operating principle, APS is only designed to detect low concentrations of the order of  $1000\ \text{particles}/\text{cm}^3$ .

#### 5.6.8 Other extractive measurement methods

Other extractive methods cited in the literature are:

- Beta gauges, which allow a time-dependent measurement of the mass of an aerosol impacted on a collection filter. The physical principle is based on electron attachment to an aerosol that has been deposited on a substrate. It is based on the assumption that electron attachment is proportional to the mass of the deposited aerosol. Limitations occur due to varying dimensions of aerosols, non-homogeneity of the substrate, and the dependence of the measurement on the atomic numbers of the chemical elements in the aerosol. The method is particularly influenced by high atomic numbers.
- Diffusion Mobility Analyser (DMA) electric classifications, presented for SMPS and EEPS devices above, can also be used with detectors other than the condensation particle counter (CPC). Different suitable technologies of CPC are also available. Another detector type cited in the literature is the electrometer-filter.
- Multistage liquid impinger device, consisting of a glass cylindrical vessel typically of diameter 80 mm and height 20 mm (the sizes can be varied) divided horizontally into three chambers. The particulate-laden gas stream (with the flow depending on the actual apparatus used) enters the top chamber via a relatively large jet and flows over a wetted disk that traps particles larger than  $10\ \mu\text{m}$ . The gas stream then enters the central chamber, via a smaller-sized jet and impinges on a second wetted disc. Particle sizes between  $2\ \mu\text{m}$  and  $10\ \mu\text{m}$  are trapped here. The gas stream then passes into the lower chamber via a smaller jet and through a third wetted disc, trapping particles in the  $0,5\ \mu\text{m}$  to  $5\ \mu\text{m}$  range. The trapping process is analogous to the principle of particle trapping in the lung and the results are, therefore, particularly significant in inhalation hazard studies.<sup>[39]</sup> A sample flow system similar to that used with the particle concentration/gravimetry technique is suitable.

## 6 Aerosol measurement metrology

### 6.1 Standard aerosol generators for calibration of instrumentation

#### 6.1.1 Need for standard aerosols

To ensure a proper aerosol measurement, standard aerosols are needed. Standard aerosols must represent the three main characteristics of an aerosol: its concentration, its granulometric distribution, and its morphology. Various devices are used to produce these controlled aerosols. Parameters governing the selection of a standard aerosol generator are dimensions, range, maximum and minimum concentrations to be produced, chemical nature and phase state (liquid or solid aerosol), morphology of the aerosol particles, and electrical charge state and/or electrical neutrality of the aerosol.

#### 6.1.2 Polymer ball generators

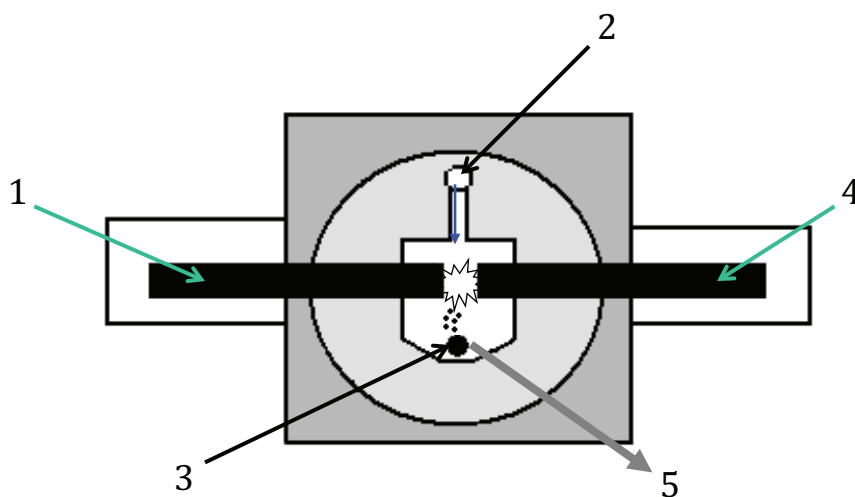
The simplest way to produce a monodispersed aerosol is to disperse spherical balls of polystyrene or polyvinyl latex in a liquid and then evaporate the liquid. Standard liquids are available for granulometric ranges from  $10\ \text{nm}$  to  $30\ \mu\text{m}$ . The standard deviation of such dispersions is, in general, very good. Nevertheless, there are some difficulties with this technique. The first is the possible formation of doublets and triplets of the latex particles in the solution. Using only high dilutions of latex in the solvent

liquid reduces this effect.<sup>[40]</sup> The second difficulty concerns the removal of the liquid to retain only the latex balls. The liquid has to be very pure, and its removal must be performed without modifying the latex aerosol.

Few other materials are adapted to this technique because of various incompatibilities and interactions with the liquid phase needed for such generators.

### 6.1.3 Spark discharge generators

From the work of Helsper et al.,<sup>[41]</sup> the spark discharge generator (Figure 18) is able to produce a nanostructured aerosol of particles by electrical arc discharge between two electrodes.<sup>[42]</sup> As the electrodes are consumed, the space between them is kept constant, ensuring a stable and reproducible arc and therefore aerosol generation. The arc necessary for the production of particles is the result of the discharge of a capacitor/resistor oscillator, whose frequency is controlled via a variable resistor. To avoid oxidation of the electrodes, a flow of inert argon gas flows around the arc. The primary particles formed as a result of the arc can then form aerosol clusters, the extent of which depends on their concentration. This cluster-forming agglomeration can be partially reduced and controlled by subsequent dilution of the generated aerosol in filtered air.



#### Key

- 1 Graphite electrode connected to the ground
- 2 Argon
- 3 Compressed air
- 4 Graphite electrode connected to a high voltage generator
- 5 Argon + air + graphite particles (30 to 300 nm)

**Figure 18 — Spark discharge principle**

When the frequency of the spark increases, the particle size distribution shifts to higher diameters, and the total concentration increases. This increase in the median diameter with the frequency of electrical discharge between the two electrodes is linked to the particle concentration generated within the arc chamber. In practice, as the frequency of the arc increases, the number of primary particles produced may become so great that the charges between adjacent particles may lead to them agglomerating.

Figure 19 shows the influence of the chemical nature of the electrodes. The physicochemical properties of the materials used for the electrodes have a great influence on the nature of the aerosols generated. Carbon electrodes have weaker electrical and thermal conductivities, and the generation of primary

particles is more effective because the energy dissipated between the electrodes is relatively low. This leads to particle size distributions shifted towards larger diameters by the process of coagulation.

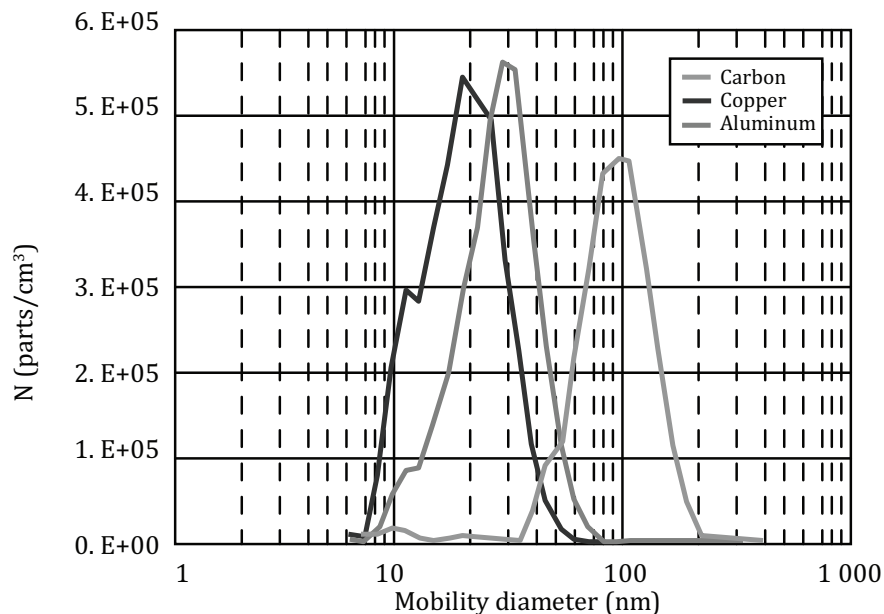


**Figure 19 — Granulometric distribution  $N(dm)$  for different chemical nature of electrodes**  
 $P_{air} = 0$ ,  $P_{ar} = 1$  bar,  $w = 500$  (from Reference [42])

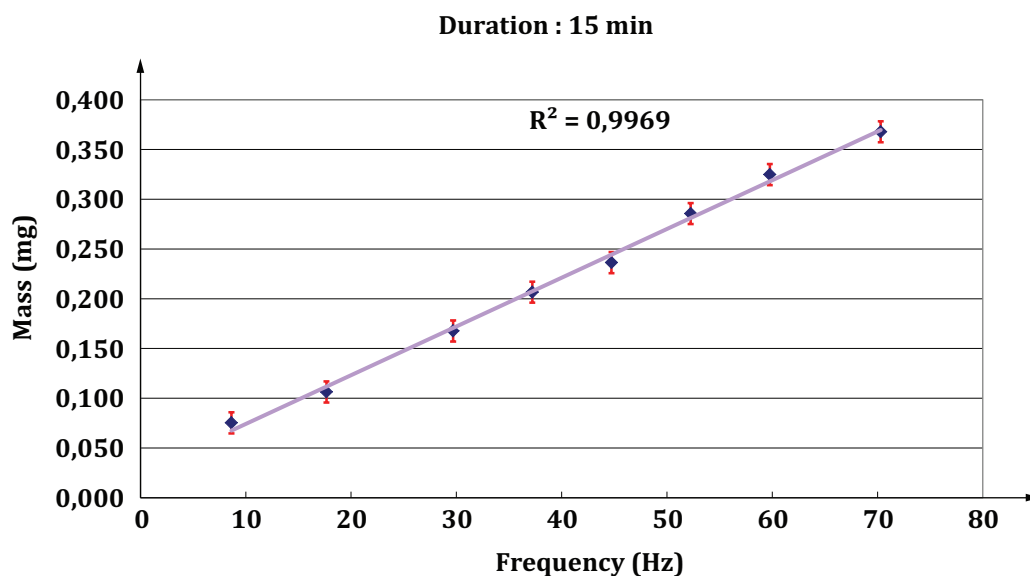
#### 6.1.4 Other generators

Direct dispersion of calibrated powders is currently under development, but is subject to many difficulties, especially because it is difficult to produce monodispersed powders. Nevertheless, granulometric distribution in the resulting aerosol can be very close to the original powder, and the chemical composition may not be altered significantly. Such direct dispersion of powders is normally performed in two steps. The first step consists of feeding the powder into an enclosure at a constant flow through a disperser. The second step is the dispersion of the powder as an aerosol. The technique mainly used is based on a pneumatic principle.

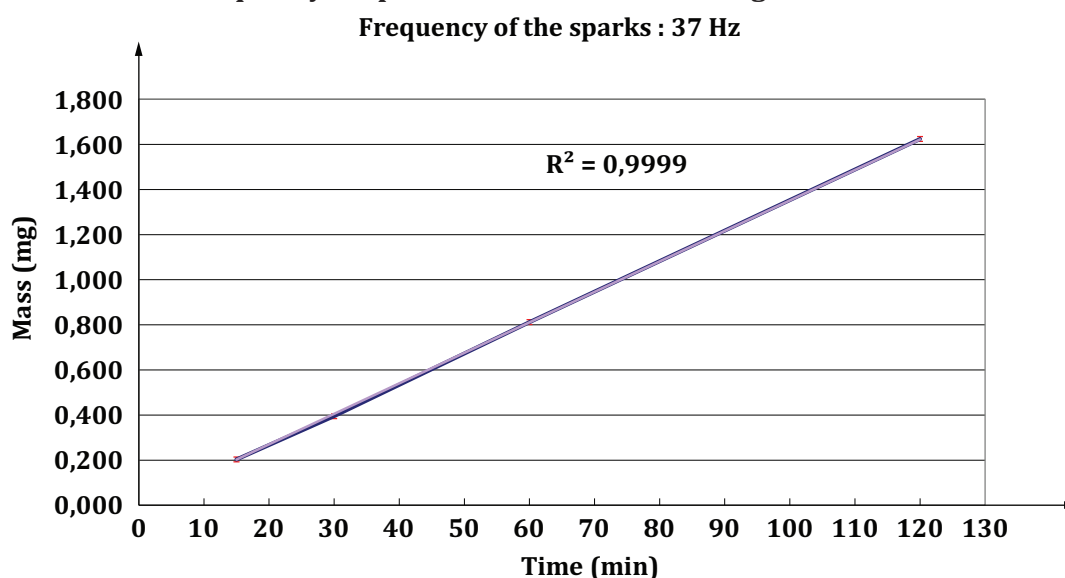
Dispersion of liquid droplets in aerosols is also possible with various techniques. The most cited is a pneumatic nebulisor, where the droplets produced vary from 1  $\mu m$  to 10  $\mu m$  with a geometric standard deviation between 1,7 and 2,5 and a mass concentration between 1  $g/m^3$  and 50  $g/m^3$ . Other techniques have been adapted to produce a monodispersed liquid aerosol and include the rotating disk, vibrating orifice, vibrating needle, and methods used in electrostatic spraying.

## 6.2 Qualification (Verification) of generators

Qualification of standard aerosol generators is essential to ensure their repeatability, reproducibility and time stability (drift). The most common technique is to deposit the entire generated aerosol on a filter and to check, with a gravimetric method (as presented in 5.6.2) the relationship between expected and measured weight, as presented on [Figures 20 a\)](#) and 20 b).



a) Example of qualification of the linearity of a spark discharge generator by comparison between frequency of sparks and mass of aerosols generated in 15 min



b) Example of qualification of drift of a spark discharge generator

**Figure 20**

### 6.3 Calibration methods exigencies

To calibrate a device for measuring aerosols in fire effluents, it is important to produce an aerosol with characteristics as close as possible to the characteristics of the aerosols in the fire effluent. With this objective, it is possible to produce aerosols very close in granulometric distribution and concentration to the fire aerosols to be measured, but the accurate representation of particle morphology is difficult to achieve.

When a suitable generator has been established, it is connected to the fire model or directly to the sampling and measuring device, with care taken to ensure the connections are appropriate. For example, it is especially important to regulate the pressure between the generator and the calibrated device. For extractive measurements, the recommendations of 5.6.1 must be applied, and the devices must be heated under the same conditions as for fire aerosol measurement. For example, for devices like cascade

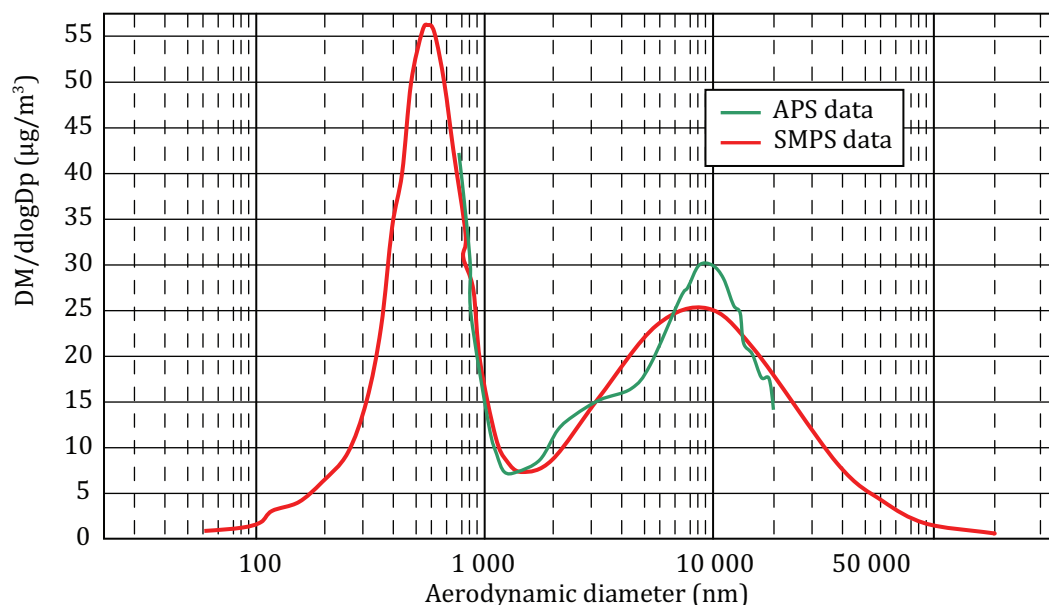
impactors, the cut-off diameter of each stage depends on temperature and is given at ambient conditions by manufacturers. It has to be measured in real end-use fire model conditions and the results corrected.

Depending on the characteristics of the calibrated device and on the parameters obtained, such calibration ensures the validation of the installation. Nevertheless, calibration can never reproduce all aspects of aerosols produced in fire, and deviations have to be taken into account based on the physical and chemical properties of the aerosols.

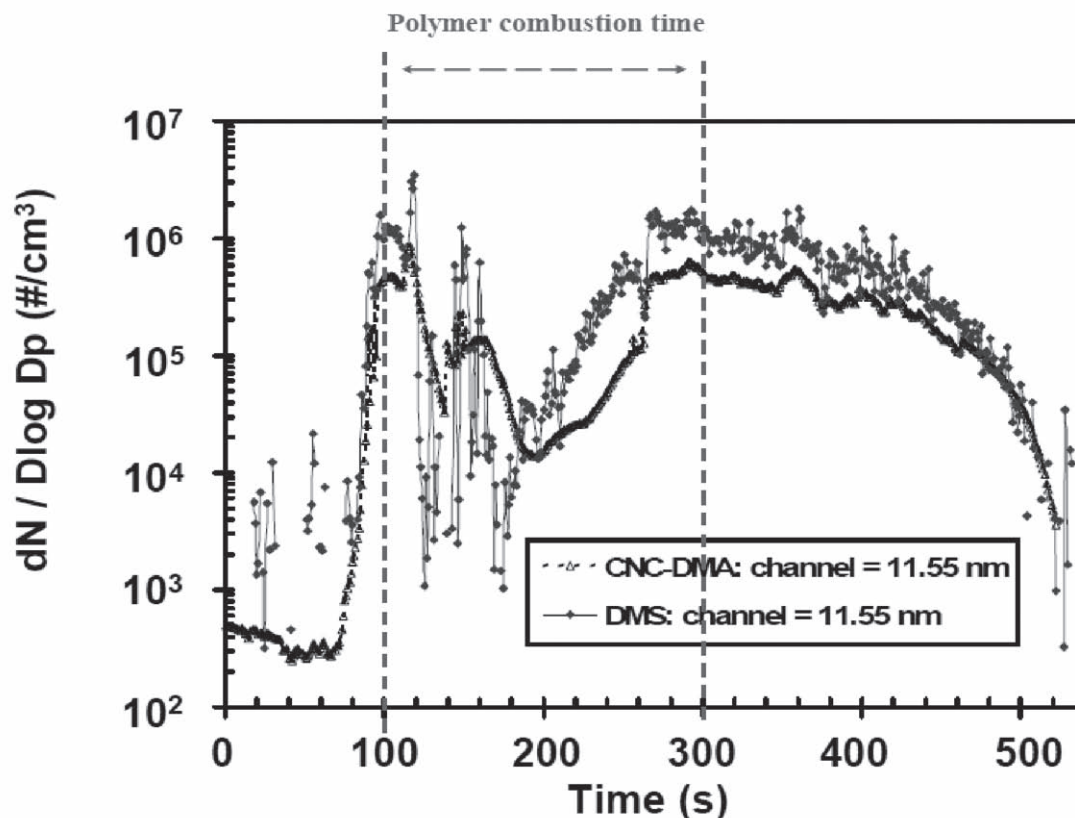
## 6.4 Validation

### 6.4.1 Comparison among devices

Validation of an aerosol measurement can be performed by comparing the data obtained from different devices based on different measurement principles. With aerosol measurement, it is also essential to understand the scope and limitations of the various sampling and measurement methods if a meaningful interpretation is to be made and results compared. The [Figure 21 a\)](#) shows a successful comparison between SMPS and APS devices for a bi-dispersed aerosol. Each system is based on a different physical measuring principle. SMPS uses a model to interpret electric mobility diameter measured in aerodynamic diameter. The [Figure 21 b\)](#) shows a comparison between SMPS and EEPS for a 11,55 nm region scan during combustion of PA-6 in cone calorimeter.<sup>[43]</sup>



a) Example of comparison between SMPS and APS measurements

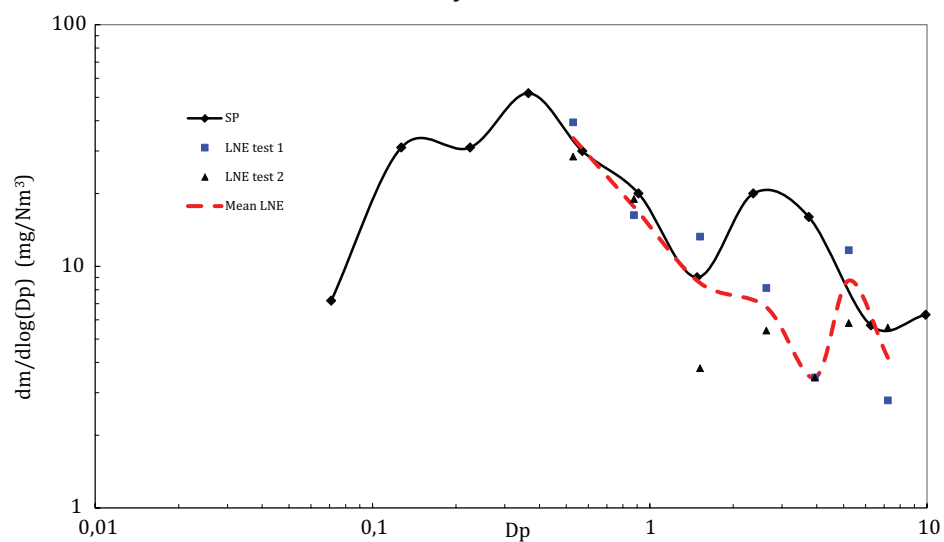
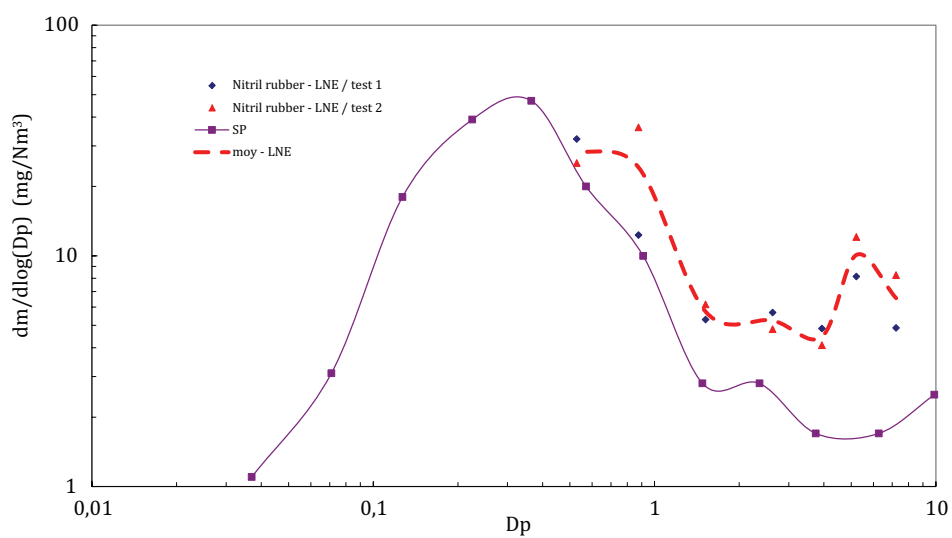


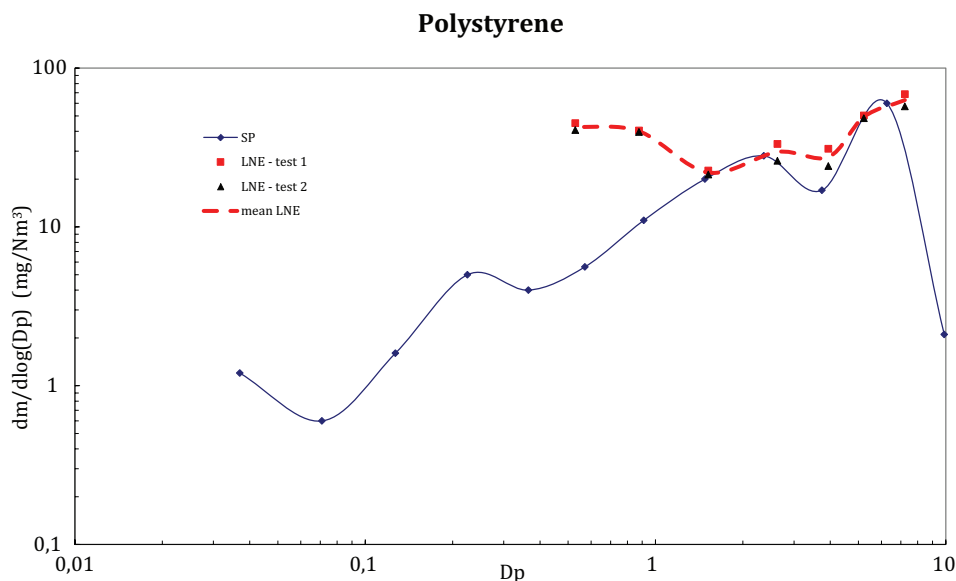
b) Example of comparison between SMPS and EEPs (DMS) measurements for 11,55 nm region<sup>[43]</sup>

Figure 21

#### 6.4.2 Comparison between laboratories

There are few data on interlaboratory trials in the measurement of fire effluents. Reference <sup>[36]</sup> presents results obtained for three materials tested at SP (Sweden) and LNE (France) laboratories. The fire model was the ISO 5660-1 cone calorimeter, and the materials studied were an expanded polystyrene, a flexible polyurethane foam, and a nitrile rubber. SP used a low-pressure cascade impactor, whereas LNE used a classical cascade impactor. The comparisons for the three materials are presented in [Figure 22](#). The results show a good agreement on distribution for micronic particles.

**Polyurethane****Nitril rubber**



**Figure 22 — Example of comparison between laboratories**

### 6.4.3 Interpretation of scale effects and comparison with literature

Blomqvist<sup>[4]</sup> compared particle distribution data from fire tests with the data compiled by Butler and Mulholland.<sup>[44]</sup> The mass median aerodynamic diameter (MMAD), as described by Hinds,<sup>[45]</sup> was calculated for a set of cone calorimeter tests, for an enclosure test with a sofa,<sup>[46]</sup> and for a test where a complete automobile was burned.<sup>[47]</sup>

The data are presented in [Figure 23](#) as particle yields versus MMAD. The quantitative particle distribution results compiled by Butler and Mulholland consist of data from various sources and various fire sizes, but they are all from flaming combustion. From these data, only data from fires with solid fuels have been included in the figure. The data includes fuels such as different types of wood materials and polymers from various studies and authors.



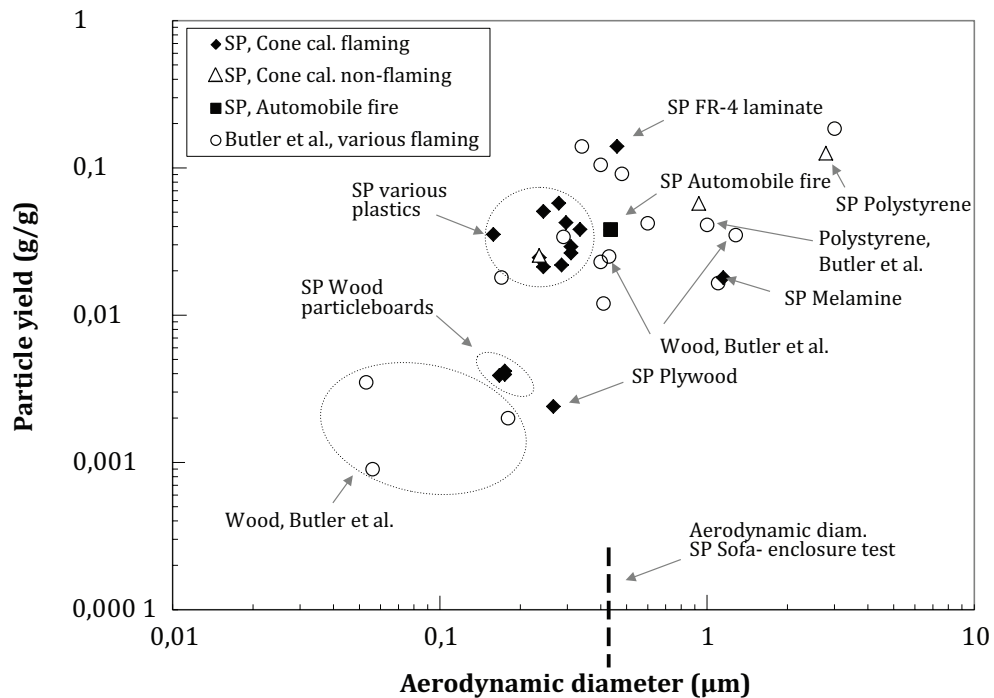


Figure 23 — Smoke yield versus median aerodynamic diameter according to reference[4]

A trend, where the aerodynamic diameter increases with increasing smoke yield, was observed by Butler and Mulholland. It can be seen that the tested wood products from the cone calorimeter tests produce low particle yields with a particle mass distribution with a small MMAD. This is in line with the “low end” group of wood data from Butler and Mulholland. Further, there are two additional data points for wood from Butler and Mulholland, the highest of these was from a large, underventilated wood crib fire.

The interpreted data from flaming combustion with melamine and an FR-4 laminate (brominated laminate) are at the “high end” of the plot. Both of these products burn poorly due to their chemical composition, and especially the FR-4 laminate produced a very high particle yield. The data point for “SP polystyrene” showed a high particle yield and a large MMAD. This product did not ignite in the cone calorimeter test. The higher values compared to the data provided by Butler and Mulholland are therefore to be expected.

The trend of increasing MMAD with increasing particle yield for the cone calorimeter tests should mainly be due to differences in the chemical composition of the materials, as the combustion in a standard cone calorimeter test is well ventilated. Strongly oxygenated materials, such as wood, burn well, whereas aromatic polymers such as polystyrene burn poorly and give a high soot yield.[48] The combustion conditions are also of importance for the particle yield, with higher yields obtained as the fire becomes less well ventilated.[48]

Data from large-scale tests conforms well to the particle mass size distribution results seen from the cone calorimeter tests and the data from Butler and Mulholland. Both large-scale tests show an MMAD slightly above 0,4 μm, and the result from the automobile fire fits well in the overall particle yield-MMAD trend. In the case of the sofa-enclosure fire tests it was not possible to calculate a particle yield as the mass-loss from the sofa was unknown.

## 7 Presentation of results

### 7.1 Calculations

The main descriptive parameters that characterize an aerosol concentration are the number of particles per cubic meter or the mass concentration. These parameters are directly given or interpreted from

the devices described in this International Standard. The main descriptive parameters produced in an aerosol analysis concerning its granulometric distribution are its mass median aerodynamic diameter (MMAD) and its geometrical standard deviation. Reference [49] details the calculation methods presented below. The morphologic characteristics of an aerosol are complex to express. Refer to 5.2.3 for more details.

### 7.1.1 Mass Median Aerodynamic Diameter (MMAD)

To calculate MMAD, construct a 'Cumulative Percent Found - Less Than Stated Particle Size' table and calculate the total mass of test substance collected in the cascade impactor. Start with the test substance collected on the stage that captures the smallest particle size fraction, and divide this mass of the test substance by the total mass found above. Multiply this quotient by 100 to convert to percent. Enter this percent opposite the effective cut-off diameter of the stage above it in the impactor stack. Repeat this step for each of the remaining stages in ascending order. For each stage, add the percentage of mass found to the percentage of mass of the stages below it. Plot the percentage of mass less than the stated size versus particle size in a probability scale against a log particle-size scale, and draw a straight line best fitting the plotted points. A weighted least squares regression analysis may be used to achieve the best fit. Note the particle size at which the line crosses the 50 % mark. This is the estimated Mass Median Aerodynamic Diameter (MMAD).

### 7.1.2 Geometric Standard Deviation (GSD)

To calculate GSD, refer to the log probability graph used to calculate the Mass Median Aerodynamic Diameter. Provided that the line is a good fit to the data, the size distribution is log normal, and the calculation of the Geometric Standard Deviation is appropriate. Note that particle size at which the line crosses the 84.1 % mark. Note the particle size at which the line crosses the 50 % mark and calculate as follows:  $GSD = 84.1 \% \text{ mark} / 50 \% \text{ mark}$ .

To verify graphically that the aerosol is in fact unimodal and log-normally distributed, the normalized mass per stage ( $f_H'$ ) is evaluated as a histogram.  $\Delta \log D_p$  is equal the difference  $\log D_{p+1} - \log D_p$ , whereas  $D_p$  is the lower cut-size limit and  $D_{p+1}$  the higher cut-size limit of the corresponding impactor stage. Calculate the histogram  $f_H'$  by equation:

$$f_H' = \frac{1}{N_f} \times \frac{\text{mass} / \text{stage}}{\Delta \log D_p}$$

Calculate the log-normal mass distribution  $y'(D_{ae}) = 1/N_f \times y(D_{ae})$  as a function of the aerodynamic diameter ( $D_{ae}$ ) using by equation:

$$y'(D_{ae}) = \exp\left(-\frac{(\log D_{ae} - \log MMAD)^2}{2 \times \log^2 GSD}\right)$$

and use the normalization factor ( $N_f$ ):

$$N_f = \frac{\Sigma \text{mass}}{\log GSD \times \sqrt{2\pi}}$$

The algorithm for the calculation of particle size characteristics is taken from relevant reference works on aerosol physics[50][51] and proves to be generally applicable.[6] The size distributions shown in Figure 24 are constructed utilizing these equations.

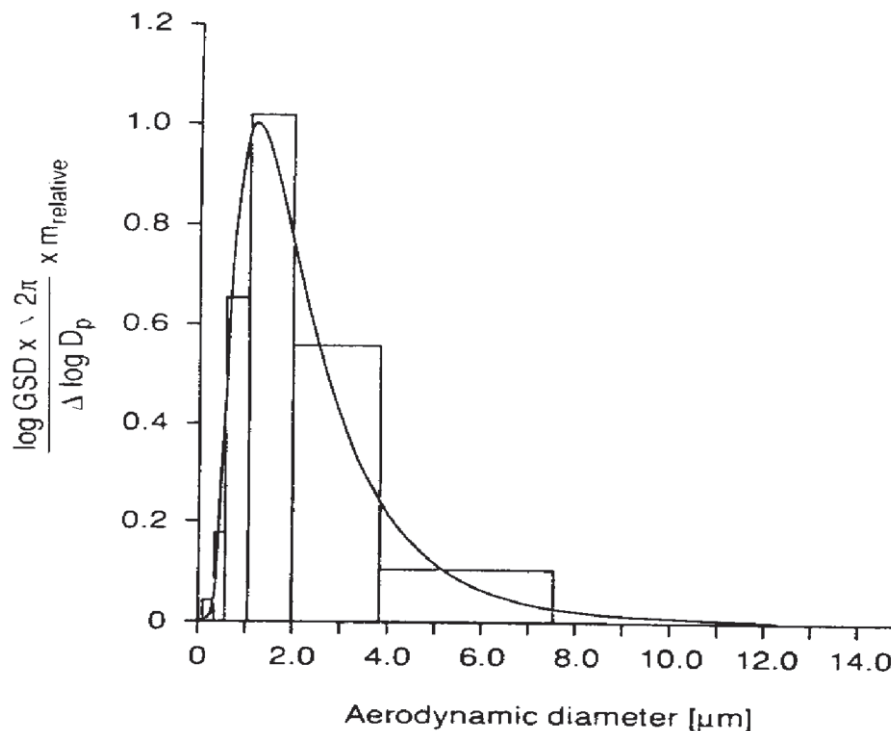


**Figure 24 — Principle of characterization of aerosol atmosphere**

The relative mass with an aerodynamic diameter  $\leq 3 \mu\text{m}$  ("Respirable mass fraction") [52][53][54] is calculated from the regression line. For probit transformation and linear regression, algorithms published by Rosiello *et al.* [55] can be suitable. The MMAD was calculated using published formulas. [51][6][56]

## 7.2 Measurement report

The report of an aerosol measurement shall contain:

- Description of the installation, including diameters of the sampling lines or tubes, distance between the fire and the sampling point.
- Flow of the sample.
- Description of the device used and the operating conditions (temperature and pressure).
- Description of the ambient conditions in terms of temperature, pressure, and relative humidity.
- The direct data produced by the device, for example,  $D_p$  for SMPS and  $D_a$  for cascade impactors.
- Description of the nature of the interpretation and of the calculations used, including all assumptions, especially those regarding particle morphology.

Results of the calculated data with uncertainties.

An example of a suitable report is presented in [Annex E](#).

## 7.3 Uncertainties

Uncertainties during aerosol measurement in fire tests stem from a variety of difficulties in obtaining a representative result. Trueness errors for concentration and granulometric distribution can have their origins in soot deposited or impacted on undesired surfaces. This difficulty can be limited by the care taken in choosing and using the particular measurement device. Temperature and moisture can also cause systematic errors. Repeatability and reproducibility uncertainties can come from the fire model

and/or aerosol generation itself, but also from ambient conditions (temperature, pressure, and relative humidity) and from the measuring device, all of which may allow unwanted effects such as coagulation or sedimentation of the aerosol.

Measurements normally deliver average values. The distribution of aerosol concentration (soot volume fraction) is needed when the soot volume fraction variation leads to large uncertainties in the values. An example of soot volume fraction distribution is given in [Figure 25](#), with a shape defined by truncated Gaussian curve associated to Dirac value for soot's absence. The effect of uncertainties of the refractive index  $m$  on the determination of  $F_v$  from extinction measurements has been shown by Joyeux.[\[57\]](#)

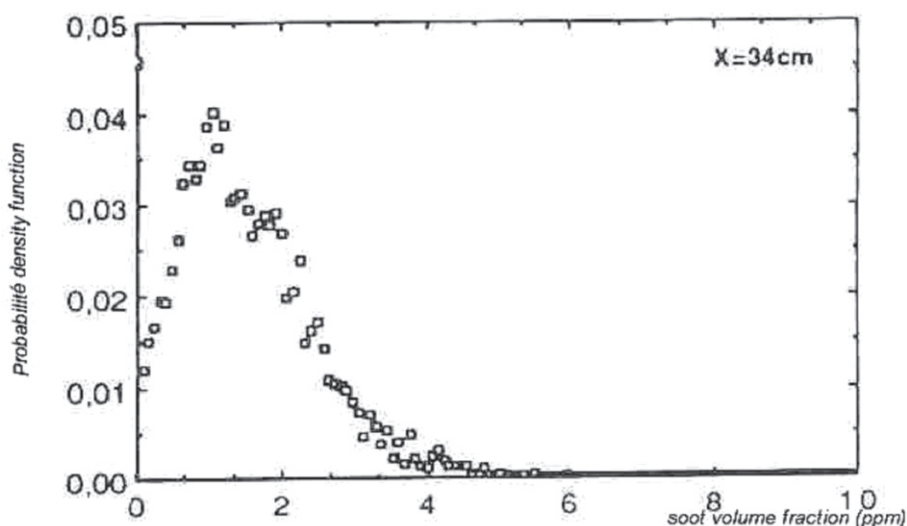


**Figure 25 — Example of soot volume fraction distribution in one location on the centreline axis of a jet flame[\[57\]](#)**

## Annex A (informative)

### Experimental measurements of $D_{pp}$ , $N_p$ , $R_g$ , $D_f$ and $k_f$

**Table A.1 — Published values of  $D_{pp}$ ,  $N_p$  and  $R_g$**

Fuel	Flame type	$D_{pp}$ (nm)	$N_p$	$R_g$ (nm)	Reference
Acetylene	-	20-30	-	-	[58]
Acetylene	Turbulent diffusion flame	47	417	472	[59]
Acetylene	Turbulent diffusion flame	17-34	50-180	-	[60]
Acetylene	Turbulent diffusion flame	64-66	70	277	[61]
Benzene	Turbulent diffusion flame	50	552	824	[59]
Butadiene	Turbulent diffusion flame	42	-	-	[62][63]
Cyclohexane	Turbulent diffusion flame	42	-	-	[62][63]
Ethylene	Laminar diffusion flame	30-37	-	-	[64]
Ethylene	Turbulent diffusion flame	32	467	452	[59]
Ethylene	Turbulent diffusion flame	19-35	20-50	20-60	[60]
Ethylene / air	Laminar diffusion flame	18-31	5-190	-	[18]
Hydrocarbons	Laminar flame	20-40	-	-	[65]
Isopropanol	Turbulent diffusion flame	31	255	330	[59]
Kerosene	Turbulent diffusion flame	19-30	-	-	[66]
Methane / oxygen	Premixed flame	20	-	-	[67]
n-Heptane	Turbulent diffusion flame	35	260	359	[59]
Propane	Turbulent diffusion flame	30	364	366	[59]
Propane / oxygen	Premixed flame	15-26	-	-	[68]
Propylene	Turbulent diffusion flame	41	460	518	[59]
Toluene	Turbulent diffusion flame	14-20	-	-	[69]
Toluene	Turbulent diffusion flame	51	526	807	[59]
Toluene	Turbulent diffusion flame	52-65	100	260	[70]
Toluene / ethylene	Premixed flame	20-25	-	-	[71]
Diesel	Diesel engine	Nearly 30	-	-	[72]
Oil	Turbulent diffusion flame	Nearly 45	-	-	[73]
Polymer	Diffusion flame	13-43	-	-	[61]
Polymer	Turbulent diffusion flame	42-54	-	-	[61]

**Table A.2 — Values of  $D_f$  and  $k_f$  given by various authors**

Fuel	Region	Flame type	Method	$D_f$	$k_f$	Reference
Acetylene	Flame	Laminar diffusion flame	2D TEM	1,8	1,7	[74]
Acetylene	Flame	Turbulent diffusion flame	2D TEM	1,82	2,41	[22][23]
Acetylene	Flame	Turbulent nonpremixed flame	2D TEM	1,82	1,9 ± 0,3	[60]
Acetylene	Plume	Laminar diffusion flame	2D TEM	1,85-1,93	1,68-2,31	[61]
Acetylene	Plume	Turbulent diffusion flame	2D TEM	1,79	-	[75]
Acetylene - ethylene	Flame	Laminar diffusion flame	ALS	1,75	2,78	[22][23]
Acetylene - ethylene	Plume	Laminar diffusion flame	2D TEM	1,66	2,35	[75]

**Table A.2** (continued)

Fuel	Region	Flame type	Method	$D_f$	$k_f$	Reference
Butane	-	-	Light scat.	1,96	-	[76]
Butane	Plume	Diffusion flame	SEM	1,97	-	[77]
Diesel	-	-	2D TEM	1,7	-	[78]
Ethylene	Flame	Laminar diffusion flame	2D TEM	1,72	2,8	[18]
Ethylene	Flame	Premixed flame	DMA-ELPI	2,15	-	[79]
Ethylene	Flame	Turbulent nonpremixed flame	2D TEM	1,74	2,2 ± 0,4	[60]
Ethylene	Plume	Turbulent diffusion flame	2D TEM	1,73	-	[75]
Isopropanol	Plume	Turbulent diffusion flame	2D TEM	1,7	-	[75]
Methane	-	Premixed flame	2D TEM	1,74	2,45	[80]
Methane / air	Flame	Premixed laminar flame	ALS/TEM	1,80-1,95	-	[81]
Methane / oxygen	-	-	Light scat.	1,73	-	[76]
n-Heptane	Plume	Turbulent diffusion flame	2D TEM	1,73	-	[75]
Propane	Plume	Turbulent diffusion flame	2D TEM	1,74	-	[75]
Propylene	Plume	Turbulent diffusion flame	2D TEM	1,75	-	[75]
Toluene	Plume	Turbulent diffusion flame	2D TEM	1,73	-	[75]
Toluene	Plume	Turbulent diffusion flame	2D TEM	1,73-1,86	1,89-2,66	[61]
Hydrocarbons	Flame	Turbulent diffusion flame	ALS	1,86	2,25	[22][23]
Hydrocarbons	Plume	Turbulent diffusion flame	2D TEM	1,67	2,33	[75]
Diesel	Engine exhaust.	Diesel engine	DMA-ELPI	2,3	-	[79]
Diesel	Plume	Diffusion flame	SEM	2,04	-	[77]
Fuel oil	Plume	Diffusion flame	SEM	1,88	-	[77]
Polymer	Plume	Turbulent diffusion flame	2D TEM	1,74-1,78	2,63-2,84	[61]
Wood	Plume	Diffusion flame	SEM	2,35	-	[77]

## Annex B (informative)

### Adsorption of combustion gases on particles

Weak chemical forces can lead to the adsorption of toxic combustion gases on the surface of soot particles and the addition of these gases to aerosol droplets. Inhalation of the aerosol provides a mechanism for the transport of the toxicants past the body's defences, as described further in [Annex C](#).

Carbonaceous soot particles have a behaviour similar to activated charcoal, which is in widespread use as a gas/vapour adsorber. The structure of these particles is porous, with a large surface often composed mainly of aromatic rings. The pi electrons of these aromatic rings can produce an electrostatic charge and facilitate the formation of van der Waals bonds. Because of the relatively large surface area of these particles, the quantities of combustion gases that can be adsorbed are considerable.

The adsorption of species on carbonaceous soot particles occurs with a low thermodynamic enthalpy, i.e. the bonds are weak. The strength of the bonding is dependent on temperature and pressure. Species adsorbed initially can be re-released readily if the temperature increases, if pressure decreases, or in the presence of a solvent with greater affinity for the adsorbed species than the soot. This dynamic state can be characterized by adsorption isotherms and isobars (and isosteres), which show the relationship between the forces between the particles and adsorbed species with respect to temperature and pressure changes. However, as a practical matter, these plots are difficult to establish experimentally, particularly when considering gases and particles in fire effluents.

The first layer of gas adsorbed at the surface of the particle is the known as the Langmuir layer. This is the only layer present for non-porous media and for surfaces with micropores smaller than 2,5 nm. The entire adsorbed content can normally be recovered.

For solids with macropores (over 25 nm), there can be many layers of molecules adsorbed. These layers can be expressed in terms of adsorbed gas volume plotted against pressure. Examples of Langmuir single layer, macroporous adsorbant aerosol and polar aerosol are presented in [Figure B.1](#).

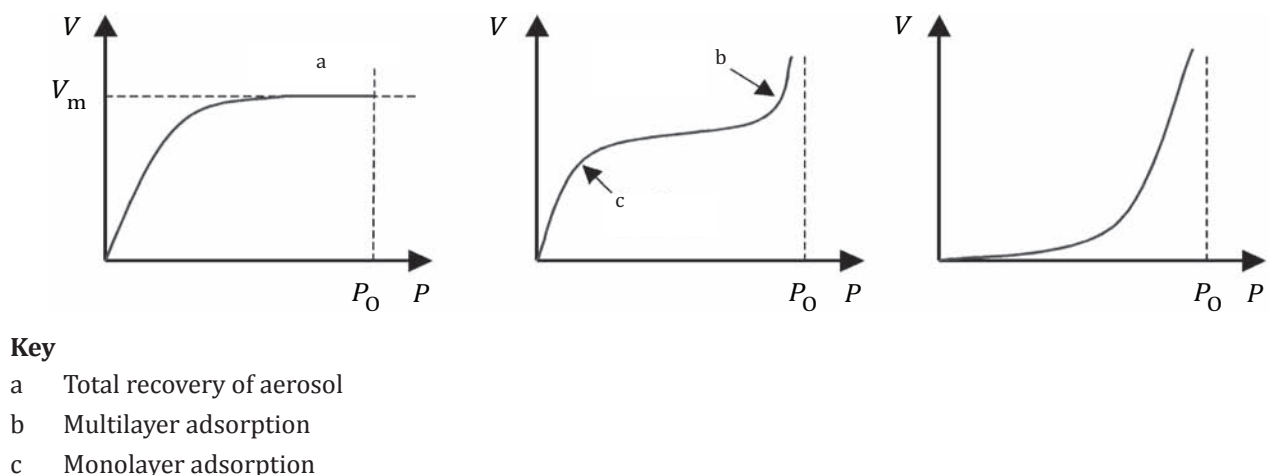


**Figure B.1 — Examples of adsorption isotherms on non-porous, macroporous and polar aerosol**

$P_0$  is the saturating vapour pressure of the adsorbed gas and  $p$  its partial pressure of the gas. The quantity of gas adsorbed by a given quantity of aerosol is described by the Freundlich equation for monolayer Langmuir adsorption. The Freundlich equation is:

$$\frac{x}{m} = K \cdot p^{1/n} \quad V = K \cdot p^{1/n}$$

where

$x$  is the mass of adsorbed gas,

$m$  is the mass of adsorbant aerosol,

$V$  is the adsorbed volume,

$K$  and  $n$  are dimensionless constants that are characteristic of the adsorbant/gas pair. These values are dependent on the temperature and are determined experimentally,

$n$  is between 1 and 2.

For multilayer adsorption, Brunauer, Emmet and Teller proposed in 1935 a model where there are multiple adsorption layers after the first one. The relation they established is known as a BET isotherm and allows calculation of the volume of species adsorbable on the surface. A BET isotherm is defined as follows:

$$V = \frac{V_m \cdot c \cdot p}{(p_0 - p) \left[ 1 + (c - 1) \left( \frac{p}{p_0} \right) \right]}$$

where

$V_m$  is the volume adsorbed on a layer,

$c$  is a constant specific to the aerosol/gas pair.

The graphical representation of this relation is a straight line, as shown in [Figure B.2](#).



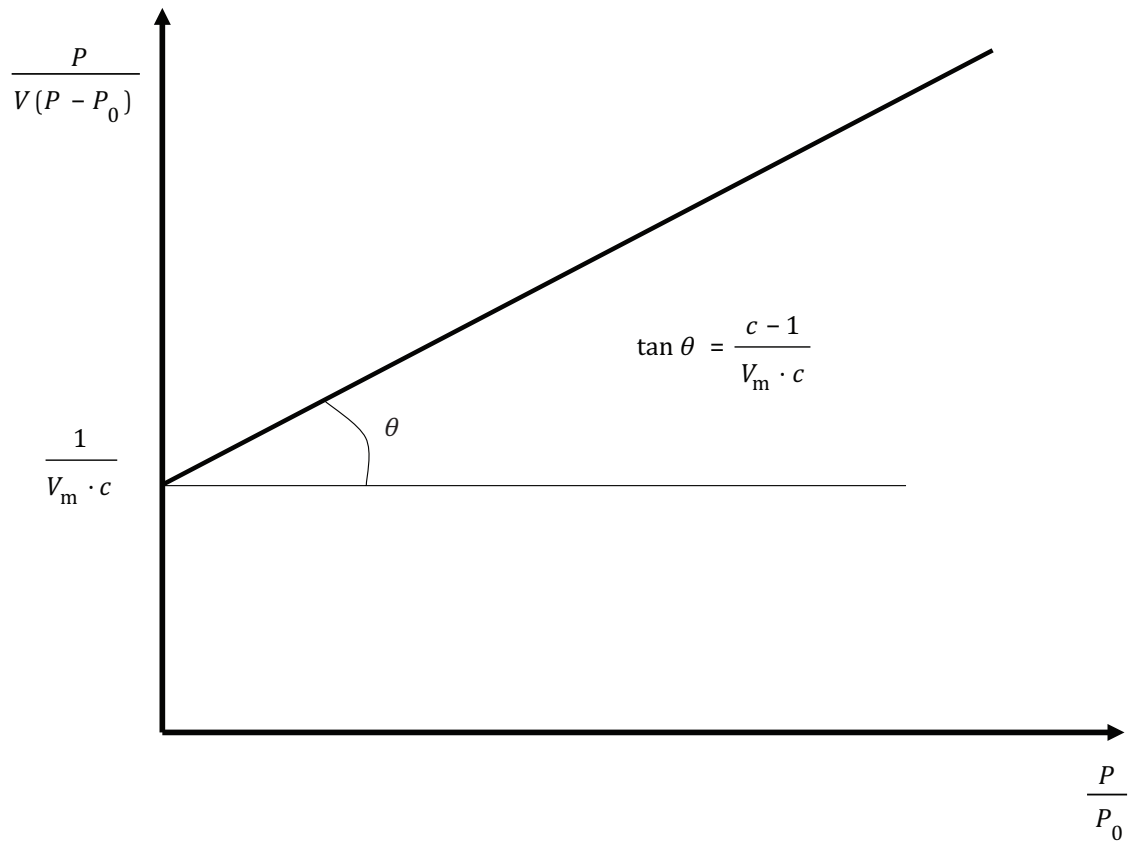


**Figure B.2 — Graphical representation of a BET isotherm**

The application of the BET equation allows the calculation of the adsorbant specific surface,  $S_0$ . This surface is the total surface of one gram of adsorbant when molecules of a particular chemical occupy the surface. It is different from the apparent surface of the aerosol presented in 5.2.3. The specific surface is given by the relation:

$$S_0 = N \cdot \sigma \cdot \frac{V_m}{V_M}$$

where

$N$  is Avogadro's number ( $6,02 \times 10^{23}$ ),

$\sigma$  is the surface occupied by a molecule,

$V_M$  is the molar mass of the gas.

Typically,  $\sigma$  has been determined using molecular nitrogen, and the measured value is  $0,162 \text{ nm}^2$ .

These calculations are difficult to perform for real fire effluents. This is because of the number of adsorbable gases present and the variability of concentrations and temperatures with time and location. These thermodynamic relationships can give the maximum adsorbed gas but measurements such as presented in 5.2.4 are needed to determine the actual quantity of adsorbed species.

## Annex C (informative)

### Inhalation dynamics and toxicity of particles

#### C.1 Standard inhalation curves

Before determining the effect on the people, it is necessary to provide a basis for quantifying how far these particles penetrate into the organism.<sup>[82]</sup> Globally speaking, for one aerosol, there are three possible areas of action: the upper respiratory tract, the bronchial tree or the periodontal pockets. These different parts of the organism are physiologically different.

The definition of the different breathable fractions was given previously. The alveolar fraction is the most dangerous for the health: as the upper tract is ciliated and can mechanically evacuate the particles but the alveoli are not equipped to achieve this. When they penetrate into the alveoli, the particles will become trapped and can be eliminated only through cellular digestion. The alveolar and thoracic fractions depend upon the respiratory rhythm and are only approximations of an average case.

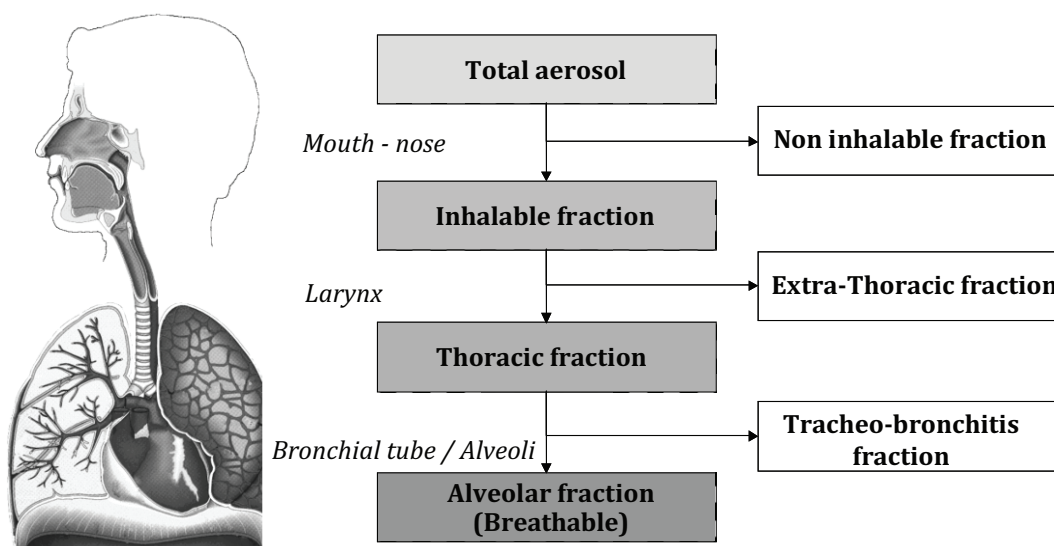


**Figure C.1 — Definition of the penetration fractions of the particles**

This represents the general mechanism of, the respiratory insult possible and the depth of penetration of the particles will increase as their size decreases. The biggest particles, with diameters in excess of 10 µm, will settle on the nasal meatus.<sup>[7]</sup> According to Mahaffey and Miller<sup>[83]</sup> and Peterson,<sup>[84]</sup> particles of less than 10 µm in diameter are too small to be filtered by the human respiratory system. They can cross the upper respiratory tract (nose and mouth) and penetrate into the lower respiratory tract.

Standard definition curves for the different fractions mentioned above have been established and fully described in ISO 7708. They give the probability that one particle of a given size can reach the different levels of the respiratory tree. These curves are conventional. There are precise tables for these values in ISO 7708.<sup>[56]</sup>

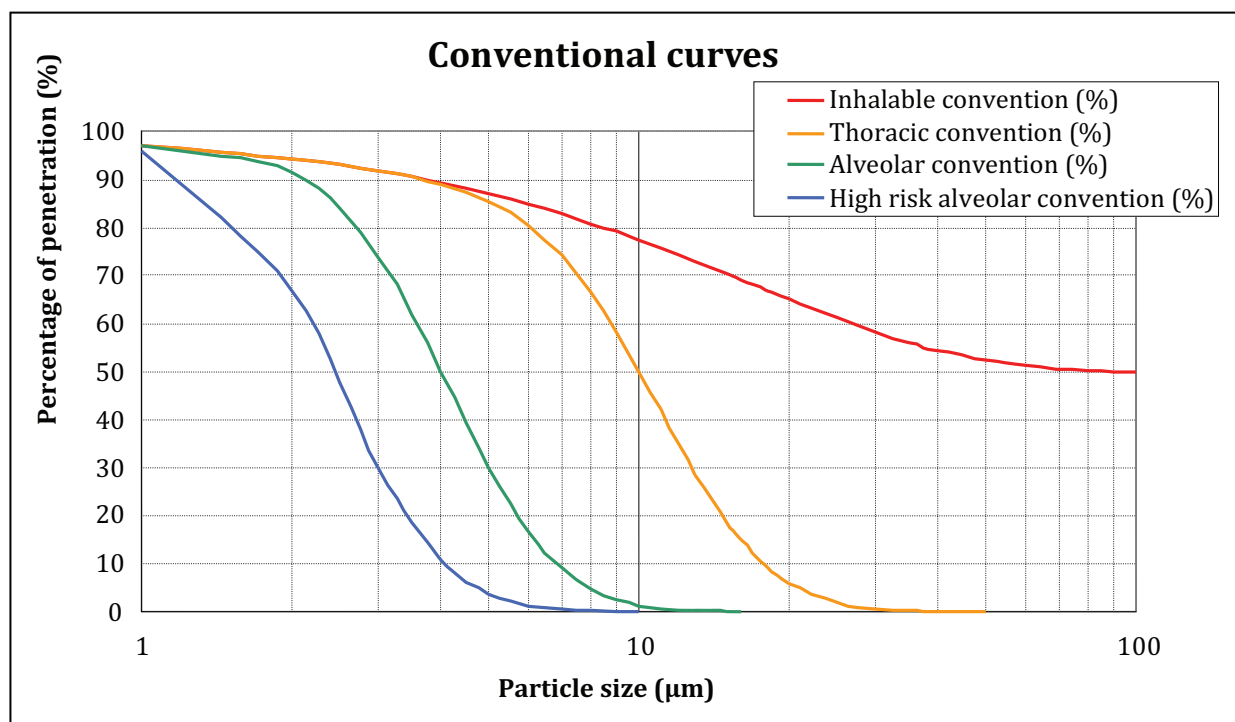


**Figure C.2 — Conventional penetration curves of particles**

These curves mean for instance that one particle of 4 μm has a probability of 89 % to be present up to the larynx, 89 % of probability to be present between the larynx and the bronchiole, 50 % to still be present at the level of the alveoli in healthy subjects and 11 % in high risk subjects<sup>1)</sup>.

The choice of which curve to use depends on the risk to be evaluated. The inhalable convention will be chosen if the particles cause the effect studied at all the levels of the pulmonary tree, while the alveolar convention will be selected for the particles having a local effect at the bottom of the lungs. Each convention corresponds to the fractions that penetrate into one area of the organism, and not to those that settle in it. More particularly, for the alveolar convention, part of the particles inspired is expired without settling and therefore there will be no biological effect.

## C.2 Physiological and pathological effects of particles deposited in different parts of the respiratory tract

The particles settling at the different levels in the respiratory tract cause varied health effects that depend on their toxicological properties and their settling site.<sup>[2]</sup> During inhalation, large particles (called PM<sub>10</sub>, with diameters under 10 μm) can reach the upper thoracic and bronchial ion the lungs. Those under 2,5 μm (PM<sub>2,5</sub>) are more dangerous, as they can penetrate more deeply into the lungs and may reach the alveolar region PM<sub>10</sub> particles may settle out of suspension within a few hours following their generation whereas PM<sub>2,5</sub> particles can remain suspended for days or even for several weeks after their generation.

The United States Department of Agriculture (USDA)<sup>[2]</sup> considers that particles with an average diameter of between 5 μm and 10 μm have a tendency to settle in the respiratory tract within average size bronchioles but may then eliminated by ciliary action and by coughing. Correlations have been established between the concentration of particles with diameter under 10 μm (PM<sub>10</sub>) and a reduction

1) For children and adults affected by certain respiratory diseases, the tracheobronchitis region collects more particles with low aerodynamic diameter, relative to healthy adults. A so-called “degraded” curve, called “high risk alveolar convention,” is then used.

in the pulmonary functions (there are similar correlations between concentrations of carbon monoxide, formaldehyde and acrolein).

Particle size distribution has a marked effect on the proportion of a fire atmosphere that is inhaled and the site of deposition. Particles size is described in terms of the aerodynamic diameter: any particle irrespective of its actual size, shape, and density behaves as a unit density sphere of a certain diameter, and this determines where it deposits. Deposition depends upon impaction, sedimentation, diffusion, and/or electrostatic attraction. Particles greater than approximately 5 µm in aerodynamic diameter deposit mainly in the nose. Particles 2 µm to 5 µm in diameter mainly in the airways. Particles less than 1 µm in diameter reach the alveoli and deposit there. At rest or under light activity, humans and other primates breathe mainly via the nose. However, during exercise or under stress, mouth breathing becomes more common and the tidal volume is higher than when breathing through the nose. Under these conditions, large particles (up to approximately 50 µm diameter) can penetrate more deeply into the airways than during nose breathing.

The smallest breathable particles (diameter between 0,5 µm and 5 µm<sup>[7]</sup>), under 3 µm<sup>[85]</sup> or under 2,5 µm<sup>[86]</sup> can reach the alveolar region of the lungs where they may be ingested by macrophages. These particles carry any adsorbed chemical compounds into the lungs where they can be “absorbed” by the blood circulation. The particles can cause lesions in the surroundings of their settling site, especially if corrosive gases are present as the adsorbed species. The presence of soot particles therefore always strongly increases the toxic potency of fire gases.<sup>[5]</sup> As the particles of soot are mainly made up of “activated charcoal they can release some compounds present on their surface. These compounds may also be released over and extended time, increasing their effect. It has been shown<sup>[87]</sup> that the SO<sub>2</sub> is particularly well adsorbed by soot.

Very small particles (less than 0.01 µm) behave more like gases, and their absorption depends upon diffusion and solubility. They are aerostable and may be exhaled unabsorbed if insoluble. There are differences between deposition in different species of animals, but they are not so extreme as to render rodents an inappropriate model for man.

Aerosol droplets may change in size during inhalation, i.e. small droplets can evaporate or aggregate. For example, cigarette smoke particles are 0.2 µm to 0.5 µm in diameter, but they absorb water vapour and reach diameters of 2 µm to 5 µm when inhaled, with the capability then of partial deposition in airways.

The toxic effects of inhaled particles depend upon their chemical properties and the site of deposition. The tissues lining each part of the respiratory tract have particular structural and functional properties which determine the physiological and pathological effects of deposited toxic particles. Parts of the upper respiratory tract, including the mouth and parts of the nose and larynx have a squamous epithelium that is relatively resistant to injury, although stimulation of trigeminal nerve endings by irritant vapours and large particles results in pain and physiological effects such as respiratory rate depression, breath holding, and coughing. The ciliated epithelium lining the main airways is more susceptible to toxic insult. Immediate effects involve stimulation of vagal nerve receptors resulting in bronchoconstriction (as in asthma attacks) with accompanying hyperinflation of the lungs and difficulties with exhalation. Deposition of irritant particles also stimulates mucus secretion from goblet cells and submucosal glands in the airways. The resulting combination of particles and mucus can block the airways, further increasing respiratory distress during and after exposure during fires. Exposure of the airways to irritants over a period of a day or so results in cilia stasis and deciliation, which occurs as a result of cigarette smoking. Inflammation of the airways results in acute bronchitis following a fire incident, with throat and chest discomfort, bronchoconstriction and breathing difficulties persisting over several days to weeks, depending upon the individual. The effects are likely to be more extreme and persistent in individuals with existing respiratory disease conditions. Single exposures such as fires can also result in permanent respiratory disease such as asthma (due to inhalation of sensitizers in smoke) and RADS (Reactive Airway Disease Syndrome), whereby subjects become especially sensitive to bronchoconstriction upon exposure to a range of stimuli (such as inhalation of cold air).

Deposition of irritant vapours or particles in the smaller airways can have more serious consequences, such as the development of fatal bronchiolitis obliterans – an inflammatory obstruction of the bronchioles.

The most sensitive part of the respiratory system is the delicate respiratory epithelium of the alveolar region. Small particles (approximately 0.5 µm to 1 µm diameter) deposit preferentially on the alveolar

surface, while smaller ultrafine particles ( $\sim 0.01 \mu\text{m}$  diameter), not only deposit on the alveolar surface but also penetrate into the lung interstitium, the region containing the small blood capillaries. The initial response to irritant deposition in the deep lung is lung oedema and inflammation, which develop over a period of a few hours after exposure in fires. This involves release of inflammatory mediators and fluid into the interstitium and alveolar lumen. This results in impairment of gas exchange due to the increased distance for gas diffusion between the alveolar air space and blood. The release of oedema fluid also interferes with lung surfactant, further impairing the mechanical performance of the lung and gas exchange. Inflammation can result in destruction of the respiratory epithelium, leading to development of emphysema or lung fibrosis.

The finest particles, usually present in relatively low concentrations, can, particularly in a child, irritate the respiratory tract or alter the respiratory functions. Some very fine particles ( $0,2 \mu\text{m}$  to  $0,5 \mu\text{m}$ ) do not settle and can pass out of the lungs again through the respiratory tract during expiration.<sup>[7]</sup>

Ultrafine particles penetrating into the blood stream have been associated with increased cardio-pulmonary mortality, including effects on the heart such as angina and infarction resulting from effects clot formation and interactions with atheroma.

In addition to their short-term/acute or immediate effect, the particles can have a longer-term effect. At first a reduction in the pulmonary capacity can occur through the mechanical obstruction of certain alveoli. As the periodontal pockets are not ciliated, and some particles are too big for cellular digestion by the macrophages, the organism does not have the efficient elimination means for this type of aggression. The lung capacity will decrease accordingly, and may result in asthmatic - like symptoms and the chronic syndrome of loss of lung capacity.

The finest particles will settle at the bottom of the periodontal pockets and hinder the alveolar gaseous exchanges. They can also be related to the occurrence or the development of lung cancers even after long periods following the cessation of acute symptoms. It is nevertheless extremely difficult to obtain toxicological data of this kind, because of the variety of aggressions that are sustained by the lungs during lifetime (cigarette, automotive pollution, asbestos etc. The effect of the particles on mortality has nevertheless been established in the case of chronic environmental emissions.

The effect of the particles on the lungs is thus related to the appearance of chronic asthma, and/or a reduction in lung capacity. Over the long term, cancers can develop. These effects may be effective several days after the fire and the risks remain for the persons present after one disaster that should wear the respiratory masks adapted to the finest particles.

The World Health Organization (WHO) stresses that 80,000 lives could be saved in Europe by 2010 thanks to the implementation of the Directive 1999/30/CE. This directive sets the daily limit values of the PM 10 at  $50 \mu\text{g}/\text{m}^3$  and their annual limit value at  $40 \mu\text{g}/\text{m}^3$ . The figures concerning the PM 2,5 have not yet been defined. However, the PM2,5 particles are by far the most toxic. Moreover, there are currently no threshold values defined for the acute exposures. A content of  $250 \mu\text{g}/\text{m}^3$  was encountered in several sources of PM10 particles.

## Annex D (informative)

### Non-toxicological effects of particles

#### D.1 Radiative heat flux

At room flashover, virtually all the combustibles in a room are burning, including those that are not in contact with the initial burning item. Much of this secondary ignition is caused by thermal radiation from the flames and especially from the layer of hot combustion gases that increasingly fills the upper portion of the room. The radiative flux from this smoke layer is determined by its temperature and optical density. The optical density is determined by the concentration of particles and their optical properties. Well before flashover, the radiation from the upper layer is sensitive to the optical properties of the smoke particles. As the room approaches flashover, the temperature is rising quickly and the particle density is high, decreasing the importance of the detailed nature of the particles.

#### D.2 Filtration and electrical effects

Carbonaceous soot particles may be electrically conductive. This can cause short circuits on and damage to electrical components, including those that might be part of a safety system.

In systems where filtration is essential, such as in electronic clean rooms, knowledge of the fire aerosol particle granulometry is crucial for dimensioning the filters for effective particle removal in emergency situations. In the nuclear industry, this is even more important, since the particles have the capacity to adsorb radioactive species.

#### D.3 Loss of visibility

People needing to function in a burning building include those trying to escape and those who are trying to find the fire in order to control it. High concentrations of visible smoke interfere with these functions, and the optical properties are central to the degree of loss of visibility. On a mass basis, particles all diffuse light,<sup>[84]</sup> but not in the same way or to the same extent. Particles with a size close to the wavelengths in the visible spectrum (i.e. between 0,3 µm and 0,8 µm) scatter most light.<sup>[88]</sup> Schaefer<sup>[89]</sup> specified that the diameter of the particles producing the most obscuration is close to 0,6 µm. With submicrometer particles, light scattering is proportional to the sixth power of its radius.<sup>[84]</sup> Generally, a particle of over 1 µm scatters light proportionally to the square of its radius. Recall that if a person is far enough from the fire that heat is not a serious threat, the initial particles will have coagulated, favouring a predominance of particles with larger diameters.<sup>[88]</sup>

#### D.4 Environmental considerations

The effects of airborne aerosol particles on the environment have been and remain of great concern. Occupational hygienists have realized that the potential effect on health was related to the exposure to fine particles. These particles partly originate from combustion. However, the contribution of unwanted fires to atmospheric particle release is negligible when compared with the sources such as supply of energy, automotive traffic, and industry at large, except considering locally wildland fires.

When settling on vegetation, the particles act to block their stomata, (the organelles that intervene in chlorophyllous respiration), which results in the withering of plants. With animals, the effects are similar to those observed in man. Toxic effects through digestion of particles have not been observed, and only the inhalation of particles appears to have any effect.

## Annex E (informative)

### Example of report

#### Report – Cascade impactor

N	Impactor Stage ( $\mu\text{m}$ )	Cut-off diameter ( $\mu\text{m}$ )	Mass stage (mg)	Relative mass (%)	Cumulative mass (%)
1	0.06 – 0.12	0.060	0.000	0.00	0.00
2	0.12 - 0.25	0.120	0.002	0.14	0.00
3	0.25 - 0.49	0.250	0.049	3.43	0.14
4	0.49 - 0.90	0.490	0.378	26.43	3.57
5	0.90 - 1.85	0.900	0.745	52.10	30.00
6	1.85 - 3.69	1.850	0.230	16.08	82.10
7	3.69 - 7.42	3.690	0.021	1.47	98.18
8	7.42 –14.80	7.420	0.005	0.35	99.65
9	14.80 –30.00	14.800	0.000	0.00	100.00

Mass Median Aerodynamic Diameter (MMAD): 1.28  $\mu\text{m}$

Geometric standard deviation (GSD): 1.77

Number Median Aerodynamic Diameter (NMAD): 0.49  $\mu\text{m}$

Surface Median Aerodynamic Diameter (SMAD): 0.93  $\mu\text{m}$

System: BERNER-IMPACTOR I

Air flow: 5.85 L/min

Sampling time: 3600.00 s

Concentration (computed): 4.07 mg/m<sup>3</sup> air

#### Respirability (percent < 1.0 $\mu\text{m}$ ):

1. Mass related: 33.3 % (measured)

2. Number related: 89.7 % (extrapolated)

#### Respirability (percent < 3.0 $\mu\text{m}$ ):

1. Mass related: 93.3 % (measured)

2. Number related: 99.9 % (extrapolated)

#### Respirability (percent < 5.0 $\mu\text{m}$ ):

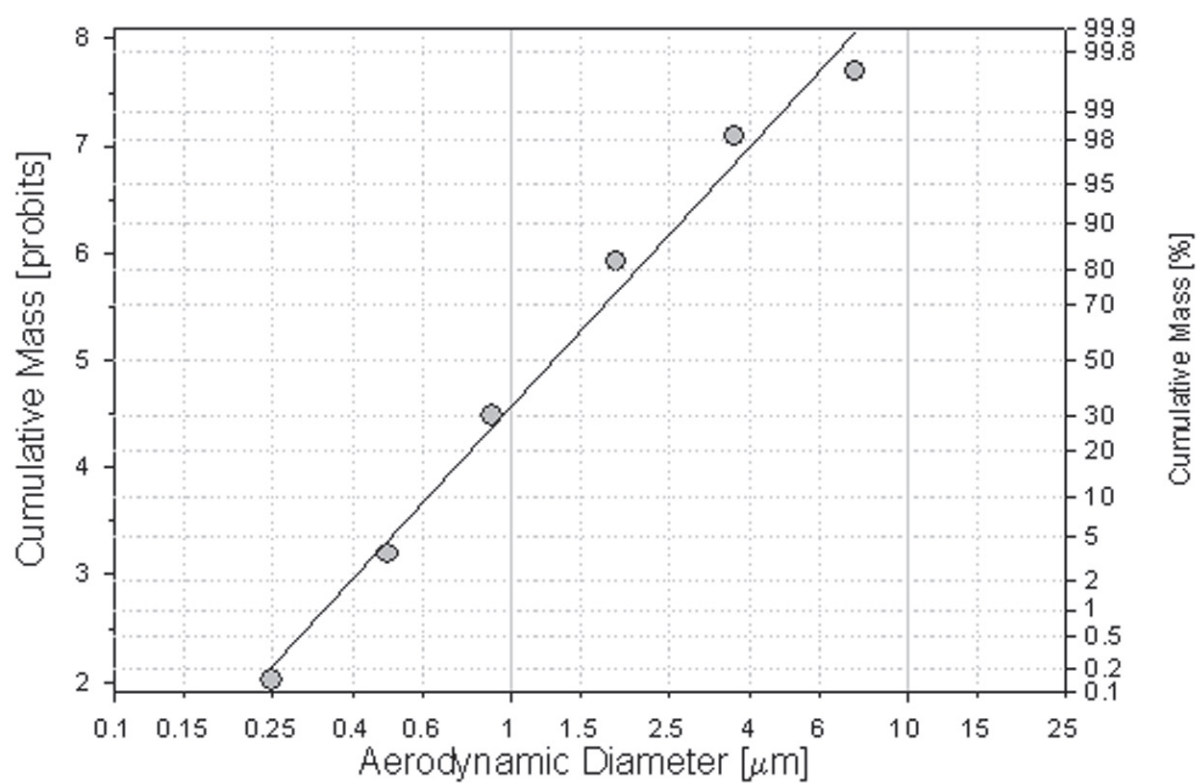
1. Mass related: 99.3 % (measured)

2. Number related: 99.9 % (extrapolated)

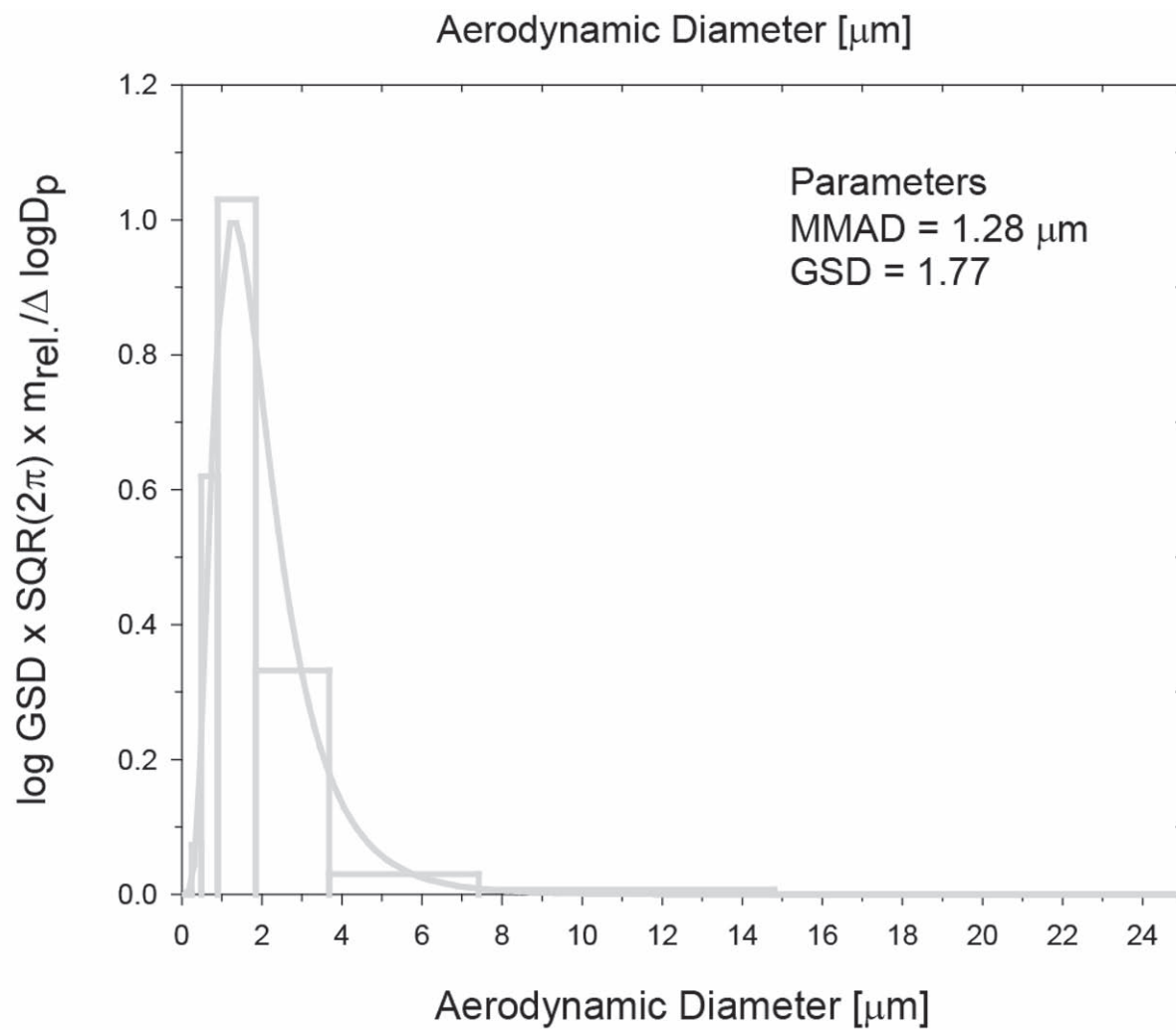
ECD-definition: right cut-size ( $D_p+1$ )



Particle-size Analysis  
(Target concentration: 3.0 mg/m<sup>3</sup> air)







## Bibliography

- [1] OUF F.X. Caractérisation des aérosols émis lors d'un incendie, PhD Thesis, University of Rouen, 2006, ISRN IRSN-2006/62-FR.
- [2] RENOUX A., & BOULAUD D. Les aérosols – Physique et métrologie – Editions Lavoisier Tec & Doc – Paris. ISBN 2-7430-0231.
- [3] WILLEKE K., & BARON P.A. *Aerosol Measurement. Principles, Techniques and Applications*. J. Wiley & Sons, 1993
- [4] BLOMQUIST P. Emissions from Fires – Consequences for Human Safety and the Environment, PhD thesis, Report 1030, Lund University, 2005.
- [5] LEVIN B.C., & KULIGOWSKI E.D. Toxicology of Fire and Smoke. *in Inhalation Toxicology*. 2nd Edition. Chapter 10, pp. 205-228. CRC Press (Taylor and Francis Group), Boca Raton, FL, Salem, H.; Katz, S. A., Editor(s), 2005.
- [6] PAULUHN J. Retrospective Analysis of Acute Inhalation Toxicity Studies: Comparison of Actual Concentrations obtained by Filter and Cascade Impactor Analyses. *Regul. Toxicol. Pharmacol.* 2005, **42** pp. 236–244
- [7] USDA. 1991, Health Hazards of Smoke, USDA Forest Service, Missoula Technology and Development Center, 9167-2809-MTDC, 8 p.
- [8] HARVEY R.G. *Polycyclic Aromatic Hydrocarbons: Chemistry and Carcinogenicity*. Cambridge University Press, 1991, pp. 11–15.
- [9] WITTEN T.A., & SANDERS J.M. Diffusion-Limited Aggregation, a Kinetic Critical Phenomenon. *Phys. Rev. Lett.* 1981, **47** pp. 1400–1403
- [10] JULLIEN R., & BOTET R. *Aggregation and fractal aggregates*. World Scientific Pub Co Inc. 1987
- [11] PUTORTI A.D. *Design parameters for stack-mounted light extinction measurement devices, NISTIR 6215*. National Institute of Standards and Technology, Gaithersburg, 1999
- [12] VAN HULLE P. Caractérisation des aérosols émis par la combustion des hydrocarbures: Application a la mesure de l'indice de réfraction des suies. PhD Thesis, University of Rouen, 2002.
- [13] WU J.S., KRISHNAN S.S., FAETH G.M. Refractive indices at visible wavelengths of soot emitted from buoyant turbulent diffusion flames. *J. Heat Transfer*. 1997, **119** pp. 230–237
- [14] BUSHELL G.C., YAN Y.D., WOODFIELD D., RAPER J., AMAL R. On techniques for the measurement of the mass fractal dimension of aggregates. *Adv. Colloid Interface Sci.* 2002, **95** pp. 1–50
- [15] SORENSEN C.M. Scattering and absorption of light by particles and aggregates. In: *Handbook of Surface and Colloid Chemistry*, (BIRDI K.S.ed.). CRC Press, 1997, pp. 533–558.
- [16] GREEN H.L., & WATSON H.H. *Medical Research Council Special Report, 199 HMS*. HMSO, London, 1935
- [17] DOBBINS R.A., & MEGARIDIS C.M. Morphology of flame-generated soot as determined by thermophoretic sampling. *Langmuir*. 1987, **3** pp. 254–259
- [18] KÖYLÜ Ü.Ö., MCENNALLY C.S., ROSNER D.E., PFEFFERLE L.D. Simultaneous measurements of soot volume fraction and particle size/microstructure in flames using a thermophoretic sampling technique. *Combust. Flame*. 1997, **110** (Issue 4) pp. 494–507
- [19] THOMASSEN Y., KOCH W., DUNKHORST W., ELLINGSEN D.G., SKAUGSET N., JORDBEKKEN L. et al. Ultrafine Particles at Workplaces of a Primary Aluminium Smelter. *J. Environ. Monit.* 2006, **8** pp. 127–133

- [20] Model 3089 Nanometer Aerosol Sampler, TSI Manual
- [21] SPURNY K.R. *Physical and Chemical characterization of Individual Airborne Particles*. John Wiley & Sons Inc, New York, 1986, pp. 40–71.
- [22] KÖYLÜ Ü.Ö., FAETH G.M., FARIAS T.L., CARVALHO M.G. Fractal and projected structure properties of soot aggregates. *Combust. Flame*. 1995, **100** pp. 621–633
- [23] KÖYLÜ Ü.Ö., XING Y., ROSNER D.E. Fractal morphology analysis of combustion-generated aggregates using light scattering and electron microscope images. *Langmuir*. 1995, **11** pp. 4848–4854
- [24] SORENSEN C.M., & FEKE G.D. The morphology of macroscopic soot. *Aerosol Sci. Technol.* 1996, **25** pp. 328–337
- [25] VAN GULIJK C., MARIJNISSEN J.C.M., MAKKEE M., MOULIJN J.A., SCHMIDT-OTT A. Measuring diesel soot with a scanning mobility particle sizer and an electrical low-pressure impactor: performance assessment with a model for fractal-like agglomer. *J. Aerosol Sci.* 2004, **35** pp. 633–655
- [26] FARDELL P., & GUILLAUME E. Sampling and analysis of fire effluents, in *Fire Toxicity* (chapter 11) 1st edition, ISBN 1 84569 502 X, Woodhead publishers / CRC ed., April 2010.
- [27] Rasbash. D.J., Philips R.P., Quantification of smoke produced by fires. *Fire Mater.* 1978, **2** pp. 102–109
- [28] DURST F., & ZARE N. Laser Doppler Measurements in Two-Phase Flows. Proceedings of LDA75, University of Denmark, 1975.
- [29] GREHAN G., GOUESBET G., NAQWI A. Trajectory Ambiguities in Phase Doppler Systems: Use of Polarizers and Additional Detectors to Suppress the Effect, International Symposium on application of laser techniques to fluid mechanic, Lisboa, 12.1. 1992.
- [30] WIENER B.B. Particles Sizing Using Photon Correlation Spectroscopy. In: *Modern Method of Particle Size Analysis*, (BARTH H.G. ed.). Wiley, New York, 1984, pp. 93–116.
- [31] CRANE R.I., & EVANS R.L. Inertial deposition of particles in a bent pipe. *J. Aerosol Sci.* 1977, **8** (3) pp. 161–170
- [32] PUI D.Y.H., ROMAY-NOVAS F., LIU B.Y.H. Experimental Study of Particle Deposition in Bends of Circular Cross Section. *Aerosol Sci. Technol.* 1987, **7** (3) pp. 301–315
- [33] DEKATI. *Fine Particle Sampler FPS-4000* documentation, available online at [http://www.dekati.com/cms/fps\\_4000](http://www.dekati.com/cms/fps_4000).
- [34] DEKATI. *Diluter DI-1000* documentation, available online at [http://www.dekati.com/cms/dekati\\_diluter](http://www.dekati.com/cms/dekati_diluter).
- [35] MATTER ENGINEERING Rotating disk diluter for Emissions documentation, available online at <http://www.matter-aerosol.ch/>.
- [36] LE TALLEC Y., SARAGOZA L., HERTZBERG T., BLOMQUIST P. Particles from Fire: Evaluation of the particulate fraction in fire effluents using the cone calorimeter. Proceedings of Interflam Conference, Edinburgh University, 2004.
- [37] LALL A.A., SEIPENBUSCH M., RONG W., FRIEDLANDER S.K. On-line measurement of ultrafine aggregate surface area and volume distributions by electrical mobility analysis: II. Comparison of measurements and theory. *J. Aerosol Sci.* 2006, **37** pp. 272–282
- [38] LEITH D., & PETERS T.M. Concentration Measurement and Counting Efficiency of the Aerodynamic Particle Sizer 3321. *J. Aerosol Sci.* 2003, **34** (5) pp. 627–634
- [39] MAY K.R. A multistage liquid impinger. *Bacteriol. Rev.* 1996, (September) pp. 559–570
- [40] RAABE O.G. The dilution of Monodisperse suspension for Aerosolization. *Am. Ind. Hyg. Assoc. J.* 1968, **29** pp. 439–443

- [41] HELSPER C., MOLTER W., LOFFLER F., WADENPOHL C., KAUFAMNN S., WENNINGER G. Investigations of a New Aerosol Generator for the Production of Carbon Aggregate Particles. *Atmos. Environ.* 1993, **27** pp. 1271–1275
- [42] BAU S.IRSN/DSU/SERAC - Journées des Thèses IRSN, 1-4 October 2007.
- [43] MOTZKUS C., CHIVAS-JOLY C., GUILLAUME E., DUCOURTIEUX S., SARAGOZA L., LESENECHAL D. et al. Count size distribution of the aerosol emitted by the combustion of nanocomposites, Posters session, European Aerosol Conference EAC2011, Manchester (UK), 4-9 September 2011.
- [44] BUTLER K.M., & MULHOLLAND G.W. Generation and Transport of Smoke Components. *Fire Technol.* 2004, **40** (2) pp. 149–176
- [45] HINDS W.C. Aerosol Technology, 2nd Ed., A Wiley-Interscience publication, 1999.
- [46] HERTZBERG T., & BLOMQVIST P. Particles from fires – a screening over common materials found in buildings. *Fire Mater.* 2003, **27** pp. 295–314
- [47] LÖNNERMARK A., & BLOMQVIST P. Emissions from an Automobile Fire. *Chemosphere.* 2006, **62** pp. 1043–1056
- [48] MULHOLLAND G.W. Smoke productions and properties, *In SFPE Handbook of Fire Protection Engineering* (NFPA, Ed.), NFPA, 2.258-2.268, Quincy, MA, USA, 2002.
- [49] O'SHAUGHNESSY P.T., & RAABE O.G. A comparison of cascade impactor data reduction methods. *Aerosol Sci. Technol.* 2003, **37** (2) pp. 187–200
- [50] DENNIS R. Handbook of Aerosols - Technical Information Center, Energy Research and Development Administration. pp. 110-114, July 1976.
- [51] MARPLE V.A., & RUBOW K.L. Aerosol Generation Concepts and Parameters. In: *Generation of Aerosols and Facilities for Exposure Experiments*, (WILLEKE K. ed.). Ann Arbor Science Publ. Inc, Mich., 1980, pp. 3–29.
- [52] RAABE O.G. Deposition and Clearance of Inhaled Aerosols. In: *Mechanisms in Respiratory Toxicology*, (WITSCHI H., & NETTESHEIM P. eds.). CRC Press, Inc, Boca Raton, Florida, **Vol. I**, pp. 27–76.
- [53] SNIPES M.B. Long-Term Retention and Clearance of Particles Inhaled by Mammalian Species. *Crit. Rev. Toxicol.* 1989, **20** pp. 175–211
- [54] Sot-commentary. Recommendations for the Conduct of Acute Inhalation Limit Tests, prepared by the Technical Committee of the Inhalation Specialty Section. *Society of Toxicology. Fundam. Appl. Toxicol.* 1992, **18** pp. 321–327
- [55] ROSIELLO A.P., ESSIGMANN J.M., WOGAN G.N. Rapid and Accurate Determination of the Median Lethal Dose (LD<sub>50</sub>) and its Error with Small Computer. *J. Toxicol. Environ. Health.* 1977, **3** pp. 797–809
- [56] ISO 7708, *Air quality — Particle size fraction definitions for health-related sampling*
- [57] JOYEUX D. Numerical and experimental assessment of soot formation in Ethylene diffusion flame, PhD Thesis, University of Rouen, 1993.
- [58] SAMSON R.J., MULHOLLAND G.W., GENTRY J.W. Structural analysis of soot agglomerates. *Langmuir.* 1987, **3** pp. 272–281
- [59] KÖYLÜ Ü.Ö., & FAETH G.M. Carbon monoxide and soot emissions from buoyant turbulent diffusion flames. *Fire Safety Science: Proceedings of the Third International Symposium*, pp 625-634, 1991.
- [60] HU B., YANG B., KÖYLÜ Ü.Ö. Soot measurements at the axis of an ethylene/air non-premixed turbulent jet flame. *Combust. Flame.* 2003, **134** pp. 93–106
- [61] OUF F.X., COPPALLE A., VENDEL J., WEILL M.E., YON J. Characterization of soot particles in the plume of over-ventilated diffusion flames. *Combust. Sci. Technol.* 2008, **180** (4) pp. 674–698

- [62] KRISHNAN S.S., LIN K.-C., FAETH G.M. Optical properties in the visible of overfire soot in large buoyant turbulent diffusion flames. *J. Heat Transfer*. 2000, **122** pp. 517–524
- [63] KRISHNAN S.S., & FAETH G.M. Buoyant turbulent jets and flames: II. Refractive index, extinction and scattering properties of soot, NIST GCR 00-796, 2000.
- [64] MEGARIDIS C.M., & DOBBINS R.A. Comparison of soot growth and oxidation in smoking and non-smoking ethylene diffusion flames. *Combust. Sci. Technol.* 1989, **66** pp. 1–16
- [65] LEE K.B., THRING M.W., BEÉR J.M. On the rate of combustion of soot in a laminar soot flame. *Combust. Flame*. 1962, **6** (Issue C) pp. 137–145
- [66] PRADO G.P., LEE M.L., HITES R.A., HOULT D.P., HOWARD J.B. Soot and hydrocarbon formation in a turbulent diffusion flame. International Symposium on Combustion Vol. 16 (1), pp. 649–661, 1977.
- [67] ZHANG H.X., SORENSEN C.M., RAMER E.R., OLIVIER B.J., MERKLIN J.F. In situ optical structure factor measurements of an aggregating soot aerosol. *Langmuir*. 1988, **4** (4) pp. 867–871
- [68] PRADO G., JAGODA J., NEOH K., LAHAYE J. A study of soot formation in premixed propane/oxygen flames by in-situ optical techniques and sampling probes. International Symposium on Combustion, Vol. 18(1), pp. 1127–1136, 1981.
- [69] WEY C., POWELL E.A., JAGODA J. I. The effect on soot formation of oxygen in the fuel of a diffusion flame. International Symposium on Combustion, Vol. 20(1), pp. 1017–1024, 1985.
- [70] JAGODA I. J., PRADO G., LAHAYE J. An experimental investigation into soot formation and distribution in polymer diffusion flames. *Combust. Flame*. 1980, **37** pp. 261–274
- [71] HARRIS S.J., & WEINER A.M. Detection of Incipient Soot particles in a premixed ethylene flame. Chemical and Physical Processes in Combustion, Fall Technical Meeting, The Eastern States Section, pp. 67.1–67.4, 1984.
- [72] ROESSLER D.M. Diesel particle mass concentration by optical techniques. *Appl. Opt.* 1982, **21** (22) pp. 4077–4086
- [73] EVANS D., BAUM H., MCCAFFREY B., MULHOLLAND G., HARKLEROAD M., MANDERS W. Combustion of Oil on Water. Proceedings of the Ninth Annual Arctic and Marine Oilspill Program - Technical Seminar; Edmonton, Alberta, Can; Code 10157, 1986.
- [74] SORENSEN C.M., & FEKE G.D. The morphology of macroscopic soot. *Aerosol Sci. Technol.* 1996, **25** pp. 328–337
- [75] KÖYLÜ Ü.Ö., & FAETH G.M. Structure of overfire soot in buoyant turbulent diffusion flames at long residence times. *Combust. Flame*. 1992, **89** (2) pp. 140–156
- [76] SORENSEN C.M., CAI J., LU N. Light-Scattering measurements of monomer size, monomers per aggregate, and fractal dimension for soot aggregates in flames. *Appl. Opt.* 1992, **31** pp. 6547–6557
- [77] COLBECK I., ATKINSON B., JOHAR Y. The morphology and optical properties of soot produced by different fuels. *J. Aerosol Sci.* 1997, **28** pp. 715–723
- [78] WENTZEL M., GORZAWSKI H., NAUMANN K.H., SAATHOFF H., WEINBRUCH S. Transmission electron microscopical and aerosol dynamical characterization of soot aerosols. *J. Aerosol Sci.* 2003, **34** pp. 1347–1370
- [79] MATTI MARICQ M., & XU N. The effective density and fractal dimension of soot particles from premixed flames and motor vehicles. *J. Aerosol Sci.* 2004, **35** pp. 1251–1274
- [80] CAI J., LU N., SORENSEN C.M. Analysis of Fractal cluster morphology parameters : structural coefficient and density autocorrelation function cutoff. Journal of Colloidal and interface science, Vol. 171:470–473, 1995.



- [81] KIM H.W., & CHOI M. In situ line measurement of mean aggregates size and fractal dimension along the flame axis by planar laser light scattering. *J. Aerosol Sci.* 2003, **34** (12) pp. 1633–1645
- [82] HEYDER J., GEBHART J., RUDOLF G., SCHILLER C.F., STAHLHOFEN W. Deposition of particles in the human respiratory tract in the size range 0.005-15 µm. *J. Aerosol Sci.* 1986, **17** (5) pp. 811–825
- [83] MAHAFFEY L., & MILLER M. Introduction to fire effects RX 340, Chap IV Air Quality. Northern training center, 13 p., 1995.
- [84] PETERSON J.L. Air quality, smoke management, and prescribed fire. Proceeding of the 1990 Pacific Northwest Range Management Short Course, Fire in Pacific Northwest Ecosystems, January, 23-25th 1990, Pendleton, OR, Corvallis, OR, Departement of Rangeland Resources, Oregon State University, pp. 132-136, 1990.
- [85] MOBLEY H.E., BARDEN C.R., BIGLER CROW A., FENDER D.E., JAY D.M., WINKWORTH R.C. Southern forestry smoke management guidebook. USDA Forest Service general technical report SE-10, 140p, 1976.
- [86] WARD D., & HARDY D.C. Smoke emissions from wildland fires. *Environ. Int.* 1991, **17** pp. 117–134
- [87] Plan régional Qualité de l'air - Généralités sur la pollution de l'air et ses effets sur la santé et l'environnement- DRIRE région Nord Pas de Calais, 2000.
- [88] SANDBERG D.V., & MARTIN R.E. Particle sizes in slash fire smoke. USDA Forest Service research paper PNW-199, 7 p., 1975.
- [89] SCHAEFER V.J. Some physical relationships of fine particle smoke. Proceedings annual: 13 Tall Timbers Fire Ecology Conference; Tallahassee, Florida, March 22-23rd, 1973, pp. 283-294.
- [90] ISO 19701, *Methods for sampling and analysis of fire effluents*
- [91] ISO 5660-1:2002, *Reaction-to-fire tests — Heat release, smoke production and mass loss rate — Part 1: Heat release rate (cone calorimeter method)*
- [92] ISO 5660-2:2002, *Reaction-to-fire tests — Heat release, smoke production and mass loss rate — Part 2: Smoke production rate (dynamic measurement)*
- [93] ISO 9705:1993, *Fire tests — Full-scale room test for surface products*
- [94] ISO 13571, *Life-threatening components of fire — Guidelines for the estimation of time to compromised tenability in fires*



